

THESIS

DEVELOPMENT OF AN ASYMMETRIC INTERMOLECULAR STETTER REACTION
AND ORGANOCATALYST DESIGN

Submitted by

Garrett S. Glover

Department of Chemistry

In partial fulfillment of the requirements

for the Degree of Master of Science

Colorado State University

Fort Collins, Colorado

Spring 2012

Master's Committee:

Advisor: Tomislav Rovis

John L Wood

Shane Kanatous

ABSTRACT

DEVELOPMENT OF AN ASYMMETRIC INTERMOLECULAR STETTER REACTION AND ORGANOCATALYST DESIGN

The intermolecular Stetter represents a powerful carbon-carbon bond forming reaction that involves addition of an acyl anion equivalent to an untethered Michael acceptor. Despite the appeal of rendering the intermolecular reaction asymmetric, this area remains particularly underdeveloped. We describe a catalytic asymmetric intermolecular Stetter reaction for the coupling of 2-pyridinecarboxaldehydes and β -substituted vinyl triflates.

In pursuit of increasing the efficiency of this reaction, we developed a series of base-activated NHC pre-catalysts that are capable of catalyzing the intramolecular Stetter reaction without an external base. As an indirect result of our attempts to form activated pre-catalysts, we discovered a catalyst hydration product, that itself generates free-carbene in solution. Additionally, we gathered conclusive evidence for a previously unknown S_NAR type decomposition pathway of an electron deficient triazolinylidene catalyst.

TABLE OF CONTENTS

The Development of an Asymmetric Intermolecular Stetter Reaction

1.1	Introduction.....	1
1.2	The Benzoin Reaction.....	2
1.3	The Asymmetric Stetter Reaction.....	4
1.3.1	Introduction.....	4
1.3.2	The Asymmetric Intramolecular Stetter Reaction.....	6
1.3.3	The Asymmetric Intermolecular Stetter Reaction.....	8
1.4	Development of an Asymmetric Intermolecular Stetter Reaction.....	9
1.4.1	Selection of an Appropriate Michael Acceptor.....	9
1.4.2	Optimization of Pre-Catalyst.....	11
1.4.3	Solvent Screen.....	12
1.4.4	Effect of Catechol.....	13
1.4.5	Base Screen.....	14
1.4.6	Attempts to Decrease Elimination.....	15
1.4.7	Tuning the Catalyst <i>N</i> -Aryl Substituent.....	17
1.4.8	Aldehyde Scope.....	18
1.5	Conclusion.....	19

Chapter 2. The Development of Base-Activated Organocatalysts

2.1	Introduction.....	22
2.2	Counterion Exchange in a Biphasic System.....	23
2.3	Counterion Exchange in Organic Media.....	26

2.4	Base-Activated NHC Pre-Catalysts and the Intramolecular Stetter.....	26
2.5	Toward Electron Deficient Base-Activated Pre-Catalysts.....	29
2.5.1	Attempts at a Direct Synthesis.....	29
2.5.2	Triazolium Chloride Salts by Counterion Exchange.....	32
2.6	Elucidation of Pre-Catalyst Decomposition Pathways.....	34
2.6.1	Pre-Catalyst Hydration and the Stetter Reaction.....	34
2.6.2	An Unexpected $S_{N_{AR}}$ Decomposition Pathway.....	35
2.7	Conclusion.....	37
	Appendix 1: Chapter 1 Experimental.....	40
	Appendix 2: Chapter 2 Experimental.....	57

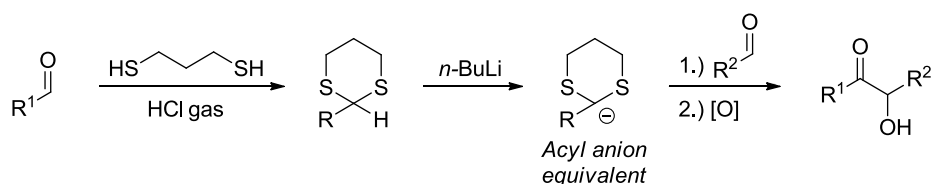
Chapter 1

The Development of an Asymmetric Intermolecular Stetter Reaction

1.1 Introduction

N-heterocyclic carbenes (NHCs) have attracted considerable interest in recent years due to their ability to reverse the normal mode of reactivity of aldehydes, rendering them nucleophilic at the carbonyl carbon. This reactivity reversal is referred to as *umpolung*.¹ Other well-known protocols to reverse the polarity of aldehydes require a protection/deprotection sequence with a stoichiometric reagent, most commonly a dithiane (Scheme 1.1) or a protected cyanohydrin. To reveal the nucleophilic acyl anion, a strong base such as *n*-BuLi is usually required.² NHC pre-catalysts, on the other hand, are used in sub-stoichiometric quantities, form an acyl anion equivalent *insitu* and catalytically under mild conditions, and eliminate the need for protection/deprotection of the aldehyde. Most importantly, it is now possible to tune enantiofacial selectivity during C-C bond forming events by rational design of chiral-NHC pre-catalysts.

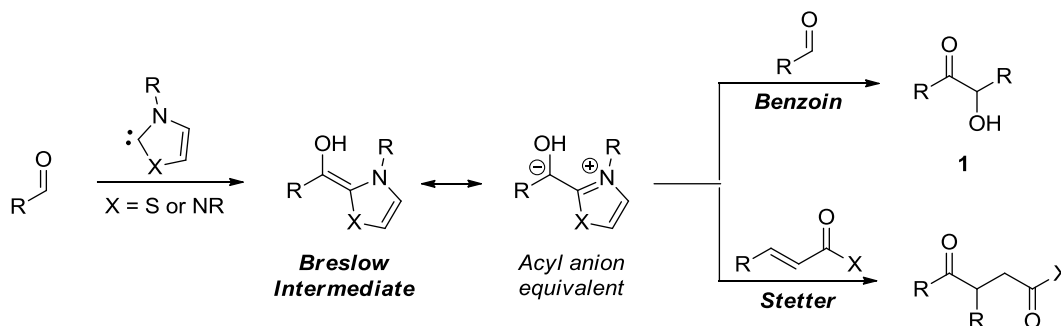
Scheme 1.1: Synthesis of α -Hydroxy Ketones Using a Dithiane Reagent



Two very important reactions that rely on the *umpolung* reactivity of aldehydes are the benzoin and Stetter reaction (Scheme 1.2). Both have undergone dramatic advancements in their catalytic asymmetric variants as a result of recent developments in chiral-NHC pre-catalyst

designs. The benzoin reaction, one of the earliest known organic reactions, is not surprisingly the first of these two to be applied toward asymmetric synthesis.

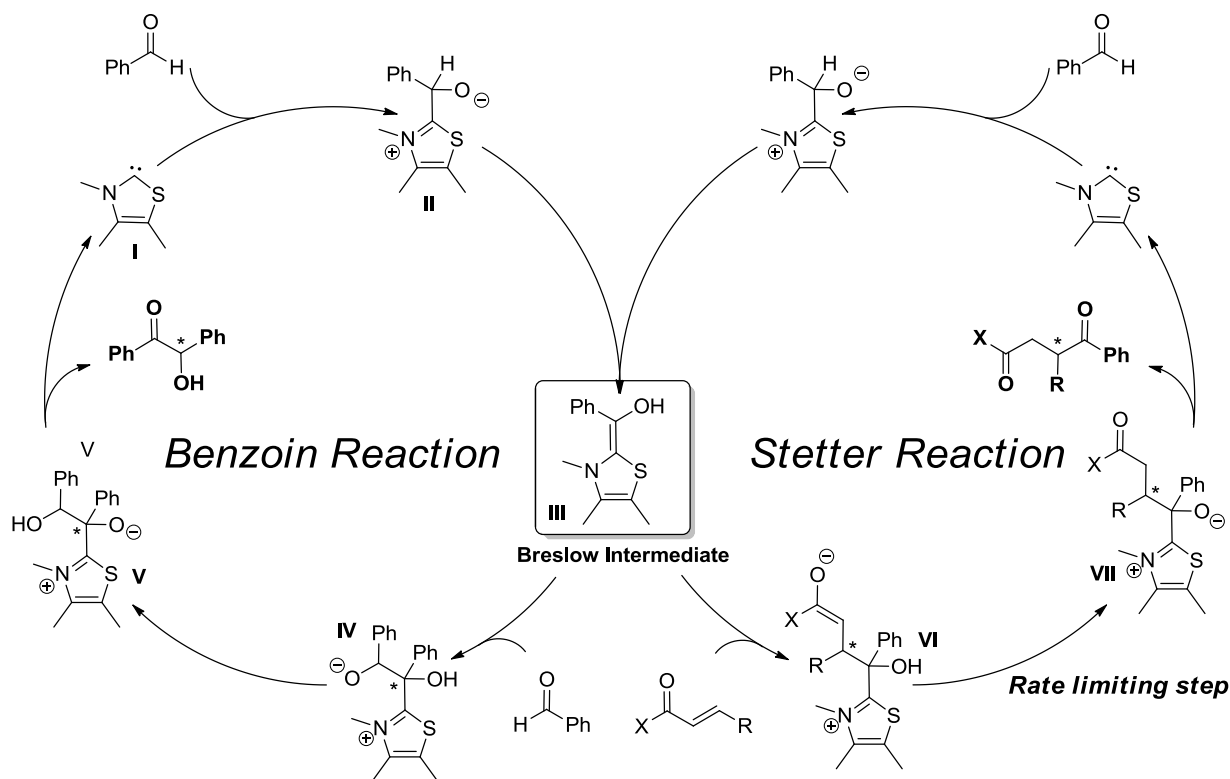
Scheme 1.2: General Benzoin and Stetter Reactions



1.2 The Benzoin reaction

The benzoin reaction was one of the earliest organic transformations found to exploit *umpolung* reactivity. Indeed, the discovery of the benzoin reaction dates back to Wohler and Liebig's 1832 communication which revealed that cyanide ion can catalyze the homocoupling of benzaldehyde to form benzoin, an α -hydroxy ketone **1** (Scheme 1.2).³ In 1943, Ukai discovered that thiazolium salts can catalyze the same reaction,⁴ and Breslow later published his landmark paper in 1958 that provided an elucidated mechanism for a thiazolium-catalyzed reaction.⁵ The Breslow mechanism, shown in Scheme 1.3, begins with *in situ* formation of carbene **I** via deprotonation of the thiazolium salt by a base. Carbene **I** then adds to an aldehyde to form tetrahedral intermediate **II**. After proton transfer, the acyl-anion equivalent **III**, termed the Breslow intermediate, is formed. This nucleophilic alkene then adds into another equivalent of aldehyde to form adduct **IV**. Proton transfer (**IV** to **V**) and collapse of tetrahedral intermediate **V** liberates carbene **I** and an α -hydroxy ketone which features a newly formed stereocenter.

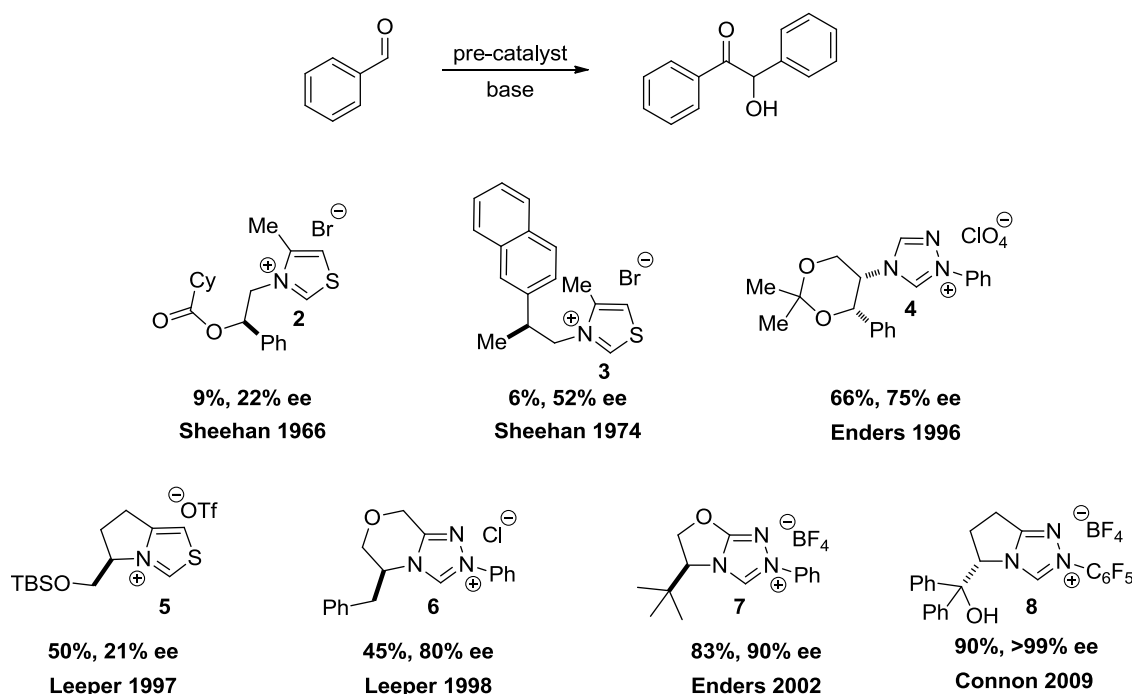
Scheme 1.3: Mechanism of the Benzoin and Stetter Reactions



The first asymmetric benzoin reaction was reported by Sheehan in 1966, and it featured chiral thiazolium pre-catalyst **2** which provided benzoin in 22% (Table 1.1). Later improvement to 52% ee was achieved using precatalyst **3**, although yields remained very low.⁶ Twenty years later, Enders utilized triazolium pre-catalyst **4**, which proved a reactive scaffold that imparted moderate levels of enantioselectivity.⁷ Leeper was among the first to prepare a bicyclic pre-catalyst, such as thiazolium **5**, for use in the benzoin reaction.⁸ He and Rawal similarly hypothesized that locking a chiral substituent into a ring rather than allowing it to have free-rotation would provide better discrimination between the two faces of the active catalyst in the C-C bond forming event.^{8,9} Although this early thiazolium bicyclic pre-catalyst design did not improve selectivities of the benzoin reaction, a related triazolium pre-catalyst **6** significantly

increased benzoin enantioselectivity to good levels.¹⁰ Further developments by Enders resulted in triazolium salt **7** which provided benzoin in 83% yield and 90% ee.¹¹ Finally, Connon's use of an electron deficient pentafluorophenyl aryl group on L-pyroglutamic acid-derived catalyst **8** substantially increased reactivity in relation to that achieved by the related *N*-phenyl catalyst, while maintaining excellent levels of enantioselectivity.¹²

Table 1.1: Catalysts Used In the Asymmetric Benzoin Reaction



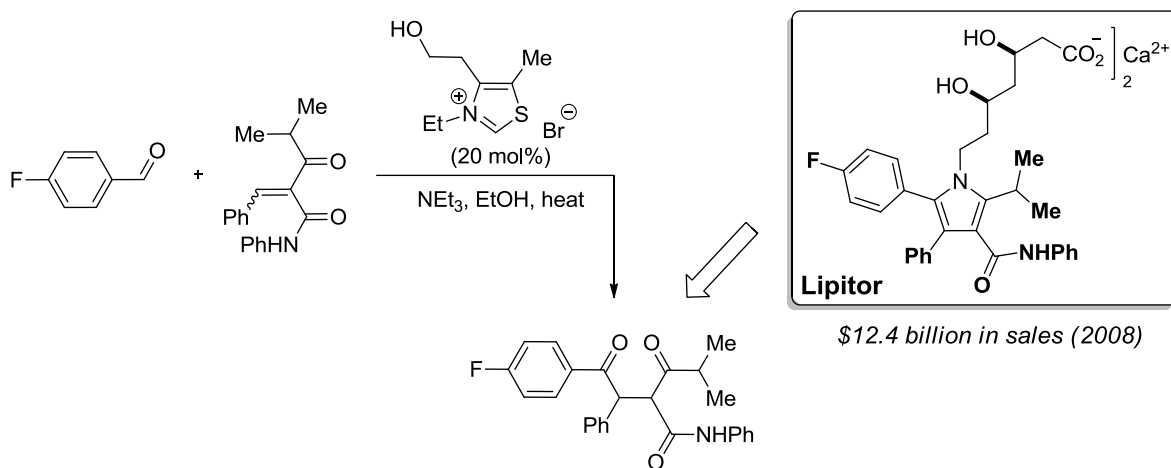
1.3 The Asymmetric Stetter Reaction

1.3.1 Introduction

In 1973, Stetter greatly expanded upon the scope of acyl anion based transformations by successfully employing α,β -unsaturated Michael acceptors as the electrophilic component. It was established that aldehydes can add in a conjugately into α,β -unsaturated esters, nitriles, or ketones in the presence of cyanide ion or a thiazolium catalysts to form highly valuable 1,4-

difunctionalized products (Scheme 1.2).¹³ 1,4-diketones, in particular, are important synthons in the total synthesis of complex molecules. One high-profile example of an industrial scale Stetter reaction is found in Pfizer's synthesis of Lipitor, a medication used to lower blood cholesterol (Scheme 1.4).¹⁴

Scheme 1.4: Pfizer's Commercial Route to Lipitor



The proposed catalytic cycle of the Stetter reaction is based on the Breslow mechanism, and proceeds through common Breslow intermediate **III** (Scheme 1.3). This nucleophilic alkene adds into a Michael acceptor to afford tetrahedral intermediate **VI**. A second proton transfer occurs to give **VII**, which collapses to release carbene **I** and provide a 1,4 difunctionalized Stetter product. It should be noted that a recent study by our group has provided compelling evidence that the first proton transfer event (**VII** to **III**) is the turnover limiting step of the intramolecular Stetter reaction.¹⁵

1.3.2 The Asymmetric Intramolecular Stetter Reaction

Over the last 15 years, the intramolecular Stetter reaction has seen rapid development, particularly in its asymmetric variation. Surprisingly, the first intramolecular Stetter reaction was not reported until 1995 by Ciganek, which was 20 years after Stetter's seminal report. In this reaction, pre-catalyst **11** mediates cyclization of aldehyde **9** to chroman-4-one **10** (Scheme 1.5).¹⁶ Soon after, Enders reported the first asymmetric intramolecular Stetter reaction on the same substrate. With triazolium salt **12**, Enders achieved a 73% yield and 60% ee of the final chromanone product.¹⁷

Scheme 1.5: First Asymmetric Stetter Reaction

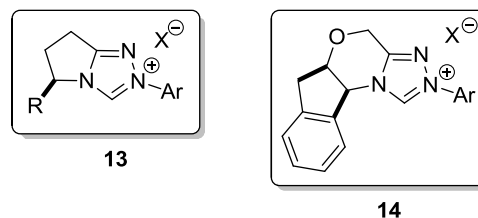
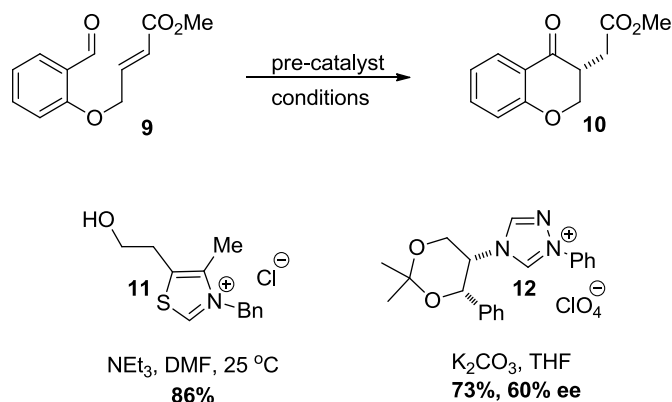
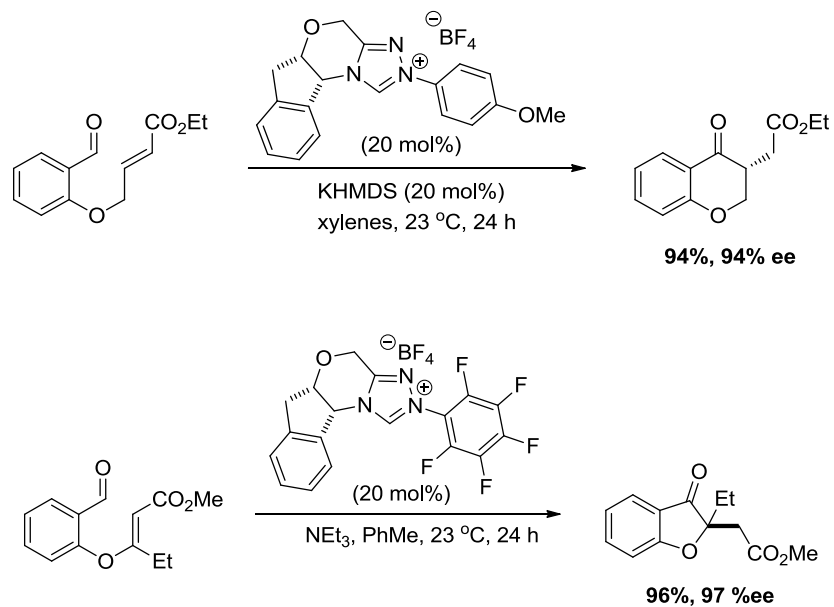


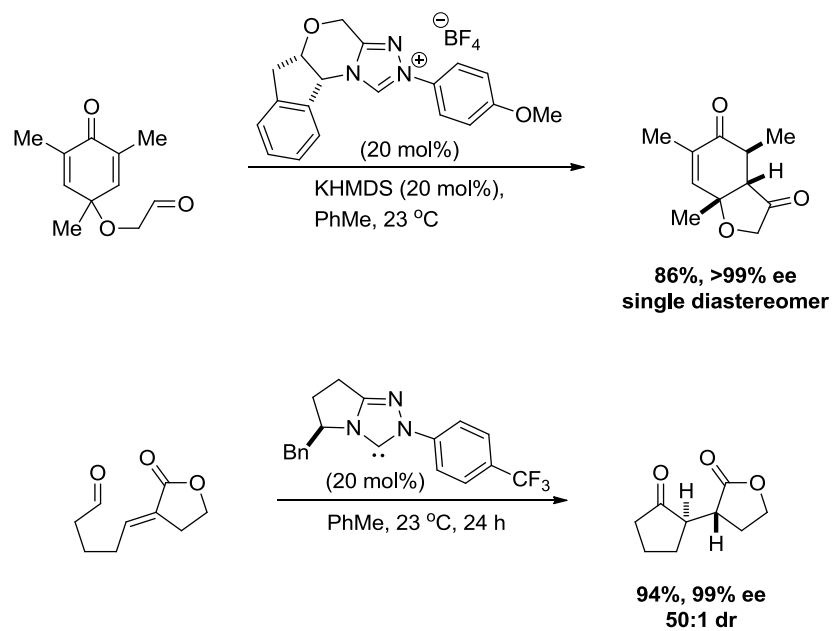
Figure 1.1: Rovis Triazolium Scaffolds

Since 2002, our group has made significant contributions to the advancement of the asymmetric Stetter reaction, particularly through development of novel chiral triazolium pre-catalysts. These can be categorized into two classes: aminoindanol-derived (**14**), and amino acid-derived (**13**) triazolium salts (Figure 1.1).^{18a,b} In a variety of intramolecular Stetter reactions, high-levels of enantioselectivity have been achieved using pre-catalysts of these general motifs. (Scheme 1.6).^{18a,c} These transformations can also be highly diastereoselective, providing Stetter products in excellent yield, enantioselectivity and diastereoselectivity (Scheme 1.7).^{19,1}

Scheme 1.6: Highly-Enantioselective Stetter Reactions Developed by the Rovis Group



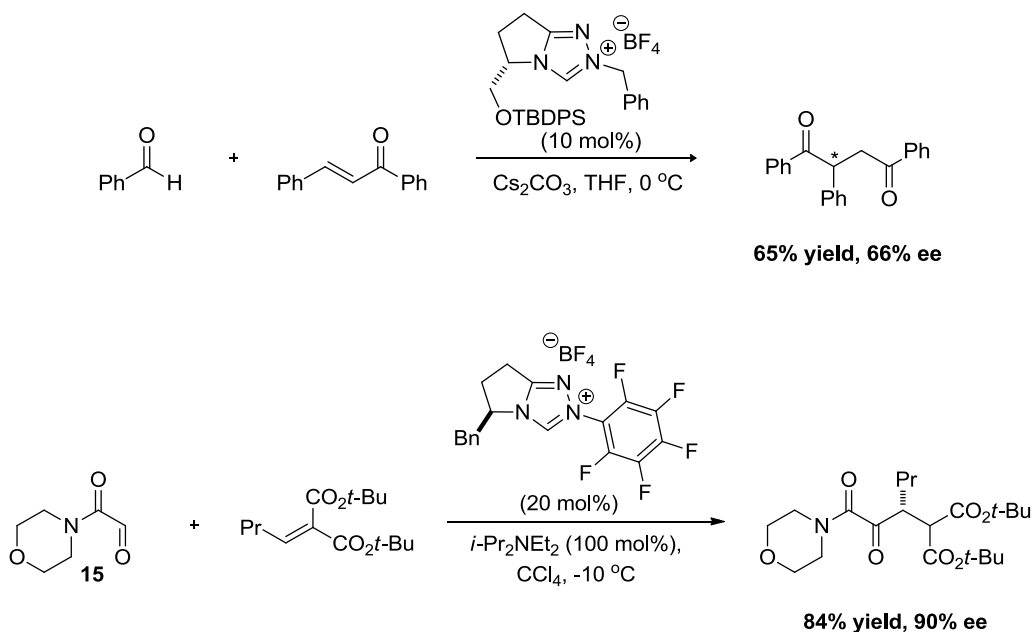
Scheme 1.7: Highly Enantio- and Diastereoselective Stetter Reactions



1.3.3 The Asymmetric Intermolecular Stetter Reaction

Despite the wealth of knowledge and success achieved in the asymmetric intramolecular Stetter reaction, transfer of this success to the asymmetric intermolecular variation has been slow to materialize. It wasn't until 2008 that two concurrent reports provided major advances in this area, one of which was submitted by our group. In this report, we showed that glyoxamide **15** could be coupled with alkylidenemalonates to access Stetter products in high yield and enantioselectivity (Scheme 1.8).^{20a} The other report was made by Enders who coupled aryl aldehydes with chalcone to form 1,4-diketones in good yields but modest ee's.²¹

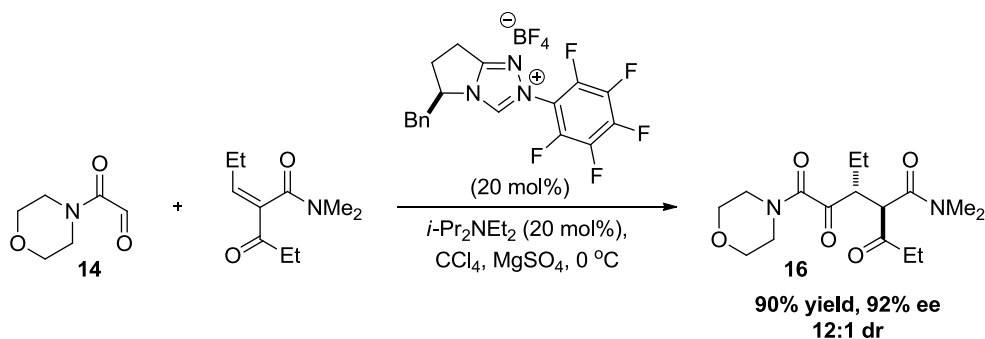
Scheme 1.8: The First Highly-Selective Asymmetric Intermolecular Stetter Reactions



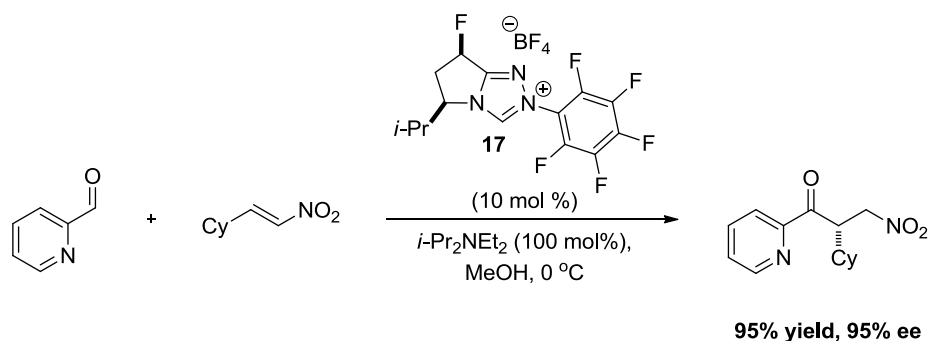
We later expanded our method to couple glyoxamide **15** with alkylidene ketoamides, which allowed us to successfully attain Stetter product **16** in high yield, high ee, and good dr (Scheme 1.9).^{20b} That same year, we issued a separate report that featured a novel fluorinated

bicyclic catalyst **17**, which efficiently and selectively couples a variety of aromatic aldehydes with β -substituted nitroalkenes in up to 95% yield and 95% ee (Scheme 1.10).²²

Scheme 1.9: An Enantio- and Diastereoselective Stetter Utilizing Alkylidene Ketoamides



Scheme 1.10: Asymmetric Stetter Reaction of Aromatic Aldehydes with Nitroalkenes



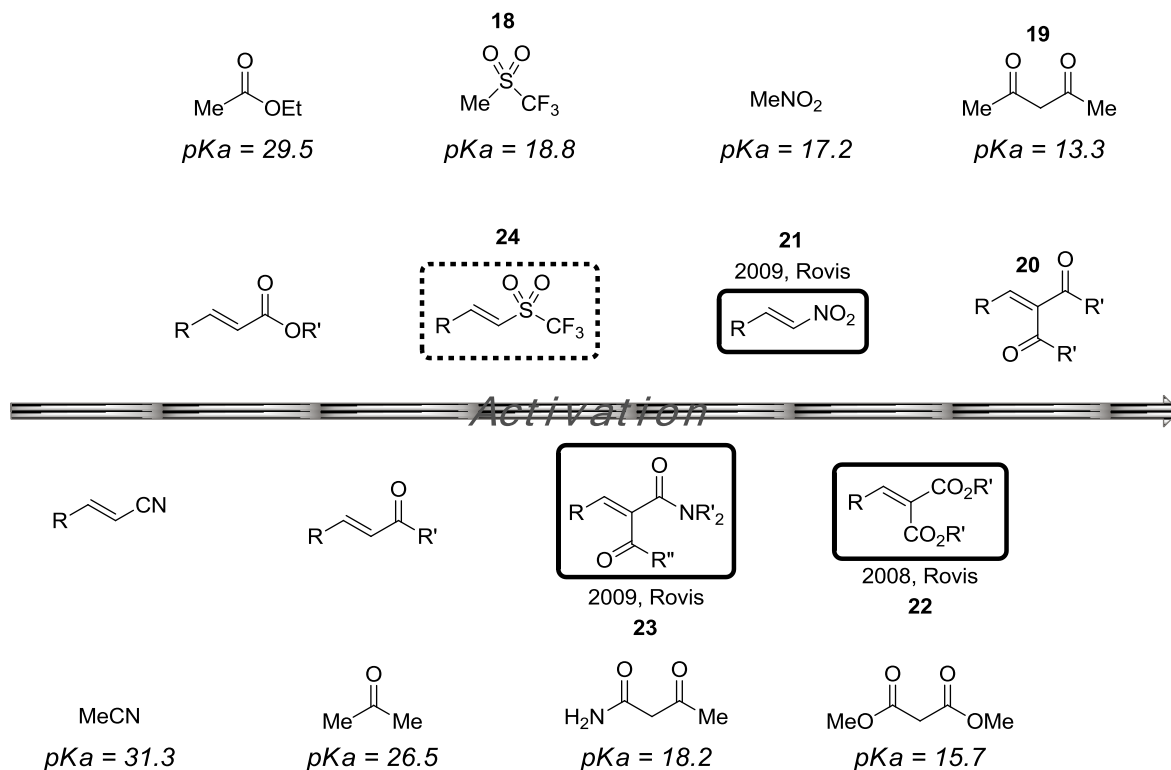
1.4 Development of an Asymmetric Intermolecular Stetter Reaction

1.4.1 Selection of an Appropriate Michael Acceptor

In the last several years, our group has made substantial progress in tackling difficult asymmetric intermolecular Stetter reactions. In general, we have had the most success with activated Michael acceptors such as alkylidenemalonates^{20a}, nitroalkenes,^{22,23} and alkylidene ketoamides^{20b}. Our goal has been to move toward less activated substrates as a way to access more general synthetic motifs.

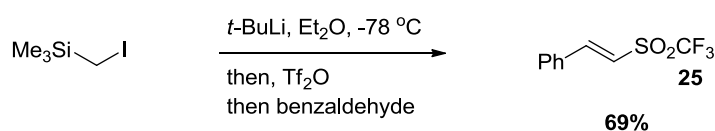
To evaluate the relative electrophilicity of Michael acceptors, we related thermodynamic acidity of α -protons of various functional groups (pK_a)²⁴ to the activation of the corresponding α,β -unsaturated Michael acceptor (Scheme 1.11). By considering that the pK_a of trifluoro(methylsulfonyl)methane **18**, for example, is 18.8, and dimethyl malonate **19** is 15.7,²⁶ we assume that alkylidene malonate **20** is a more activated Michael acceptor than vinyl trifluoromethanesulfone (triflone) **24**. We performed this analysis on a variety of Michael acceptors to form an approximate ranking of Michael acceptor activation. We sought to develop an intermolecular Stetter reaction with an acceptor that was both less-activated than substrates we had developed previously (**21,22**, and **23**), but also activated enough to provide ample opportunity for success. With these criteria in mind, we identified vinyl triflones **24** as the ideal substrates for further screening.

Scheme 1.11: Relative Activation of Michael Acceptors Based on pK_a

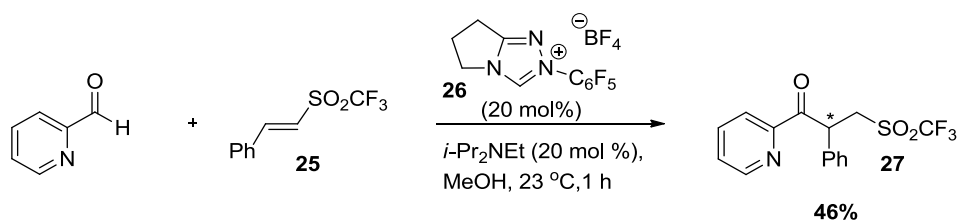


2-phenyl vinyl triflone (**25**) was prepared²⁵ (Scheme 1.12) and tested under similar Stetter reaction conditions to those developed by DiRocco for nitroalkenes (Scheme 1.10).²² When achiral triazolium pre-catalyst **26** was used, I was delighted to find that Stetter product **27** was obtained in 46% yield (Scheme 1.13). With this reactivity known, we immediately shifted our focus toward rendering this reaction enantioselective.

Scheme 1.12: Synthesis of Phenyl Vinyl Triflone



Scheme 1.13: A New Intermolecular Stetter Reaction



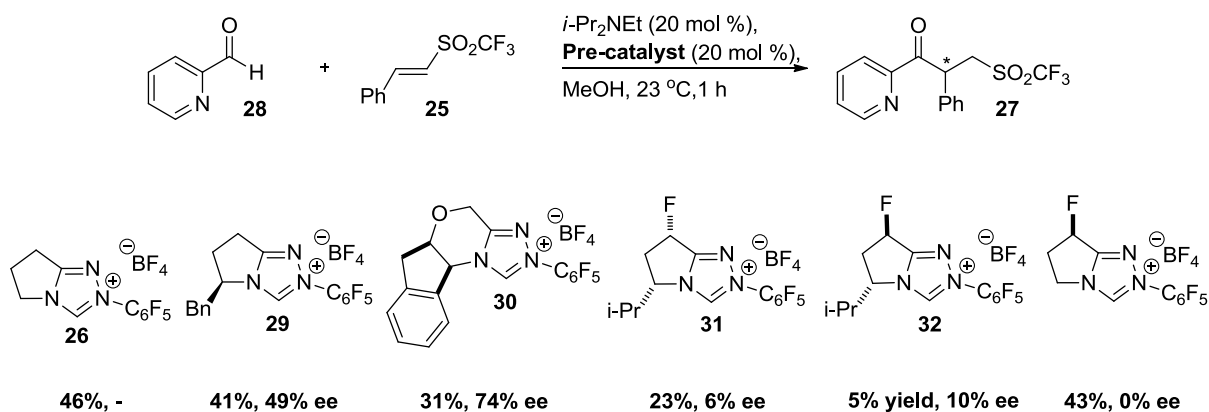
1.4.2 Optimization of Pre-Catalyst

A variety of chiral triazolium pre-catalysts that had previously been developed by our group were tested in the reaction (Scheme 1.14), and to our surprise, it was found that both the *cis*- (**31**) and *trans*-fluorinated triazoliums (**32**) lead to poor reactivity and selectivity. We had originally hypothesized that vinyl triflones would respond similarly to the Stetter reaction conditions developed for nitroalkenes, but this data indicated that the use of vinyl triflones in the Stetter reaction would require the development of a new set of reaction conditions.

Fortunately, other triazolium scaffolds that were developed within the Rovis group provided higher levels of reactivity and selectivity (Scheme 1.14). Based on the results for

triazolium **29** and **30**, bulkiness at the α -keto position resulted in lower yields but increased selectivity. This was consistent with our understanding of these catalysts as they apply to the intramolecular Stetter reaction.¹ Pre-catalyst **30** gave significantly higher levels of enantioselectivity than triazolium **29**. Therefore, further optimization was carried out using pre-catalyst **30**.

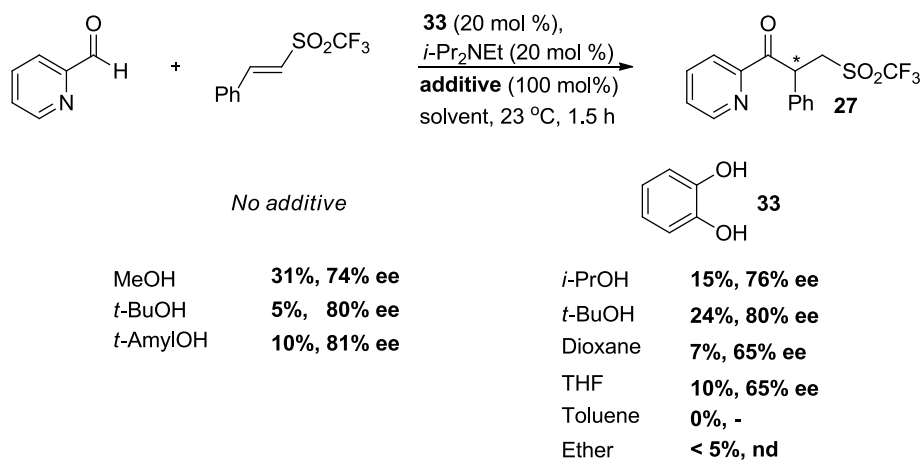
Scheme 1.14: Initial Catalyst Screen



1.4.3 Solvent Screen

In addition to pre-catalyst, solvent played a vital role in both reactivity and selectivity in the Stetter reaction. Bulkier and less polar alcoholic solvents generally favored selectivity at the cost of yield (Scheme 1.15). Non-alcoholic solvents, including THF, diethyl ether, toluene, and dioxanes lead to either trace amounts or no Stetter product. This is consistent with the intermolecular Stetter reaction of aldehydes with nitroalkenes, which also had a requirement for alcohol solvents.²²

Scheme 1.15: General Solvent Screen



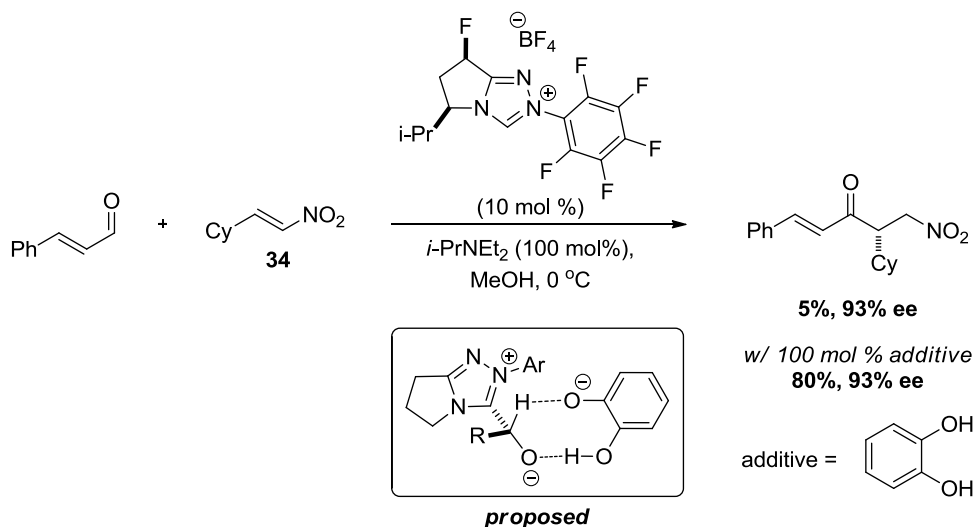
1.4.4 Effect of Catechol

Recently, DiRocco found that when 100 mol% of catechol (**33**) was added to the Stetter reaction of cinnamadehyde and nitroalkene **34**, there was a significant rate enhancement with full retention of selectivity (Scheme 1.16).²³ This prompted us to test the effect of catechol on the Stetter reaction of 2-pyridinecarboxaldehyde and 2-phenyl vinyl triflate. When catechol was added to this reaction with *t*-BuOH as the solvent, yield increased from 5% to 24% without effecting the selectivity (Scheme 1.15). Although the exact influence of catechol on this reaction is not well understood, it was proposed by DiRocco and Rovis that the catechol monoanion aids in the rate-limiting generation of the Breslow intermediate.¹⁵ Subsequently, optimization of the Stetter reaction involving phenyl vinyl triflate included 100 mol% of catechol as an additive.

t-BuOH was decidedly the best solvent of those tested when combined with catechol, yielding product **27** in 24% yield and 80% ee. In an effort to improve the yield and selectivity of this reaction, further optimizations were carried out.

Scheme 1.16: Catechol Increases Yields in the Intermolecular Stetter Reaction

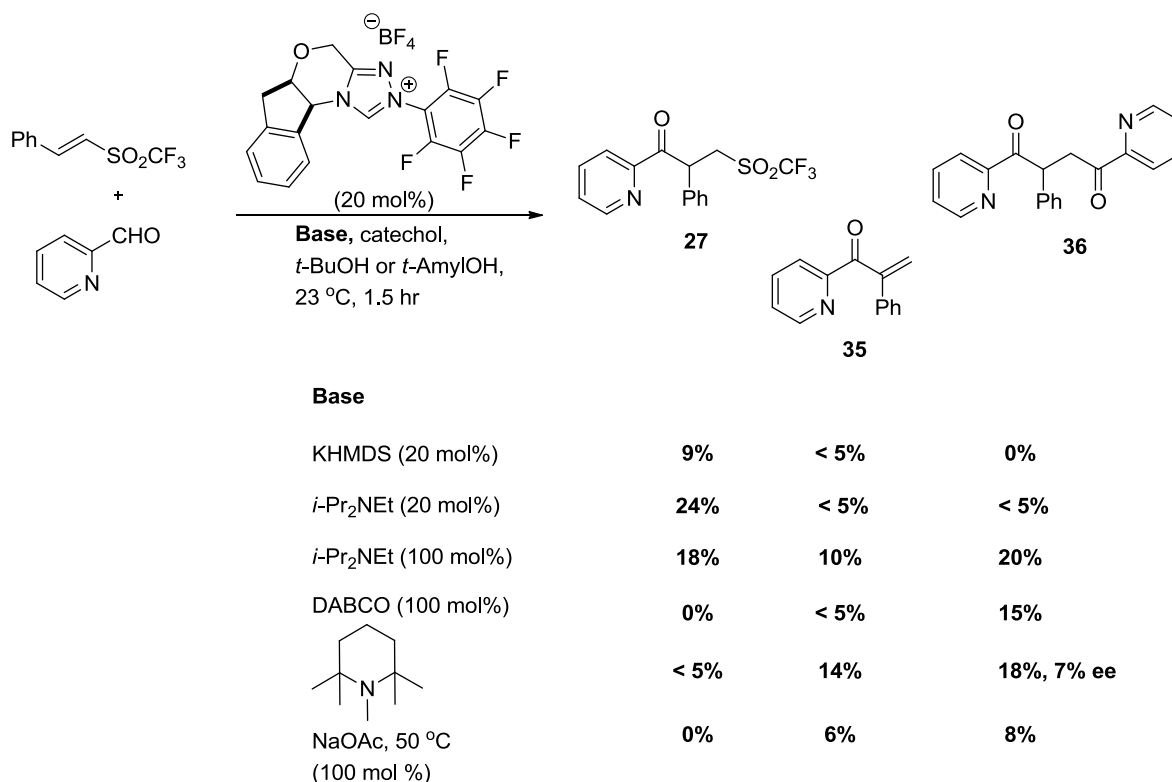
Dan DiRocco, 2011



1.4.5 Base Screen

One particular area of interest was the effect of base, especially after elimination product **35** was identified, as well as an additional byproduct **36** which arose from a competitive Stetter reaction with **2** (Scheme 1.17). A brief base screen revealed that base had a notable influence on product distribution. An increase in the quantity of base from 20 mol% *i*-Pr₂NEt to 100 mol% *i*-Pr₂NEt led to greater than 15% increase in side product **36** and greater than 5% increase in elimination product **35**. KHMDS as base resulted in poor yields of Stetter product, but no side products were observed. Other bulky amine bases such as pentamethylpiperidine and DABCO led to even higher proportions of elimination and side product **36**. Lastly, NaOAc was effective in this reaction with *t*-AmylOH, but required additional heat. At 50 °C, only a small amount of elimination product **35** and side product **36** were observed, and no Stetter product remained intact.

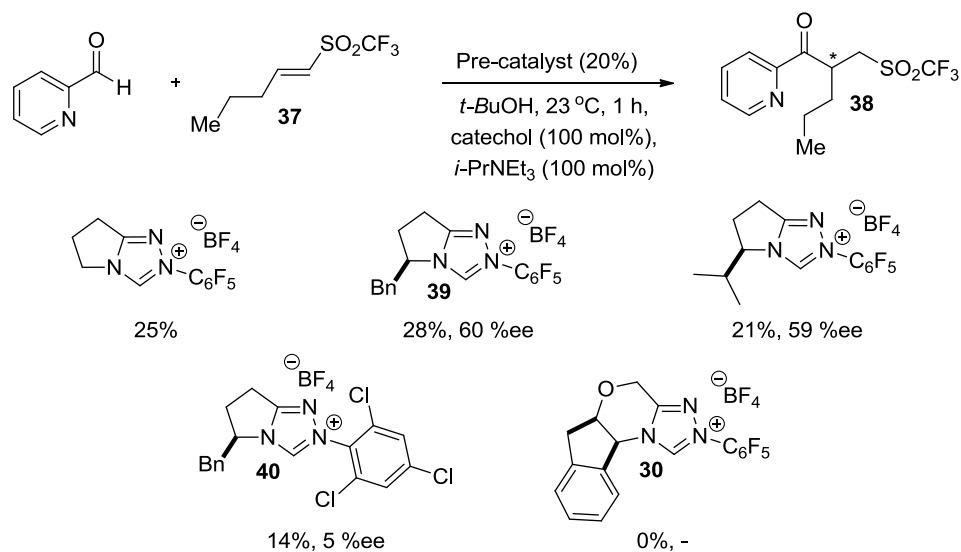
Scheme 1.17: Product Distribution Depends on Base



1.4.6 Attempts to Decrease Elimination

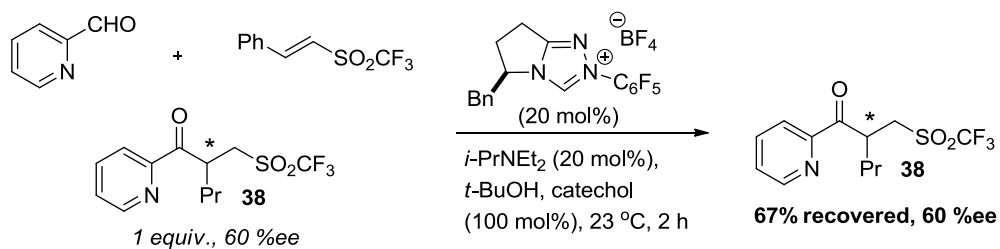
Based on the identified elimination pathway, as well as an expectation that the Stetter product would have a particularly acidic proton at the newly formed stereocenter, efforts were made to reduce the acidity at this position. 2-propyl-vinyl triflate **37** was prepared²⁵ and screened under the conditions shown in Scheme 1.18. When aminoindanol derived pre-catalyst **30** was used, no recognizable products were observed. This was unfortunate, because pre-catalyst **30** gave the highest selectivities when the more activated phenyl-vinyl triflate was used as the Michael acceptor. This study revealed that only the more reactive amino acid-derived pre-catalysts were effective, giving the best results with pre-catalyst **39** at 28% yield and 60% ee. Surprisingly, when the more sterically hindered but electronically similar 2,4,6-trichlorophenyl pre-catalyst **40** was employed, nearly racemic product was obtained.

Scheme 1.18: Catalyst Screen for Stetter Reaction with 2-Propyl-Vinyl Triflone



Despite the fact that Stetter product **38** was expected to have a less acidic α -proton than Stetter product **27**, elimination product was observed in all reactions involving triflone **37** and 100 mol% of base. We suspected that the presence of elimination product meant that epimerization might be a problem, lowering the observed ee's. To test for the epimerization of Stetter product **38** under the standard reaction conditions, 100 mol% of enantioenriched **38** was re-subjected to the Stetter reaction of phenyl vinyl triflone and 2-pyridinecarboxaldehyde (Scheme 1.19). After 2 hours, the re-subjected Stetter product was re-isolated with no decrease in enantioenrichment. From this data, we propose that when deprotonation of Stetter product occurs at the acidic α -proton, elimination proceeds more rapidly than re-protonation, meaning that epimerization of the product does not significantly influence selectivity in this reaction.

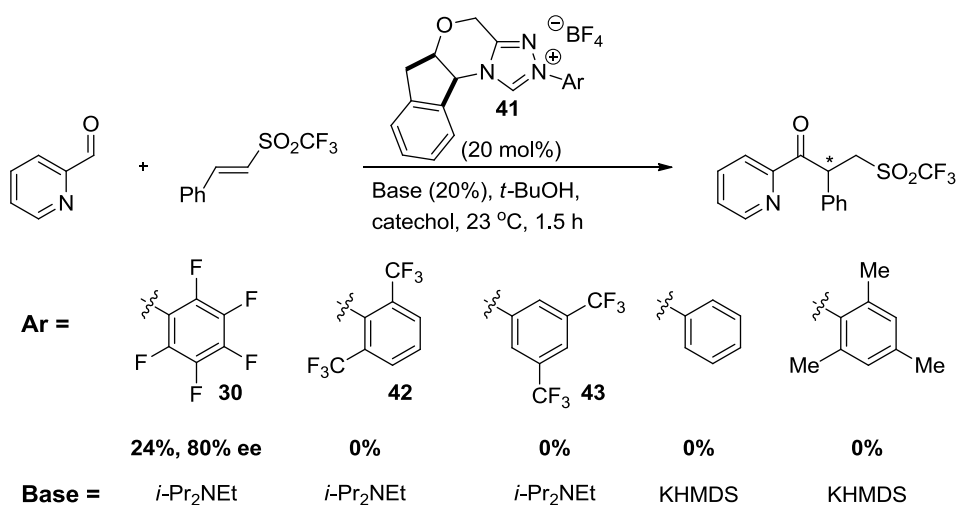
Scheme 1.19: Epimerization Experiment



1.4.7 Tuning the Catalyst *N*-Aryl Substituent

Pre-catalyst was again optimized for the Stetter reaction of 2-pyridinecarboxaldehyde and 2-phenyl vinyl triflate, this time modifying only the *N*-aryl group on the general pre-catalyst **41** (Scheme 1.20). Such changes to the electronics of the *N*-Aryl group on this particular scaffold are known to have a profound effect on the efficiency on the intramolecular Stetter.¹ Surprisingly, only the pentafluorophenyl pre-catalyst **30** leads to product formation. Even the similarly electron deficient bis(trifluoromethyl)phenyl catalysts **42** and **43** failed to yield product.

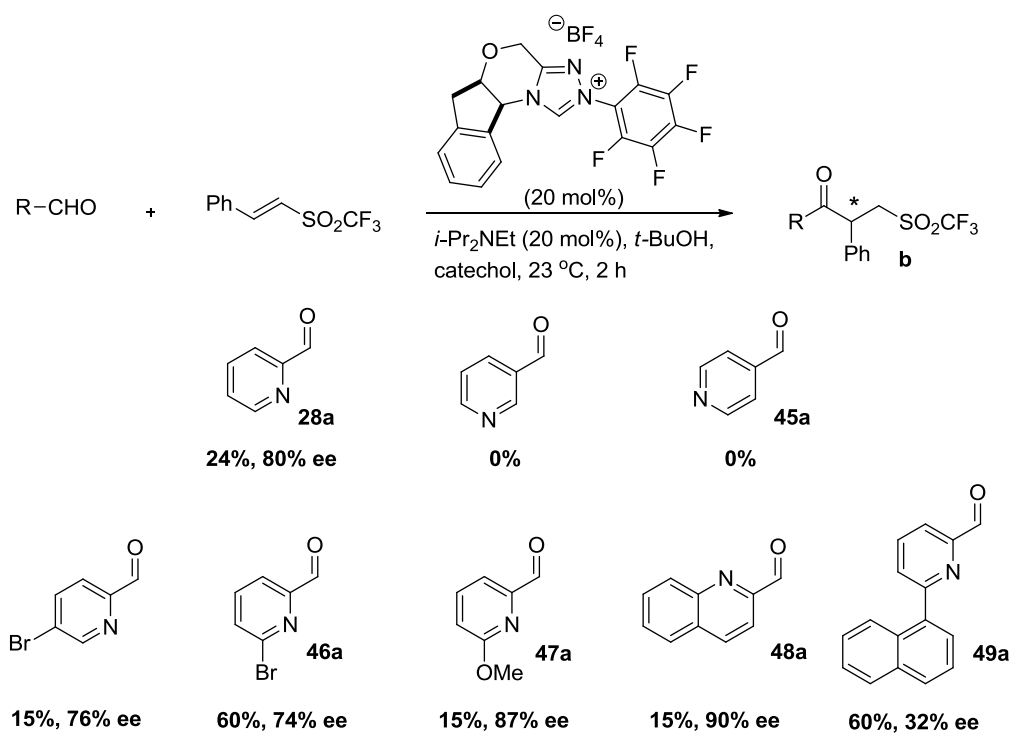
Scheme 1.20: Catalyst Optimization at the *N*-Aryl Group



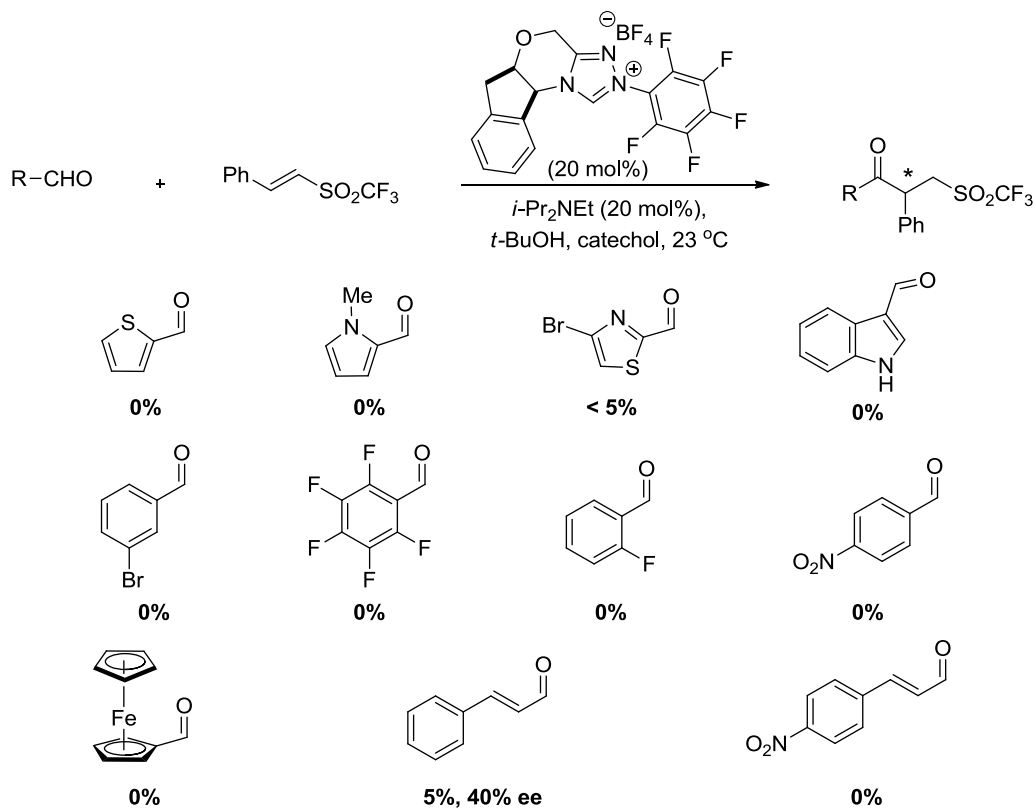
1.4.8 Aldehyde Scope

One other potential handle for boosting the low reactivity of this reaction was the aldehyde component (Scheme 1.21). Interestingly, moving the nitrogen in the pyridine ring of the carboxaldehyde from the ortho position (**28a**) to the electronically similar para position (**45a**) in pyridinecarboxaldehyde caused total loss of reactivity. Substitution at the 6-position of 2-pyridinecarboxaldehyde was beneficial for yields in the case of the 6-bromo-substituted aldehyde (**46a**), and both the methoxy-substituted aldehyde **47a** and 2-quinolinecarboxaldehyde **48a** gave significant increases in selectivity. A variety of other aromatic aldehydes were screened with very limited success (Scheme 1.22). Clearly, 2-pyridinecarboxaldehyde proves to be a privileged substrate in this reaction, the synthetic utility of which is consequently limited.

Scheme 1.21: Effect of Substitution on Parent Aldehyde



Scheme 1.22: Ineffective Aldehydes



1.5 Conclusion

In conclusion, a catalytic asymmetric intermolecular Stetter reaction has been developed for coupling 2-pyridinecarboxaldehydes and vinyl triflones. Our goal from the onset was to push the boundaries of reactivity toward the use of less-activated substrates. From that perspective, we have succeeded with our use of β-substituted vinyl triflones, which are among the least-activated Michael acceptors known to be competent in this reaction. Through our development of pre-activated NHC pre-catalysts, we expect that the scope of this reaction will be improved.

References

- ¹ Read de Alaniz, J.; Rovis, T. *Synlett* **2009**, 20, 1189.
- ² Seebach, D.; Corey, E.J. *J. Org. Chem.* **1975**, 4, 231.
- ³ Wohler, F.; Liebig, J. *Ann. Pharm.* **1832**, 3, 249.
- ⁴ Ukai, T.; Tanaka, R.; Dokawa, T. *J. Pharm. Soc. Jpn.* **1943**, 63, 296.
- ⁵ Breslow, R. *J. Chem. Soc.* **1958**, 80, 995.
- ⁶ (a) Sheehan, J. C.; Hunnemann, D. H. *J. Am. Chem. Soc.* **1966**, 88, 3666. (b) Sheehan, J. C.; Hara, T. *J. Org. Chem.* **1974**, 39, 1196.
- ⁷ Enders, D.; Breuer, K.; Teles, J. H. *Helv. Chim. Acta* **1996**, 79, 1217.
- ⁸ Knight, R. L.; Leeper, F. J. *Tet. Lett.* **1997**, 38, 3611.
- ⁹ Dvorak, C.; Rawal, V. *Tet. Lett.* **1998**, 39, 2925.
- ¹⁰ Knight, R. L.; Leeper, F. J. *Chem. Soc., Perkin Trans.1* **1998**, 1891.
- ¹¹ Enders, D.; Kallfass, U. *Angew. Chem. Int. Ed.* **2002**, 41, 1743.
- ¹² Baragwanath, L.; Rose, C.; Zeitler, K.; Connon, S. *J. Org. Chem.* **2009**, 74, 9214.
- ¹³ Stetter, H.; Kuhlmann, H. In *Organic Reactions*, Vol. 40; Paquette, L. A., Ed.; Wiley & Sons: New York, **1991**, 407.
- ¹⁴ "Pfizer 2008 Annual Report". Pfizer. 23 April 2009.
<http://media.pfizer.com/files/annualreport/2008/annual/review2008.pdf>. Retrieved 7 August 2009.
- ¹⁵ Moore, J.; Silvestri, A. P.; Read de Alaniz, J.; DiRocco, D. A.; Rovis, T. *Org. Lett.* **2011**, 13, 1742.
- ¹⁶ Ciganek, E. *Synthesis* **1995**, 1311.
- ¹⁷ Enders, D.; Breuer, K.; Runsink, J.; Teles, J. H. *Helv. Chim. Acta.* **1996**, 79, 1899.
- ¹⁸ (a) Kerr, M. S.; Read de Alaniz, J.; Rovis, T. *J. Am. Chem. Soc.* **2002**, 124, 10298. (b) Kerr, M. S.; Rovis, T. *Synlett* **2003**, 1934. (c) Kerr, M. S.; Rovis, T. *J. Am. Chem. Soc.* **2004**, 126, 8876.
- ¹⁹ Liu, Q.; Rovis, T. *J. Am. Chem. Soc.* **2006**, 128, 2552.
- ²⁰ (a) Liu, Q.; Perreault, S.; Rovis, T. *J. Am. Chem. Soc.* **2008**, 130, 14066. (b) Liu, Q.; Rovis, T. *Org. Lett.*, **2009**, 11, 2856-2869.
- ²¹ Enders, D.; Han, J.; Henseler, A. *Chem. Commun.* **2008**, 3989.
- ²² DiRocco, D.; Oberg, K.; Dalton, D.; Rovis, T. *J. Am. Chem. Soc.* **2009**, 131, 10872.
- ²³ DiRocco, D. A.; Rovis, T. *J. Am. Chem. Soc.* **2011**, 10402.
- ²⁴ Fleming, I. *Molecular Orbitals and Organic Chemical Reactions*, Ref. ed.; John Wiley & Sons: Chichester, 2010.

²⁵ Mahadevan, A.; Fuchs, P. L. *Tetrahedron Lett.* **1994**, 35, 6025-6028.

²⁶ All pKa values are for DMSO as the solvent.

Chapter 2

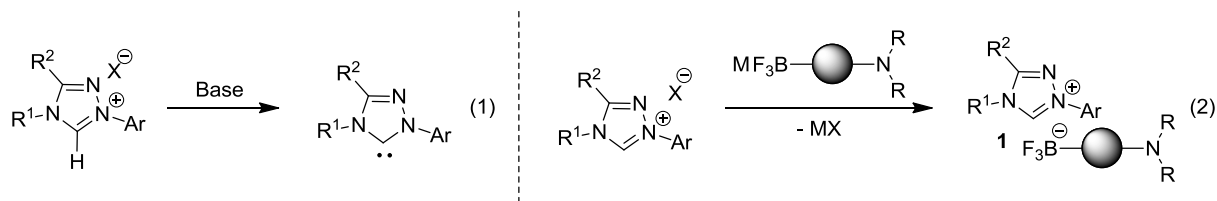
The Development of Base-Activated Organocatalysts

2.1 Introduction

The most convenient way to generate an *N*-Heterocyclic carbene is by deprotonation of a corresponding azolium salt (Scheme 2.1, eq. 1). From these bench-stable pre-catalysts, the free-carbene is usually generated by adding a stoichiometric amount of strong base such as a metal hydride, potassium *t*-butoxide, a metal bis(trimethylsilyl)amide, or in less extreme cases, a tertiary amine.¹⁻³ Unfortunately, a strong base can be incompatible with functional groups on the carbene itself, can lead to epimerization or elimination of products or reactant, and can participate in additional undesired side-reactions. These concerns are particularly relevant for the catalytic enantioselective Stetter reaction (See Chapter 1). In the Stetter reaction, it is advantageous to generate the catalytically active free carbene using milder conditions.

As illustrated in Scheme 2.1, we sought to prepare an NHC pre-catalyst with a base covalently attached to the counterion. By having the base electrostatically bound and in close proximity to an acidic triazolium moiety, we expected an increase in the concentration of catalytically active free-carbene. Likewise, we expected that the base would be less likely to participate in unwanted side reactions due to the added bulk of the electrostatically bound triazolium cation. We believed that this would be a worthwhile approach to solving the problem of low-reactivity and limited aldehyde scope in the intermolecular Stetter reaction of aldehydes and vinyl triflones. In addition, this system has the opportunity to increase the catalytic efficiency of a broad range of triazolinylidene catalysts.

Scheme 2.1: Proposed Counterion Exchange to Form a Pre-Activated NHC Catalyst Precursor

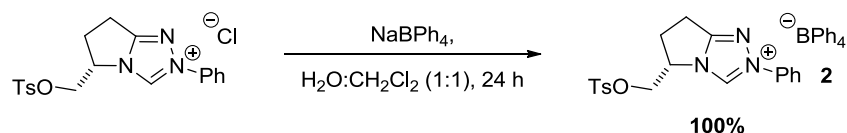


2.2 Counterion Exchange in a Biphasic System

Our initial attempts at counterion exchange were aimed toward partitioning a starting counterion X^- (Scheme 2.1, eq. 2) into the aqueous layer of biphasic system, resulting in base-activated triazolium salt **1** being dissolved in the organic layer. We hypothesized that this exchange would be particularly favorable when the byproduct MX is a highly water soluble inorganic compound, and the resulting triazolium salt **1** features a “greasy” anion to help increase its solubility in organic media. Based on Javier Read de Alaniz’s precedent for a quantitative yielding exchange of chloride for tetraphenylborate (Scheme 2.2), we anticipated that exchange with the more common triazolium tetrafluoroborate catalyst precursors would also be facile.⁴

Scheme 2.2: Counterion Exchange to Form Triazolium Tetraphenylborate **2**

Javier Read de Alaniz, 2006

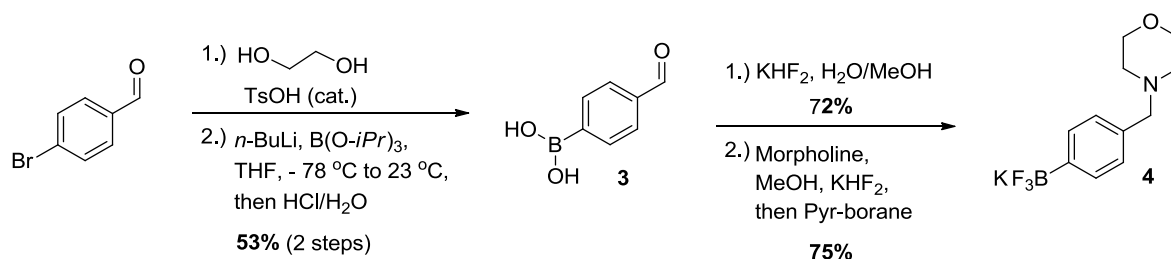


With these considerations in mind, we explored the use of potassium aryltrifluoroborates (Scheme 2.3) as counterion exchange partners, in part due to their being air-stable and crystalline solids, as well as their straightforward synthesis from a corresponding boronic acid.⁵ We also

anticipated that aryltrifluoroborates would stabilize triazolium salts similarly to the very commonly used tetrafluoroborate anion.

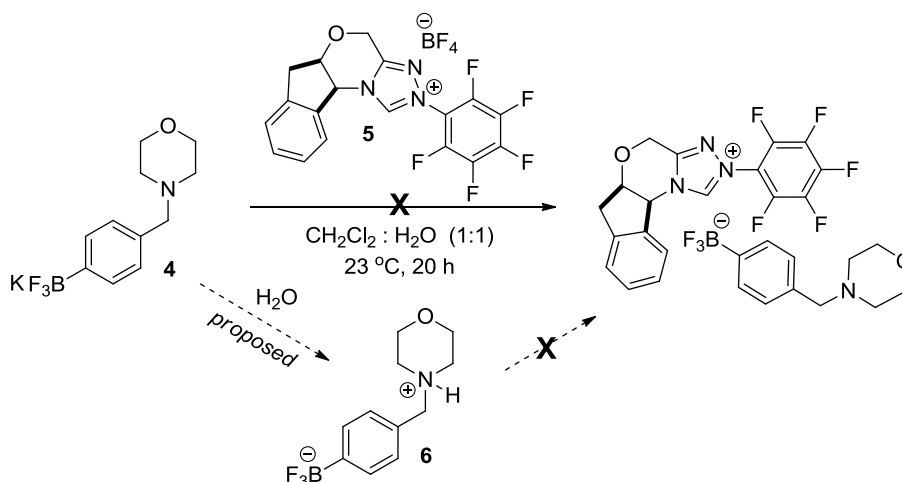
Potassium aryltrifluoroborate **4** was prepared in five steps from *p*-bromobenzaldehyde (Scheme 2.3).^{6,7a} This route was particularly advantageous due to the variety of possible amines that could be incorporated via reductive amination.⁷ With versatility at the amine functionality, it should be possible to fine-tune key properties of these potential counterions, such as their basicity.

Scheme 2.3: Synthesis of Aryltrifluoroborate 4 Via a Reductive Amination Route



The biphasic exchange reaction of potassium aryltrifluoroborate **4** and pre-catalyst **5** (Scheme 2.4) was attempted using a solvent system of CH₂Cl₂ : H₂O (1:1). After stirring for 20 hours at ambient temperature, the organic layer was separated, the aqueous layer was extracted with CH₂Cl₂, and the combined organic phase was dried over Na₂SO₄. Unfortunately, only pre-catalyst **5** was reisolated from the organic extract. We suspect that under these conditions, **4** was protonated by H₂O to form a highly water-soluble internal ammonium salt **6**. If this occurred, the fact that we did not observe counterion exchange could be rationalized.

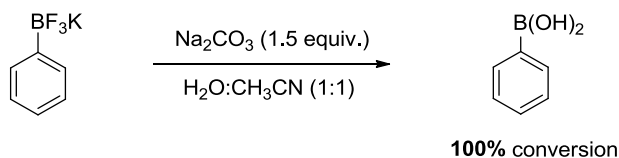
Scheme 2.4: Initial Attempt at Biphasic Counterion Exchange Reaction



To diminish the possibility of forming **6** in a biphasic mixture, we utilized alkaline buffers as the aqueous phase. Both a pH=10 and a pH=12 buffer system were tested,⁸ but with both of these buffer systems, triazolium salt **5** was still the only species to be reisolated from the organic extract in considerable quantities.⁹ In both of these cases, the alkaline buffer likely contributed to decomposition of the of the aryltrifluoroborate. This is consistent with the Hutton group's finding that basic H₂O/CH₃CN leads to complete hydrolysis of potassium phenyltrifluoroborate (Scheme 2.5).¹⁰

Scheme 2.5: Hydrolysis of Phenyl Trifluoroborate Under Basic Conditions

Alexander Yuen and Craig A. Hutton, 2005

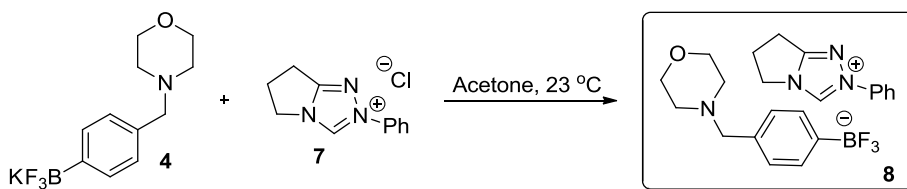


2.3 Counterion Exchange in Organic Media

Because of the difficulties we encountered with a biphasic solvent system, we pursued an alternate approach to tackle the problem of counterion exchange. We turned our focus toward devising a method that would force the precipitation of either the product triazolium salt or the byproduct inorganic salt. Because of our preference to abstain from using aqueous solvent, we chose to pursue the precipitation of an inorganic salt from organic media.

Our initial consideration was the use of aryltrifluoroborate **4** (Scheme 2.6), and in particular, how we could introduce an anion that would claim potassium from solution. Of the various triazolium salts available to us, the most common counterion was tetrafluoroborate, and less commonly chloride, bromide, and iodide. Triazolium chloride **7** was the first tested due to the very-low solubility of KCl in acetone (9.1×10^{-4} g/kg).¹¹ When triazolium chloride **7** was treated with aryltrifluoroborate **4** in acetone, we gratifyingly observed clean conversion to the newly formed triazolium salt **8** in 90% yield.

Scheme 2.6: Counterion Exchange to Form Base-Activated NHC Pre-Catalyst 8

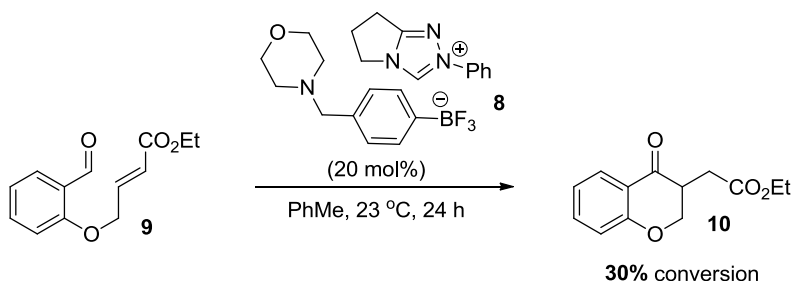


2.4 Base-Activated NHC Pre-Catalysts and the Intramolecular Stetter Reaction

Although the ^1H NMR analysis of **8** was identical to the overlaid spectra of the two starting materials, there was compelling evidence that counterion exchange did occur. For instance, the final product was highly-soluble in acetone, while the starting triazolium **7** was almost entirely insoluble. Additionally, when 20 mol% of **8** was added to aldehyde **9** in toluene

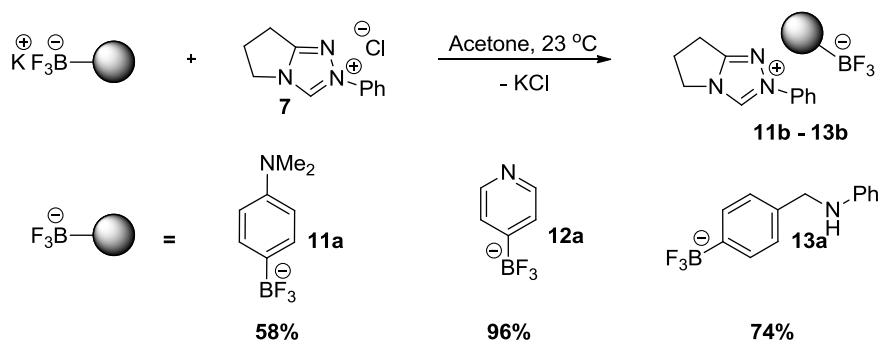
with no additional base present, I was delighted to find that pre-catalyst **8** was catalytically active in the intramolecular Stetter reaction, resulting in 30% conversion to chroman-4-one **10** (Scheme 2.7). This represents proof of concept that base-activated NHC pre-catalysts can catalyze the Stetter reaction without additional base.¹²

Scheme 2.7: Screen for Efficiency of Pre-catalyst **8** in an Intramolecular Stetter Reaction



With hopes that we could improve the level of reactivity observed by matching triazolium **7** with an appropriately matched base, we attempted counterion exchange with a series of other aryltrifluoroborates. Using the same exchange conditions from Scheme 2.6, three other base-activated pre-catalysts were prepared in 58 – 96% yield (Scheme 2.8). Of these, triazolium **11b** was slowly crystallized from acetone to yield single crystals suitable for X-ray crystallography. A crystal structure of **11b** (Figure 2.1) was obtained, which provides conclusive evidence that the method represented in Scheme 2.8 for counterion exchange is valid.

Scheme 2.8: Synthesis of New Base-Activated NHC Precursors



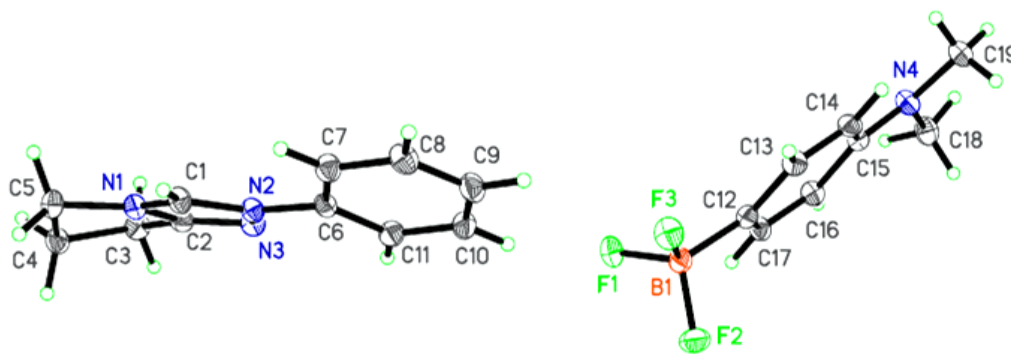
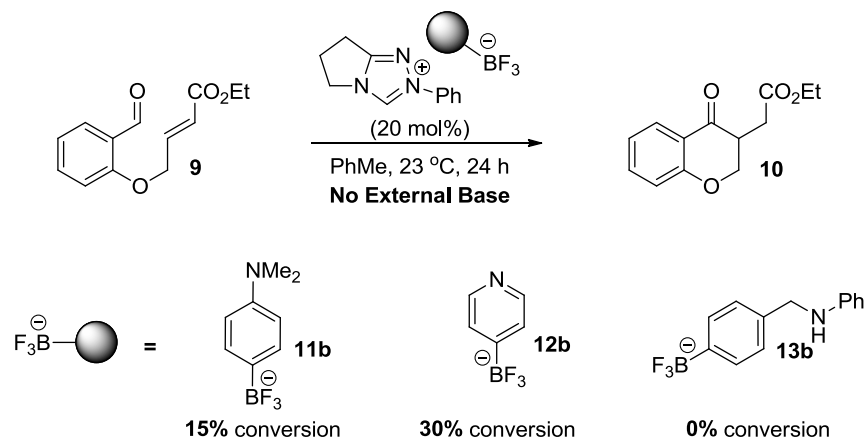


Figure 2.1: Crystal Structure of Base-Activated Pre-catalyst **11b**

Pre-catalysts **11b** - **13b** were then tested for their efficiency in the intramolecular Stetter reaction. By employing the same reaction conditions as listed in Scheme 2.7, we once again observed modest to low conversion in the case of pre-catalyst **11b** and **12b**, and undetectable conversion in the case of **13b** (Scheme 2.9).

Scheme 2.9: Pre-Activated NHC pre-catalyst in the Intramolecular Stetter Reaction



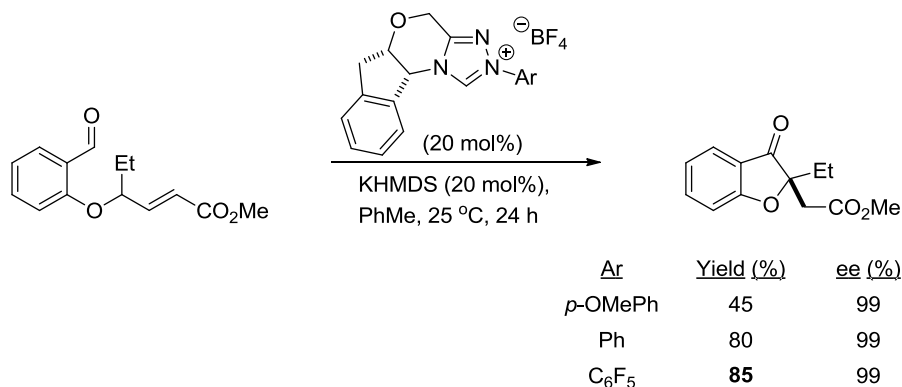
2.5 Toward Electron Deficient Base-Activated Pre-Catalysts

2.5.1 Attempts at a Direct Synthesis

Although we were pleased to observe Stetter reactivity in the case of triazolium salts **8**, **11B**, and **12B**, albeit modest, we were interested in increasing the efficiency of these pre-catalysts in the Stetter reaction through simple modifications. In particular, we directed our attention toward replacing the *N*-phenyl group of the triazolium cation for an electron withdrawing aryl group, such as pentafluorophenyl, or 2,4,6-trichlorophenyl. Triazolium pre-catalysts that feature electron withdrawing aryl groups are known to be particularly reactive in the both the intra- and intermolecular Stetter reaction.^{13,14} In fact, our group has demonstrated that a strong electron-withdrawing group on the triazole ring is the principal catalyst feature for achieving high reactivity in the Stetter reaction.¹⁵

Table 2.1: Effect of Aryl Group Electronics

Mark Kerr, 2006

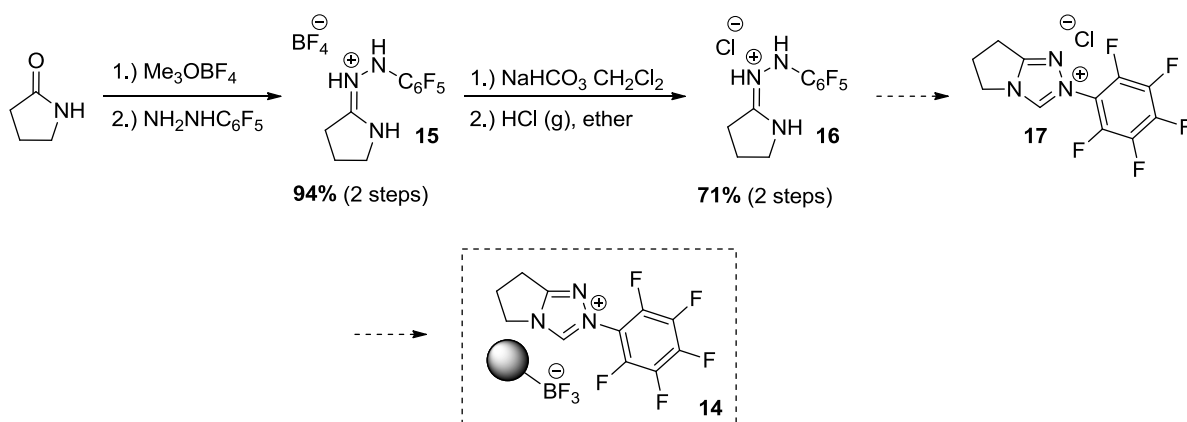


As a way to access an electron-deficient pre-catalyst with the general structure of **14** (Scheme 2.11), we set out to prepare the previously unknown pentafluorophenyl triazolium **17**. With this, we planned to attempt counterion exchange with aryltrifluoroborates as shown in

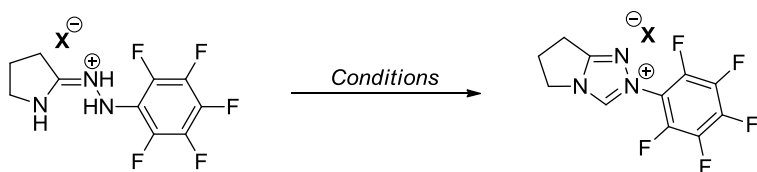
Scheme 2.8. We initiated the synthesis of **17** by first activating 2-pyrrolidinone with methyl Meerwein's reagent, and subsequently added pentafluorophenyl hydrazine to form hydrazide **15**.¹⁶ To this was added NaHCO₃ to yield a neutral hydrazone, which was acidified using HCl gas to afford hydrazide chloride **16** as a white precipitate (Scheme 2.11).

Although **15** readily undergoes cyclization to form **17** (as the tetrafluoroborate salt) when heated with (EtO)₃CH in refluxing chlorobenzene (Scheme 2.12, Entry 1),¹⁶ hydrazide **16** did not cyclize under the same conditions (Entry 2). When **16** was heated at 80 °C with trimethylorthoformate in a sealed tube, no reaction occurred (Entry 4), but when heated in a sealed tube at 120 °C for 1 hour, complete decomposition of the starting material was observed (Entry 3). A variety of other conditions were explored, including adjustments to reaction time and temperature, solvent additives, and the addition of either catalytic or stoichiometric quantities of anhydrous HCl. However, all attempts at cyclization were met without success.

Scheme 2.11: Toward the Synthesis of Triazolium Chloride 17



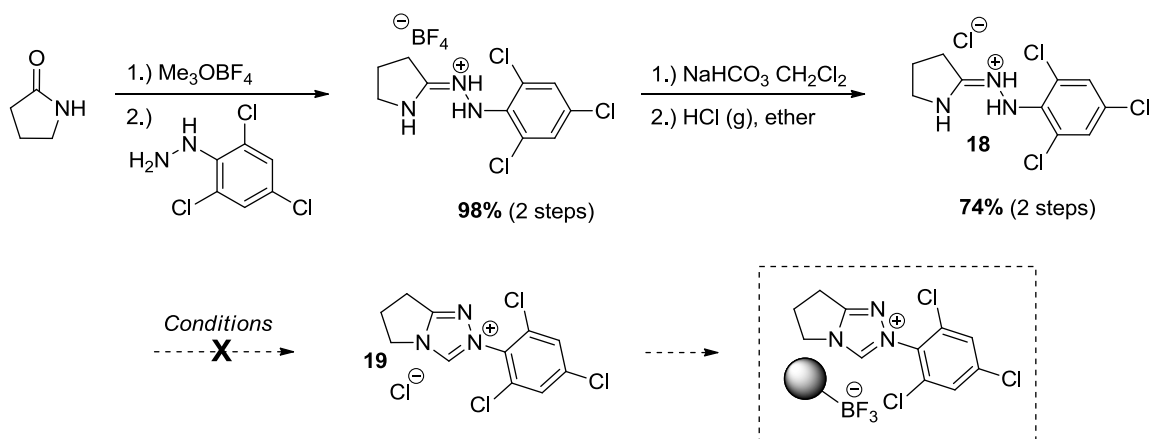
Scheme 2.12: Attempts at Cyclization of Hydrazide **16**



	Method	Entry	X	Result
A:	HC(OEt) ₃ , Chlorobenzene, 130 °C, 72 h;	A	1	BF ₄ ⁻ 75% yield ¹⁶
B:	(MeO) ₃ CH, sealed tube, 120 °C, 1 h;	A	2	Cl ⁻ NR
C:	(MeO) ₃ CH, sealed tube, 80 °C, 12 h	B	3	Cl ⁻ decomposition
		C	4	Cl ⁻ NR

We also attempted to prepare the previously unknown *N*-2,4,6-trichlorophenyl pre-catalyst **19**, commencing with the preparation of hydrazide chloride **18** (Scheme 2.13). With **18** in hand, we tested an array of cyclization techniques similar to those discussed for hydrazide **16**. Unfortunately, we have not yet succeeded in forming pre-catalyst **19**. Although we do not fully understand why the hydrazide chloride salts have been difficult to cyclize, we suspect that these salts may be more hygroscopic than the corresponding hydrazide tetrafluoroborates. If these hydrazides do retain added moisture, it is conceivable that cyclization may be inhibited.¹⁶

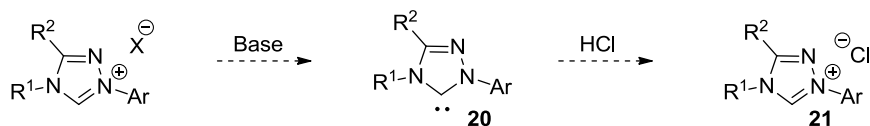
Scheme 2.13: Toward the Synthesis of Triazolium Chloride **19**



2.5.2 Triazolium Chloride Salts by Counterion Exchange

Due to the difficulties we encountered in cyclizing hydrazide chlorides, we turned our attention toward developing an alternate route for obtaining an electron-deficient triazolium chloride salt. To avoid a problematic cyclization step, we envisioned performing a counterion exchange by protonation of a free-carbene with hydrogen chloride (Scheme 2.14).

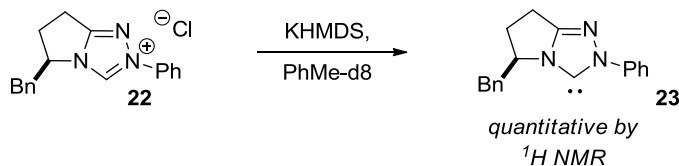
Scheme 2.14: Proposed Counterion Exchange by Protonation of a Free-Carbene



In a previous report by Read de Alaniz, free-carbene **23** was generated quantitatively by treating pre-catalyst **22** with one equivalent of KHMDS in deuterated toluene (Scheme 2.15).⁴ Free-carbene **23** was also obtained from the tetrafluoroborate salt of pre-catalyst **22** using the same route (Scheme 2.15). By passing the latter carbene solution through a syringe filter, all traces of KBF₄ were removed.^{17,18} We believed that we could utilize the insolubility of KBF₄ to isolate a free-carbene in the form of **20**, which could then be protonated to form a triazolium chloride salt.

Scheme 2.15: Formation of an Isolable Free-Carbene.

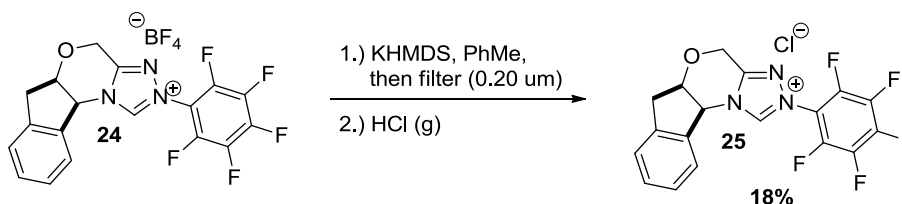
Javier Read de Alaniz, 2006



Our ultimate goal was to access a base-activated aminoindanol-derived pre-catalyst from triazolium chloride **25** (Scheme 2.16). We chose this particular scaffold because our group has frequently observed excellent enantioselectivity in the asymmetric intra- and intermolecular Stetter reaction using pre-catalyst **25**, but it is often a less-reactive catalyst than amino-acid derived scaffolds.¹⁹ For example, pre-catalyst **24** afforded the highest ee's for the intermolecular Stetter reaction of phenyl vinyl triflone with 2-pyridinecarboxaldehydes, but it failed to afford Stetter product when the less activated *n*-propyl vinyl triflone was used (see 1.4.6). We believed that installing an electrostatically-bound base to the triazolium pre-catalyst could improve the yield and substrate scope of this reaction.

To form triazolium **25**, one equivalent of KHMDS was added to a slurry of **24** in toluene, and the resulting carbene solution was quickly passed through a syringe filter. Dry hydrogen chloride²⁰ was bubbled through the filtered carbene solution under an inert atmosphere. After concentrating the reaction mixture and trituration using a small amount of acetone, triazolium **25** was collected in 18% yield as a white powder.

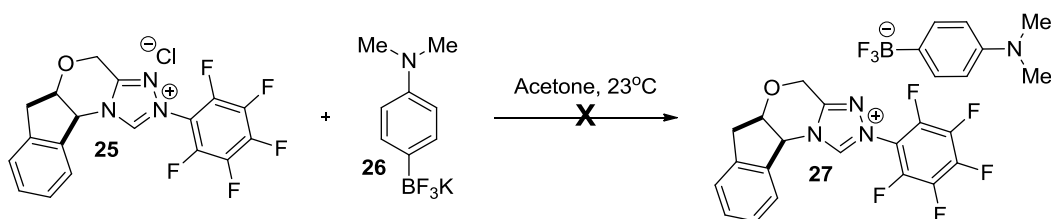
Scheme 2.16: Synthesis of Triazolium Chloride 25



The counterion exchange to form pre-activated catalyst precursor **27** was attempted by treating triazolium chloride **25** with an equimolar portion of aryltrifluoroborate **26** in acetone (Scheme 2.17). Unfortunately, counterion exchange did not take place.^{21,22} It is not clear why the exchange did not proceed as it did for triazolium **7** (Scheme 2.8), but it is possible that the more

electron-withdrawing triazolium **25** binds chloride more closely than triazolium **7**, creating a higher energy-barrier for counterion exchange.

Scheme 2.17: Failed Counterion Exchange with Electron Deficient Pre-Catalyst **25**

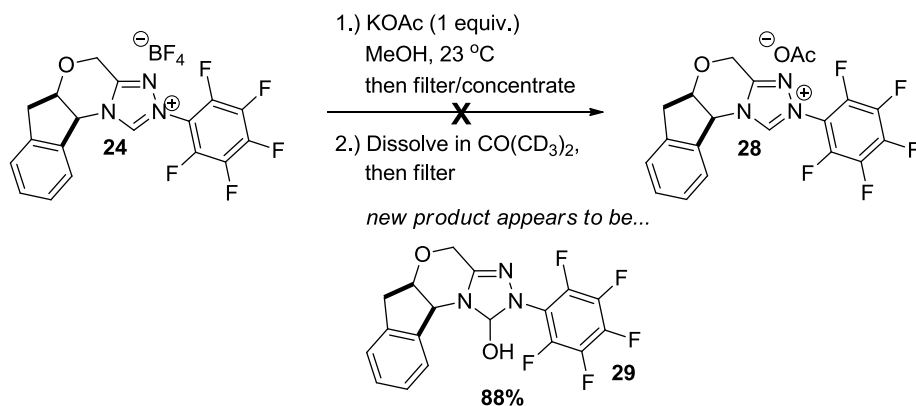


2.6 Elucidation of Pre-Catalyst Decomposition Pathways

2.6.1 Pre-Catalyst Hydration and the Stetter Reaction

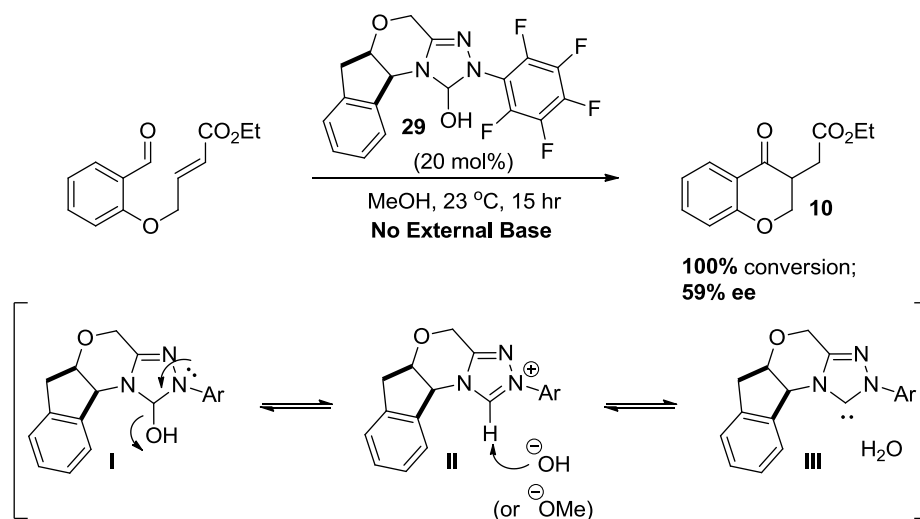
During investigations toward counterion exchange in organic media, we sought to perform a counterion exchange to generate triazolium acetate **28**. Our first attempt at such an exchange is shown in Scheme 2.18, where one equivalent each of KOAc and triazolium **24** were dissolved in methanol and stirred overnight. The solution was then concentrated, re-dissolved in *d*₆-acetone, and filtered to remove any remaining KOAc. The resulting ¹H NMR was not consistent with triazolium acetate **28**, but a new product had been formed. The mass spectra indicated that the major product was triazolium hydrate **29**.²³

Scheme 2.18: Formation of Triazolium Hydrate **29**



When hydrate **29** was subjected to standard intramolecular Stetter reaction conditions (Scheme 2.19), full conversion to chroman-4-one **10** was observed with moderate levels of enantioselectivity. In order to obtain the catalytically active free-carbene **I**, it is assumed that hydroxide must first be eliminated to form triazolium **II** with subsequent deprotonation. It is not clear if hydrate **29** will be synthetically useful as a pre-catalyst, but it may prove to be an important catalytic resting state to consider for organocatalytic reactions involving electron-poor azoliums.

Scheme 2.19: Triazolium Hydrate **29 as a Pre-Catalyst**



2.6.2 An Unexpected S_NAR Decomposition Pathway

In an effort to prepare larger quantities of hydrate **29**, the reaction shown in Scheme 2.18 was scaled to 0.8 grams of starting triazolium **24** (Scheme 2.20). However, the outcome was quite different than what was obtained on smaller scale. From the crude ¹H NMR, it appeared that the reaction had only reached 20% conversion. After column chromatography, hydrate **29** was obtained in low yield, but an interesting minor product was isolated and characterized by X-

ray crystallography (Figure 2.2).²⁴ This product represents a fascinating, if not important NHC carbene decomposition pathway.²⁵

Scheme 2.20: Unexpected Catalyst Decomposition Product 30

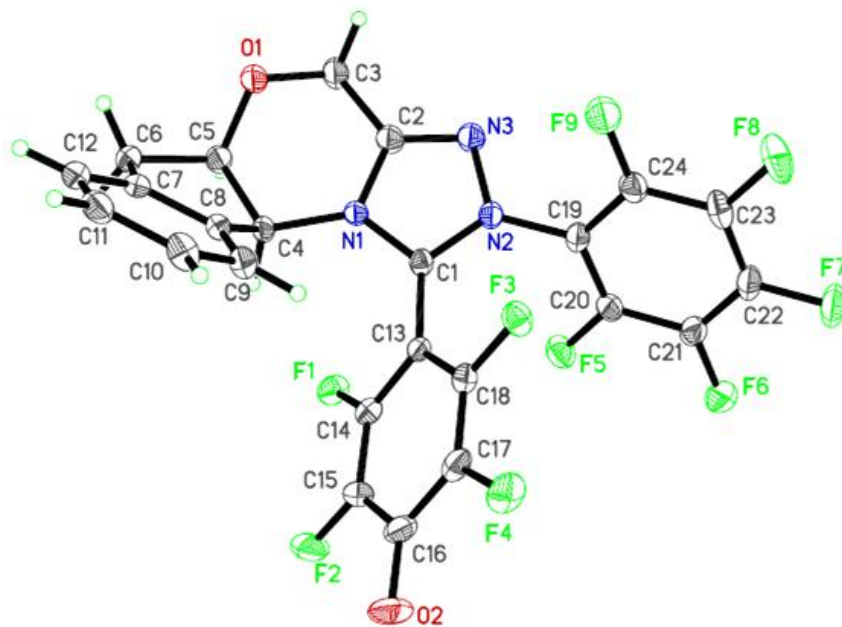
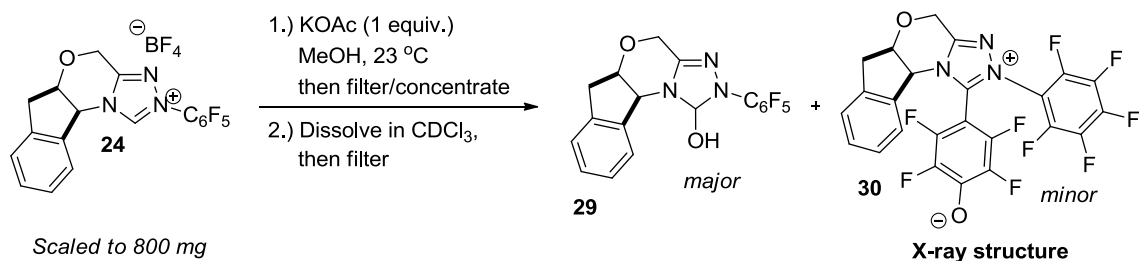
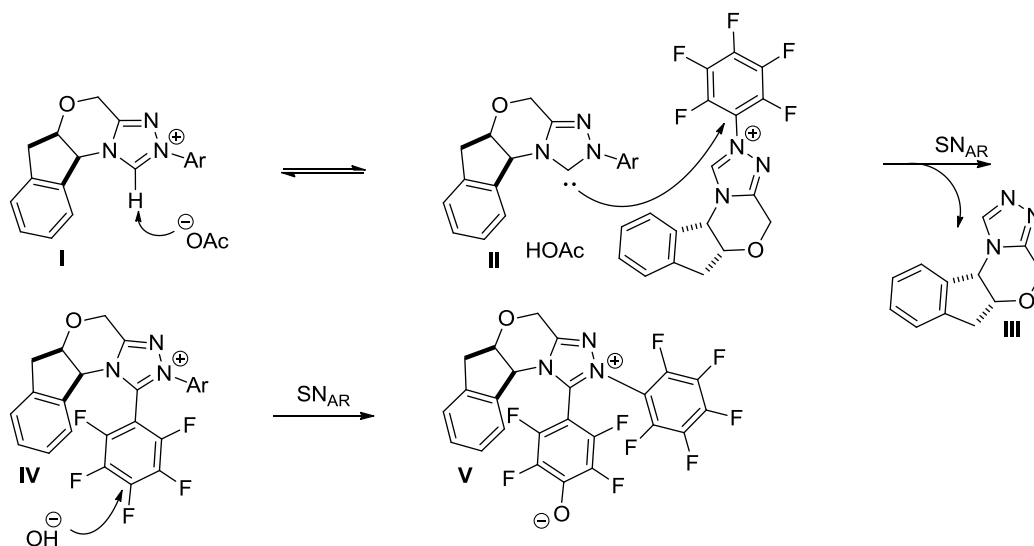


Figure 2.2: Crystal Structure of Catalyst Decomposition Product 30

We propose the following mechanism for the formation of **30** (Scheme 2.21): Triazolium **I** is first deprotonated by KOAc to form free-carbene **II**. This participates in an S_NAR reaction with the *N*-pentafluorophenyl group of another molecule of triazolium **I** to produce one equivalent each of triazole **III** and triazolium salt **IV**. We believe that hydroxide, generated from trace water and KOAc, then adds to **V**, which should be a highly-activated substrate for S_NAR

hydrolysis to yield triazolium **VI**. Another possibility is that hydroxide performs the first $\text{S}_{\text{N}}\text{AR}$ step to yield pentafluorophenol, and then free-carbene **II** performs $\text{S}_{\text{N}}\text{AR}$ on pentafluorophenol. However, the aforementioned mechanism is more likely because triazolium **I** should be a much better electrophile than pentafluorophenol.

Scheme 2.21: Proposed Mechanism for the Formation of Triazolium **30**



2.7 Conclusion:

Through the use of counterion exchange, we successfully prepared three new base-activated NHC pre-catalysts that are each capable of self-generating catalytically active free-carbene. One of these triazolium pre-catalysts was unambiguously assigned using X-ray crystallography. Additionally, in our search for new base-activated pre-catalysts, we prepared and isolated a triazolium hydrate, which itself is capable of forming free-carbene in solution. And lastly, we gathered conclusive evidence for an exciting new $\text{S}_{\text{N}}\text{AR}$ type decomposition pathway for an electron deficient triazolinylidene catalyst.

References

- ¹ Arnold, P. L.; Mungur, S. A.; Blake, A. J.; Wilson, C. *Angew. Chem. Int. Ed.* **2003**, *42*, 5981.
- ² Arduengo, A.J.; Dias, H. V. R.; Harlow, R. L.; Kline, M. *J. Am. Chem. Soc.* **1992**, *114*, 5530.
- ³ Douthwaite, R. E.; Haussinger, K.; Green, M. L. H.; Silcock, P.J.; Gomes, P.T.; Martins, A. M.; Danopoulos, A. A. *Organometallics* **1999**, 4584 .
- ⁴ Read de Alaniz, J. Ph.D. Dissertation, Colorado State University, Fort Collins, CO, 2006.
- ⁵ (a) Darses, S.; Genet, J.-P.; *Eur. J. Org. Chem.*, **2003**, 4313-4327. (b) Darses, S.; Genet, J.-P.; Brayer, J.-L.; Demoute, J.-P. *Tetrahedron Lett.* **1997**, *38*, 4393-4396.
- ⁶ Cousin, D.; Mann, J.; Nieuwenhuyzen, M. van den Berg, H. *Org. Biomol. Chem.*, **2006**, *4*, 54-62.
- ⁷ (a) Molander, G. Cooper, D. *J. Org. Chem.* **2008**, *73*, 3885–3891. (b) Molander, G.; Cavalcanti, L.; Canturk, B.; Pan, P.; Kennedy, L. *J. Org. Chem.* **2009**, *74*, 7364–7369.
- ⁸ Buffer preparations. pH=10 buffer: NaHCO₃ (105 mg) was added to a 50 mL volumetric flask. Deionized water was added to dissolve, and then 0.10 M NaOH (5.33 mL). The solution was then diluted to 50 mL. pH=12 buffer: NaHPO₄ (177 mg) was added to a 50 mL volumetric flask. Water was added to dissolve, and then 0.10 M NaOH (13.5 mL). The solution was then diluted to 50 mL.
- ⁹ Triazolium salt **5** was re-isolated quantitatively. Using this as the ¹H NMR standard, less than 5% of the starting aryltrifluoroborate was observed by ¹H NMR for each of the buffered reactions.
- ¹⁰ Yuen, A. K. L.; Hutton, C. A. *Tetrahedron Lett.* **2005**, *46*, 7899-7903.
- ¹¹ Burgess, J. 1978 *Metal Ions in Solution*; Halsted Press: New York, 1978.
- ¹² A control reaction of triazolium chloride **7** (instead of **8**) under the same conditions given in Scheme 2.7 gave no cyclization product. Additionally, a control reaction of *N*-methylmorpholine (20 mol%), triazolium chloride **7** (20 mol%), and aldehyde **9** under the same conditions resulted in 30% conversion to cyclized product.
- ¹³ DiRocco, D.; Oberg, K.; Dalton, D.; Rovis, T. *J. Am. Chem. Soc.* **2009**, *131*, 10872.
- ¹⁴ Kerr, M. S.; Rovis, T. *J. Am. Chem. Soc.* **2004**, *126*, 8876.
- ¹⁵ Kerr, M. Ph.D. Dissertation, Colorado State University, Fort Collins, CO, 2007.
- ¹⁶ Vora, H.; Lathrop, S.; Reynolds, N.; Kerr, M.; Read de Alaniz, J.; Rovis, T. *Org. Synth.* **2010**, *87*, 350-361.

- ¹⁷ Read de Alaniz, J.; Rovis, T. *J. Am. Chem. Soc.* **2005**, *127*, 6284-6289.
- ¹⁸ The authors of citation (17) noted that KBF₄ was completely insoluble in deuterated toluene. Before filtration, the ¹⁹F NMR showed no trace of tetrafluoroborate anion.
- ¹⁹ Read de Alaniz, J.; Rovis, T. *Synlett* **2009**, *20*, 1189.
- ²⁰ Dry hydrogen chloride gas was generated in small quantities by dropwise addition of concentrated H₂SO₄ to anhydrous CaCl₂. Prior to adding H₂SO₄, the system was thoroughly purged with Ar.
- ²¹ When a TLC was taken of the crude reaction mixture after filtration, the aryltrifluoroborate and triazolium chloride were separated, which indicated that they did not exist as ion pairs.
- ²² Counterion exchange also failed when attempted in acetonitrile using **25** and **26**, as well as when the tetrafluoroborate salt of **25** was used with **26** in acetone.
- ²³ Hydrate **29** was purified by column chromatography and treated with Ac₂O in CDCl₃. Within 30 minutes, ¹H NMR showed partial conversion to a triazolium salt. After 18 hours, complete conversion to a triazolium salt was observed, presumably through elimination of acetate.
- ²⁴ A co-crystallized molecule of H₂O was omitted for clarity.
- ²⁵ A test reaction of triazolium **30** with aldehyde **9** in PhMe did not result in cyclization to form Stetter product.

Appendix 1: Chapter 1 Experimental

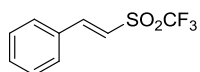
An Asymmetric Intermolecular Stetter Reaction

General Methods. All reactions were carried out under an atmosphere of argon in flame or oven-dried glassware with magnetic stirring. Commercial reagents were purchased from Sigma-Aldrich or Alfa Aesar and used without further purification, unless otherwise indicated.

Aldehydes were either purchased from Aldrich or prepared via literature procedures. Vinyl triflones were prepared according to the general procedure as described within. Tetrahydrofuran, diethylether, and dichloromethane were degassed with argon and passed through two columns of neutral alumina. Toluene was degassed with argon and passed through one column of neutral alumina and one column of Q5 reactant. Methanol was purchased from Fisher Scientific and dried with activated 3Å molecular sieves. Column chromatography was performed on EM Science silica gel 60 (230-400 mesh). Thin layer chromatography was performed on SiliCycle® 250µm 60A plates. Visualization was accomplished with UV light or either KMnO₄ or *p*-anisaldehyde stain, followed by heating.

¹H, ¹³C, and ¹⁹F NMR spectra were recorded on a Varian 300 or 400 spectrometer at ambient temperature. All ¹H and ¹³C NMR spectra are referenced to TMS or the residual solvent signal. Data for ¹H NMR are reported as follows: chemical shift in parts per million (δ, ppm), multiplicity (s = singlet, bs = broad singlet, d = doublet, t = triplet, q = quartet, and m = multiplet), coupling constants (Hz), integration. ¹³C NMR data was recorded at 75 or 100 MHz, and are reported as follows: chemical shift (δ, ppm). ¹⁹F NMR data was recorded at 376 or 282 MHz, and are reported either as (δ, ppm), or as follows for spectra containing multiple signals: chemical shift (δ, ppm), multiplicity (s = singlet, d = doublet, t = triplet, q = quartet, m = multiplet), coupling constant (Hz), integration.

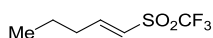
Infrared spectra were obtained on a Nicolet Avatar 320 FT-IR spectrometer. High resolution mass spectra (HRMS) were recorded on an Agilent Technologies 6210 Time of Flight LC/MS. Low resolution mass spectra (LRMS) were recorded on an Agilent Technologies 6130 Quadrupole LC/MS. HPLC spectra were obtained on an Agilent 1100 series system.



General procedure for synthesis of vinyl triflones. (E)-2-

((trifluoromethyl)sulfonyl)vinyl)benzene (25): Prepared via a slightly

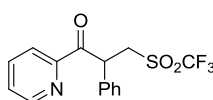
modified literature procedure.¹ (Iodomethyl)trimethylsilane (3.24 g, 0.0151 mol) was added to 75 mL of diethyl ether and cooled to -78 °C. *t*-BuLi in pentane (1.7 M, 18.6 mL, 0.0317 mol) was then added dropwise. After stirring for 1 h, freshly distilled Tf₂O (2.13 g, 7.56 x 10⁻³ mol) was added to the solution dropwise and allowed to stir for 1.5 h. Freshly distilled benzaldehyde (0.802 g, 7.56 x 10⁻³ mol) was then added, and the reaction mixture stirred for 5 h. The reaction flask was then removed from the dry ice bath and stirred for an additional 40 min. The septum was then removed, and H₂O (40 mL) was slowly added during stirring to eventually form a yellowish-brown solution. The aqueous solution was then extracted with diethyl ether (30 mL x 3), washed with brine, and dried over Na₂SO₄. Rotary evaporation afforded a crude yellow solid. Column chromatography was performed using a gradient system of 29:1 to 15:1 (hexanes to ethyl acetate), and yielded 1.23 g of **25** as a white solid (69% yield). R_f (20:1 hexanes to ethyl acetate) = 0.28; ¹H NMR (400 MHz; CDCl₃): δ 7.90 (d, *J* = 15.6 Hz, 1H), 7.62-7.55 (m, 3H), 7.51-7.48 (m, 2H), 6.83 (d, *J* = 15.5 Hz, 1H); ¹³C NMR (100 MHz; CDCl₃): δ 153.8, 133.2, 131.1, 129.5, 129.4, 116.6; IR (NaCl, CDCl₃) 3072, 1608, 1576, 1497, 1451, 1356, 1195, 1116, 975; HRMS (DART) calcd for C₉H₇F₃O₂S 236.0119, found 254.0451 (M+NH₄)⁺.



(E)-1-((trifluoromethyl)sulfonyl)pent-1-ene (37): According to the general

procedure, (Iodomethyl)trimethylsilane (4.85 g, 0.0227 mol), diethyl ether (75

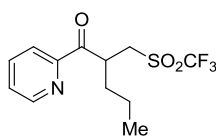
mL), *t*-BuLi in pentane (1.7 M, 32.0 mL, 0.0545 mol), Tf₂O (3.20 g, 0.0113 mol), butanal (0.817 g, 0.0113 mol), H₂O (50 mL), and diethyl ether for extraction (35 mL x 3). Column chromatography, which was performed using a gradient system of 37:1 to 15:1 (hexanes to ethyl acetate), yielded 0.946 g of **37** as a colorless oil (41% yield). R_f (20:1 hexanes to ethyl ether) = 0.30; ¹H NMR (400 MHz; CDCl₃): δ 7.29-7.21 (m, 1H), 6.29 (d, *J* = 15.3, 1H), 2.34 (dq, *J* = 7.2, 1.5 Hz, 2H), 1.53 (sextet, *J* = 7.5 Hz, 2H), 0.92 (t, *J* = 7.4 Hz, 3H); ¹³C NMR (100 MHz; CDCl₃): δ 160.4, 121.3, 34.3, 20.5, 13.3; ¹⁹F NMR (376 MHz; CDCl₃): δ -79.2; IR (NaCl, CDCl₃) 3064, 2969, 2940, 2881, 1619, 1366, 1220, 1197, 1121; HRMS (DART) calcd for C₆H₉F₃O₂S 202.0275, found 220.0619 (M+NH₄)⁺.



2-phenyl-1-(pyridin-2-yl)-3-((trifluoromethyl)sulfonyl)propan-1-one (27):

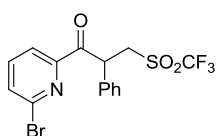
t-Butanol (0.7 mL) was added via syringe to a mixture of triazolium **30** (13.2 mg, 0.0289 mmol), **25** (41 mg, 0.174 mmol), and catechol (15.5 mg, 0.141 mmol) under argon. 2-Pyridinecarboxaldehyde (**28**) (13.5 μL, 0.141 mmol) was added at once via syringe, and *i*-Pr₂NEt (4.9 μL, 0.0289 mmol) was added last to form a homogenous yellow solution. The reaction was stirred for 2 h at 23 °C, at which time acetic acid (5.5 μL) was added to quench the reaction. The mixture was then concentrated, and purified by column chromatography with a gradient system of 15:1 Hexanes:EtOAc to 4:1 Hexanes:EtOAc to yield 7.0 mg of **27** as a colorless oil (24% NMR yield, 14% isolated yield, 80% ee). R_f (1:1 CH₂Cl₂ to hexanes) = 0.26; HPLC Analysis - Chiracel IC column, 70:30 hexanes to isopropanol, 1.0 mL/

min. Major enantiomer 4.82 minutes, minor enantiomer 5.24 minutes; ^1H NMR (400 MHz; CDCl_3): δ 8.59 (m, 1H), 7.98 (dt, $J = 7.8, 1.1$ Hz, 1H), 7.70 (td, $J = 7.7, 1.7$ Hz, 1H), 7.36-7.30 (m, 3H), 7.24-7.20 (m, 2H), 7.18-7.14 (m, 1H), 6.11 (dd, $J = 9.7, 3.8$ Hz, 1H), 4.48 (ddd, $J = 14.6, 9.7, 0.8$ Hz, 1H), 3.54 (ddd, $J = 14.5, 3.8, 0.4$ Hz, 1H); ^{13}C NMR (100 MHz; CDCl_3): δ 196.0, 151.1, 149.1, 136.9, 135.2, 129.2, 128.7, 128.2, 127.7, 123.3, 120.1, 52.0, 44.0; ^{19}F NMR (376 MHz; CDCl_3): δ -78.4; IR (NaCl, CDCl_3) 2925, 2854, 1702, 1583, 1494, 1438, 1367, 1205, 1121 cm^{-1} ; LRMS (ES+) calcd for $\text{C}_{15}\text{H}_{12}\text{F}_3\text{NO}_3\text{S}$ 343.05, found 344.1.



1-(pyridin-2-yl)-2-(((trifluoromethyl)sulfonyl)methyl)pentan-1-one (38):

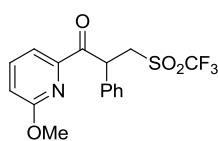
t-Butanol (1.4 mL) was added via syringe to a mixture of triazolium **29** (25.6 mg, 0.0565 mmol), **37** (66.6 mg, 0.330 mmol), and catechol (31.0 mg, 0.282 mmol) under argon. 2-pyridinecarboxaldehyde (**28**) (27.0 μL , 0.282 mmol) was added at once via syringe, and *i*-Pr₂NEt (49.1 μL , 0.282 mmol) was added last to form a homogenous brownish - green solution. The reaction was stirred for 1 h at 23 °C, at which time acetic acid (37 μL) was added to quench the reaction. The mixture was then concentrated, and purified by column chromatography with a gradient system of 15:1 to 4:1 (hexanes to ethyl acetate) to yield 27 mg of **38** as a colorless oil (28% isolated yield, 60 %ee). Rf (1:1 CH_2Cl_2 to hexanes) = 0.23; HPLC Analysis - Chiracel IC column, 98:2 hexanes to isopropanol, 1.0 mL/min. Major enantiomer 13.78 minutes, minor enantiomer 12.44 minutes; ^1H NMR (400 MHz; CDCl_3): δ 8.73-8.71 (m, 1H), 8.10 (dt, $J = 7.9, 1.0$ Hz, 1H), 7.87 (td, $J = 7.7, 1.7$ Hz, 1H), 7.51 (ddd, $J = 7.6, 4.7, 1.2$ Hz, 1H), 4.94-4.88 (m, 1H), 4.14 (dd, $J = 14.5, 9.5$ Hz, 1H), 3.38 (dd, $J = 14.4, 3.4$ Hz, 1H), 1.92-1.83 (m, 1H), 1.69-1.60 (m, 1H), 1.37 (sextet, $J = 7.5$ Hz, 2H), 0.92 (t, $J = 7.3, 3\text{H}$); ^{13}C NMR (100 MHz; CDCl_3): δ 199.6, 151.5, 149.2, 137.1, 127.7, 122.9, 50.0, 38.0, 34.3, 19.7, 13.7; ^{19}F NMR (376 MHz; CDCl_3): δ -78.4; IR (NaCl, CDCl_3) 2966, 2936, 2878, 1700, 1363, 1200, 1121 cm^{-1} ; LRMS (ES+) calcd for $\text{C}_{12}\text{H}_{14}\text{F}_3\text{NO}_3\text{S}$ 309.06, found 310.1.



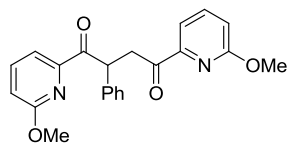
1-(6-bromopyridin-2-yl)-2-phenyl-3-(((trifluoromethyl)sulfonyl)methyl)propan-1-one (46b):

t-Butanol (0.7 mL) was added via syringe to a mixture of triazolium **30** (13.2 mg, 0.0289 mmol), **25** (41 mg, 0.174 mmol), catechol (15.5 mg, 0.141 mmol), and 6-bromo-2-pyridinecarbaldehyde (**46a**) (26.3 mg, 0.141 mmol) under argon. *i*-Pr₂NEt (4.9 μL , 0.0289 mmol) was added last. The reaction was stirred for 2.5 h at 23 °C, at which time acetic acid (5.5 μL) was added to quench the reaction (60% nmr yield, 74 %ee). A similar reaction was performed using achiral triazolium salt **26**, and was purified by column chromatography using a solvent system of 2:1 hexanes to CH_2Cl_2 to yield **46b** as a colorless oil. Rf (1:1 CH_2Cl_2 to hexanes) = 0.55; HPLC Analysis - Chiracel IC column, 199:1 hexanes to isopropanol, 2.0 mL/min. Major enantiomer 6.97 minutes, minor enantiomer 7.50 minutes; ^1H -NMR (400 MHz; CDCl_3): δ 7.94-7.92 (m, 1H), 7.59-7.52 (m, 2H), 7.34-7.31 (m, 2H), 7.27-7.23 (m, 2H), 7.21-7.17 (m, 1H), 5.90 (dd, $J = 9.8, 3.7$ Hz, 1H), 4.46 (ddd, $J = 14.5, 9.8, 0.8$ Hz, 1H), 3.54 (dd, $J = 14.6, 3.8$ Hz, 1H); ^{13}C NMR (100 MHz; CDCl_3): δ 194.3, 151.5, 141.3, 139.3, 134.7, 132.5, 129.3, 128.8, 128.5, 122.1, 51.8, 44.5; ^{19}F NMR (376 MHz;

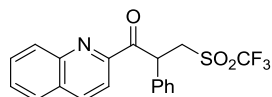
CDCl₃): δ -78.3; IR (NaCl, CDCl₃) 3088, 3034, 2995, 2937, 1706, 1557, 1431, 1368, 1210, 1122, 976, 935 cm⁻¹.



1-(6-methoxypyridin-2-yl)-2-phenyl-3-((trifluoromethyl)sulfonyl)propan-1-one (47b): *t*-Butanol (0.7 mL) was added via syringe to a mixture of triazolium **30** (13.2 mg, 0.0289 mmol), **25** (41 mg, 0.174 mmol), and catechol (15.5 mg, 0.141 mmol) under argon. 6-methoxy-2-pyridinecarbaldehyde (**47a**) (19.4 g, 17.0 μ L, 0.141 mmol) was added at once via syringe, and *i*-Pr₂NEt (4.9 μ L, 0.0289 mmol) was added last. The reaction was stirred for 2 h at 23 °C, at which time acetic acid (5.5 μ L) was added to quench the reaction (15% nmr yield, 87% ee). A similar reaction was performed using achiral triazolium salt **26**, and was purified by column chromatography using a solvent system of 2:1 hexanes to CH₂Cl₂ to yield **47b** as a colorless oil. R_f (4:1 hexanes to ethyl acetate) = 0.24, R_f (1:1 CH₂Cl₂ to hexanes) = 0.37; HPLC Analysis - Chiracel IC column, 199:1 hexanes to isopropanol, 2.0 mL/ min. Major enantiomer 6.61 minutes, minor enantiomer 7.94 minutes; ¹H-NMR (400 MHz; CDCl₃): δ 7.72-7.64 (m, 2H), 7.37-7.26 (m, 5H), 6.91 (dd, *J* = 8.0, 1.1 Hz, 1H), 5.98 (dd, *J* = 9.3, 4.0 Hz, 1H), 4.51 (ddd, *J* = 14.6, 9.3, 0.9 Hz, 1H), 3.99 (s, 3H), 3.58 (ddd, *J* = 14.6, 4.1, 0.5 Hz, 1H); ¹³C NMR (100 MHz; CDCl₃): δ 195.5, 163.3, 148.5, 139.2, 135.5, 129.3, 128.44, 128.36, 117.0, 116.5, 53.8, 52.2, 44.7; ¹⁹F NMR (376 MHz; CDCl₃): δ -78.3; IR (NaCl, CDCl₃) 2987, 2954, 1701, 1592, 1471, 1367, 1277, 1204, 1121, 1031, 982 cm⁻¹; LRMS (ES⁺) calcd for C₁₆H₁₄F₃NO₄S 373.06, found 374.1.

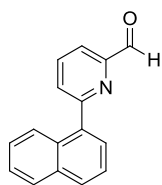


1,4-bis(6-methoxypyridin-2-yl)-2-phenylbutane-1,4-dione: Under achiral reaction conditions for the synthesis of **47b**, this elimination / re-addition product was isolated as a colorless oil. R_f (1:1 CH₂Cl₂ to hexanes) = 0.24; ¹H-NMR (400 MHz; CDCl₃): δ 7.69-7.62 (m, 3H), 7.58 (dd, *J* = 7.3, 0.9 Hz, 1H), 7.46-7.43 (m, 2H), 7.31-7.27 (m, 2H), 7.23-7.19 (m, 1H), 6.92 (dd, *J* = 8.2, 0.9 Hz, 1H), 6.87 (dd, *J* = 7.8, 1.3 Hz, 1H), 5.84 (dd, *J* = 10.7, 4.0 Hz, 1H), 4.30 (dd, *J* = 19.1, 10.7 Hz, 1H), 4.00 (s, 3H), 3.98 (s, 3H), 3.66 (dd, *J* = 19.1, 4.0 Hz); ¹³C NMR (100 MHz; CDCl₃): δ 199.7, 163.3, 163.1, 150.5, 150.0, 140.0, 138.93, 138.90, 128.8, 128.6, 126.9, 116.2, 115.4, 115.3, 115.0, 98.6, 53.6, 53.5, 46.8, 42.8; IR (NaCl, CDCl₃) 2950, 1694, 1590, 1468, 1431, 1340, 1273, 1033, 987 cm⁻¹; LRMS (ES⁺) calcd for C₂₂H₂₀N₂O₄ 376.14, found 377.2.

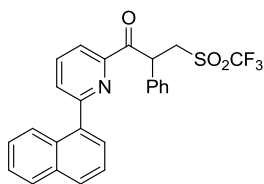


1-(isoquinolin-3-yl)-2-phenyl-3-((trifluoromethyl)sulfonyl)propan-1-one (48b): *t*-Butanol (0.7 mL) was added via syringe to a mixture of triazolium **30** (13.2 mg, 0.0289 mmol), **25** (41 mg, 0.174 mmol), catechol (15.5 mg, 0.141 mmol), and 2-quinolinecarboxaldehyde (**48a**) (22.2 mg, 0.141 mmol) under argon. *i*-Pr₂NEt (4.9 μ L, 0.0289 mmol) was added last to form a dark-red solution. The reaction was stirred for 2 h at 23 °C, at which time acetic acid (5.5 μ L) was added to quench the reaction (15% NMR yield, 90% ee). A similar reaction was performed using achiral triazolium salt **26**,

and was purified by column chromatography using a solvent system of 2:1 hexanes to CH₂Cl₂ to yield **48b** as a colorless oil. R_f (1:1 CH₂Cl₂ to hexanes) = 0.42; HPLC Analysis - Chiracel IC column, 199:1 hexanes to isopropanol, 2.0 mL/ min. Major enantiomer 8.54 minutes, minor enantiomer 12.75 minutes; ¹H NMR (400 MHz; CDCl₃): δ 8.15 (d, *J* = 8.4 Hz, 2H), 8.04 (d, *J* = 8.5 Hz, 1H), 7.75 (dd, *J* = 8.1, 1.3 Hz, 1H), 7.71 (ddd, *J* = 8.4, 6.9, 1.4 Hz, 1H), 7.56 (ddd, *J* = 8.1, 6.9, 1.2 Hz, 1H), 7.42-7.39 (m, 2H), 7.24-7.20 (m, 2H), 7.16-7.11 (m, 1H), 6.36 (dd, *J* = 9.5, 4.0 Hz, 1H), 4.53 (dd, *J* = 14.5, 9.5, 0.8 Hz, 1H), 3.62 (ddd, *J* = 14.5, 4.1, 0.6 Hz, 1H); ¹³C NMR (100 MHz; CDCl₃): δ 196.1, 150.5, 147.0, 137.2, 135.5, 130.8, 130.2, 129.8, 129.2, 129.1, 128.7, 128.2, 127.6, 119.0, 52.0, 43.9; ¹⁹F NMR (376 MHz; CDCl₃): δ -78.3; IR (NaCl, CDCl₃) 3063, 1700, 1494, 1457, 1367, 1205, 1121, 975, 927 cm⁻¹; LRMS (ES⁺) calcd for C₁₉H₁₄F₃NO₃S 393.06, found 394.1.

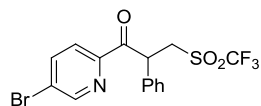


6-(naphthalen-1-yl)picolinaldehyde (49a): Prepared according to a slightly modified known procedure.² To a suspension of 6-bromo-2-pyridinecarboxaldehyde (125 mg, 0.672 mmol) and Pd(PPh₃)₄ (18.3 mg, 0.0158 mmol) in toluene (1.2 mL), aqueous 2.0 M Na₂CO₃ (0.6 mL) and **1-naphthylboronic acid** (173 mg, 1.00 mmol) dissolved in methanol (0.5 mL) were added. The suspension was then refluxed for 16 h, at which time a 2.0 M aqueous solution of Na₂CO₃ (2.5 mL) and CH₂Cl₂ (6 mL) were added after the suspension had cooled to ambient temperature. The aqueous phase was separated, extracted with CH₂Cl₂, washed with brine, and the combined organic phase was dried using Na₂SO₄. Purification by column chromatography with a gradient system of 7.5:1 to 5:1 (hexanes to ethyl acetate) yielded 114 mg of **49a** as a white solid (73% yield). R_f (5:1 hexanes to ethyl acetate) = 0.40; ¹H-NMR (400 MHz; CDCl₃): δ 10.20 (d, *J* = 0.6 Hz, 1H), 8.07-7.99 (m, 3H), 7.98-7.94 (m, 2H), 7.82 (dd, *J* = 6.8, 2.0 Hz, 1H), 7.66 (dd, *J* = 7.1, 1.4 Hz, 1H), 7.62-7.58 (m, 1H), 7.56-7.48 (m, 2H); ¹³C NMR (100 MHz; CDCl₃): δ 193.8, 159.9, 152.7, 137.5, 137.2, 134.0, 130.9, 129.5, 129.3, 128.5, 127.7, 126.8, 126.1, 125.3, 125.1, 119.8; IR (NaCl, CDCl₃) 3059, 2828, 1714, 1585, 1510, 1452, 1307, 1252, 1215, 989 cm⁻¹; LRMS (ES⁺) calcd for C₁₇H₁₅NO₂ 265.11 (MeOH sample, calcd for OMe acetal), found 266.2.



1-(6-(naphthalen-1-yl)pyridin-2-yl)-2-phenyl-3-((trifluoromethyl)sulfonyl)propan-1-one (49b): *t*-Butanol (0.7 mL) was added via syringe to a mixture of triazolium **30** (13.2 mg, 0.0289 mmol), **25** (41 mg, 0.174 mmol), catechol (15.5 mg, 0.141 mmol), and **49a** (32.9 mg, 0.141 mmol) under argon. *i*-Pr₂NEt (4.9 μL, 0.0289 mmol) was added last. The reaction was stirred for 36 h at 23 °C, at which time acetic acid (5.5 μL) was added to quench the reaction (60% nmr yield, 32% ee). A similar reaction was performed using achiral triazolium salt **26**, and was purified by column chromatography using a solvent system of 2:1 hexanes to CH₂Cl₂ to yield **49b** as a colorless oil. R_f (1:1 CH₂Cl₂ to hexanes) = 0.36; HPLC Analysis - Chiracel ODH column, 90:10 hexanes to isopropanol, 1.0 mL/ min. Minor enantiomer 8.44 minutes, major enantiomer 9.05 minutes; ¹H-NMR (400 MHz; CDCl₃): δ 8.15 (dd, *J* = 7.8,

1.1 Hz, 1H), 8.00-7.92 (m, 4H), 7.74 (dd, $J = 7.8, 1.1$ Hz, 1H), 7.62-7.58 (m, 1H), 7.56-7.53 (m, 2H), 7.45 (ddd, $J = 8.5, 7.0, 1.4$ Hz, 1H), 7.33-7.25 (m, 5H), 6.19 (dd, $J = 10.0, 3.6$ Hz, 1H), 4.58 (ddd, $J = 14.6, 10.0, 0.8$ Hz, 1H), 3.59 (dd, $J = 14.5, 3.5$ Hz, 1H); ^{13}C NMR (100 MHz; CDCl_3): δ 196.2, 158.8, 150.7, 137.6, 137.4, 135.2, 133.9, 130.9, 129.4, 129.2, 128.8, 128.4, 128.2, 127.9, 126.7, 126.1, 125.6, 125.2, 121.6, 52.2, 44.1; ^{19}F NMR (376 MHz; CDCl_3): δ -78.4; IR (NaCl, CDCl_3) 2935, 1701, 1584, 1508, 1455, 1367, 1204, 1120 cm^{-1} ; LRMS (ES+) calcd for $\text{C}_{25}\text{H}_{18}\text{F}_3\text{NO}_3\text{S}$ 469.10, found 470.1.

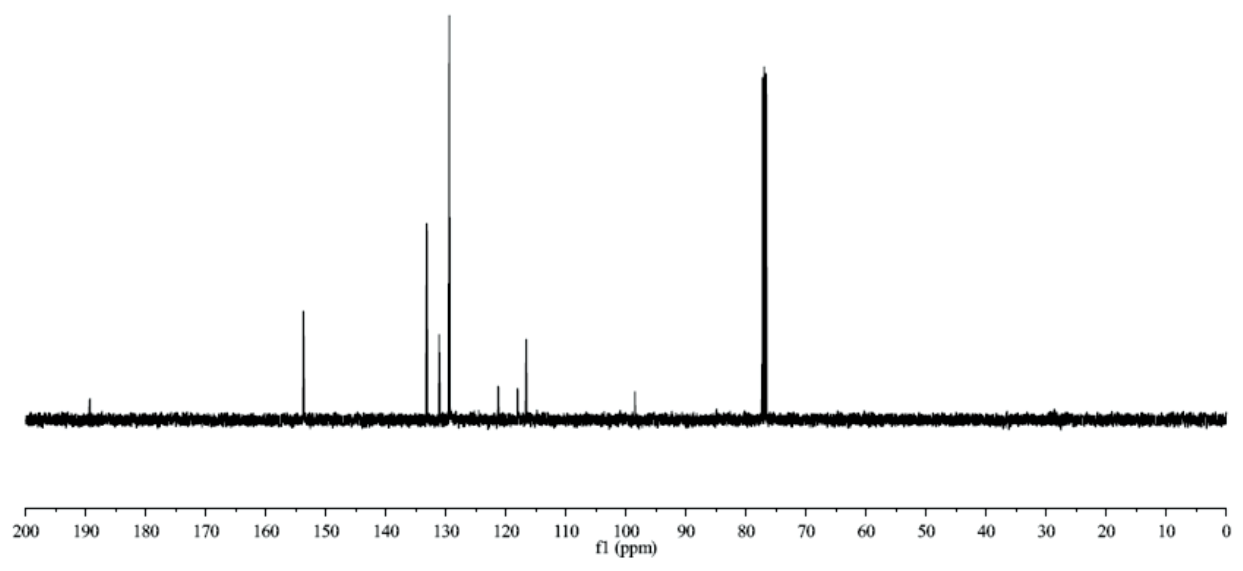
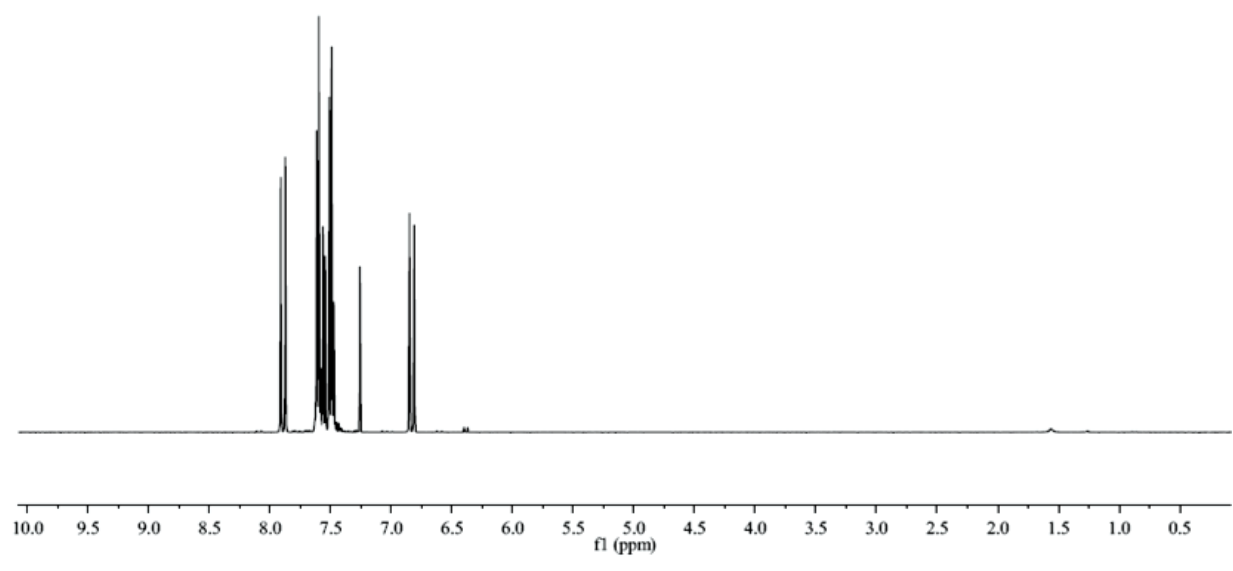
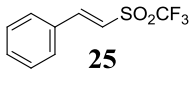


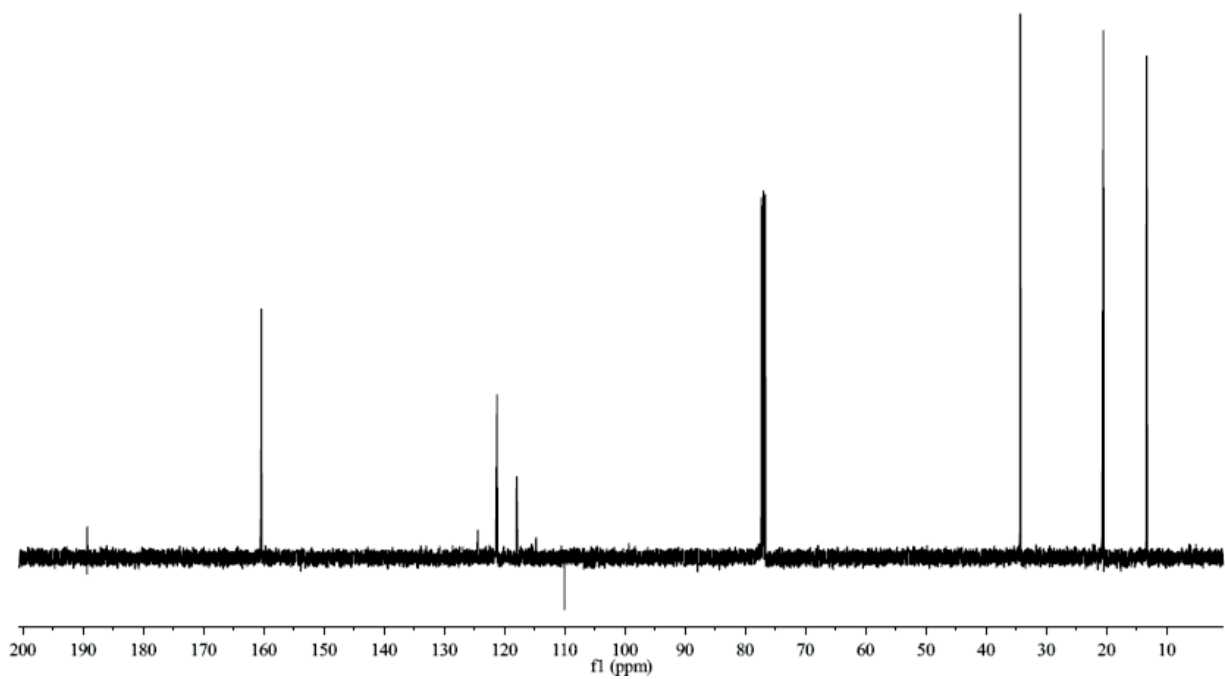
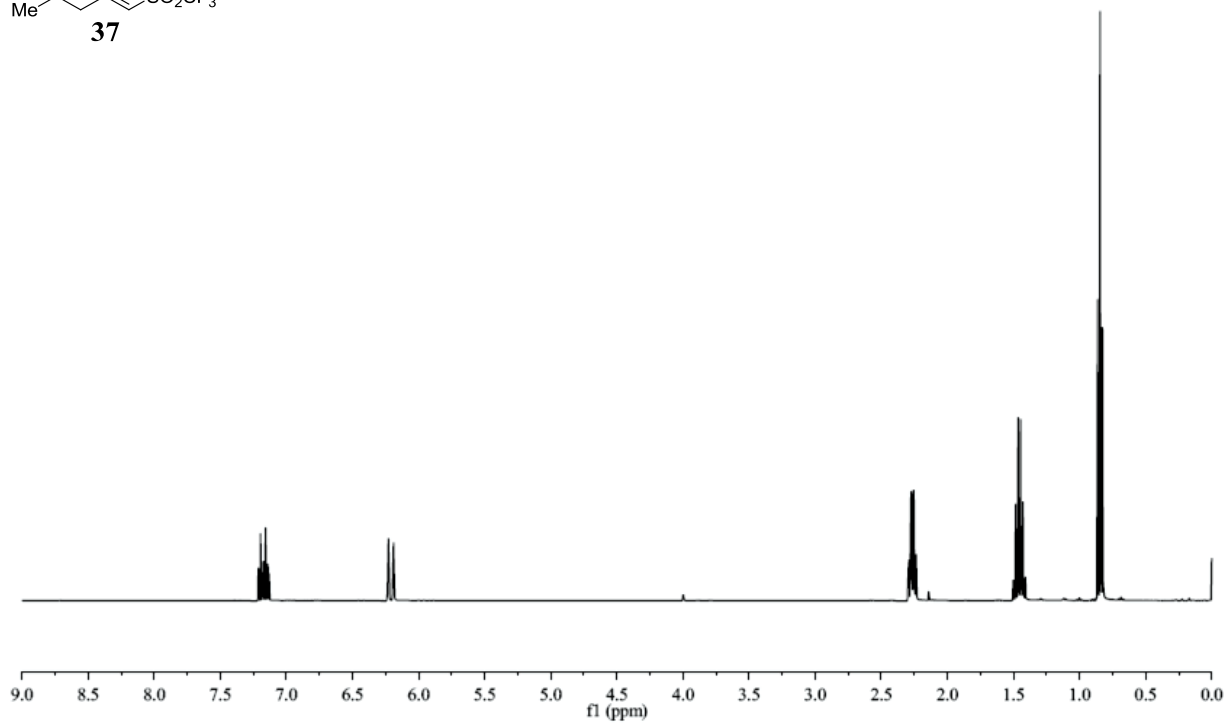
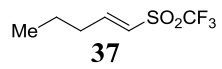
1-(5-bromopyridin-2-yl)-2-phenyl-3-((trifluoromethyl)sulfonyl)propan-1-one (50b):

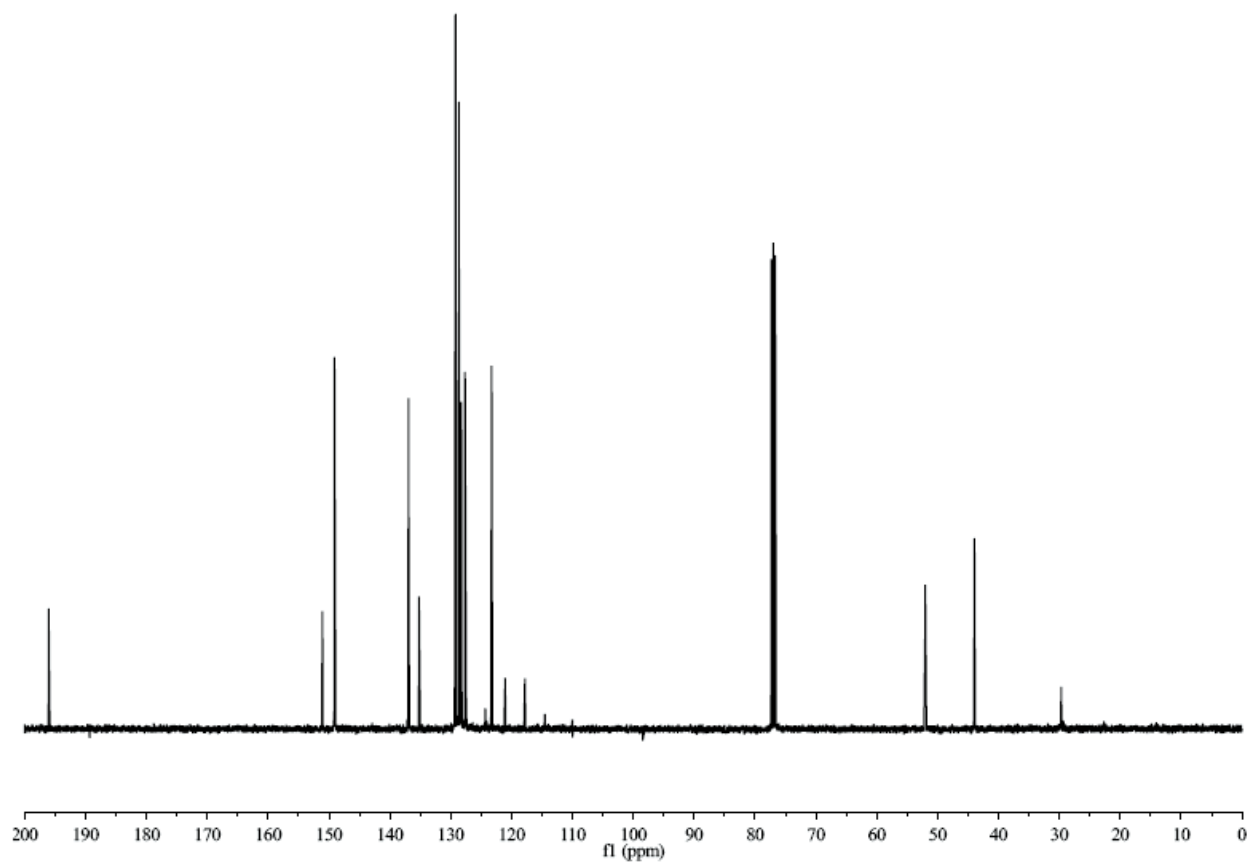
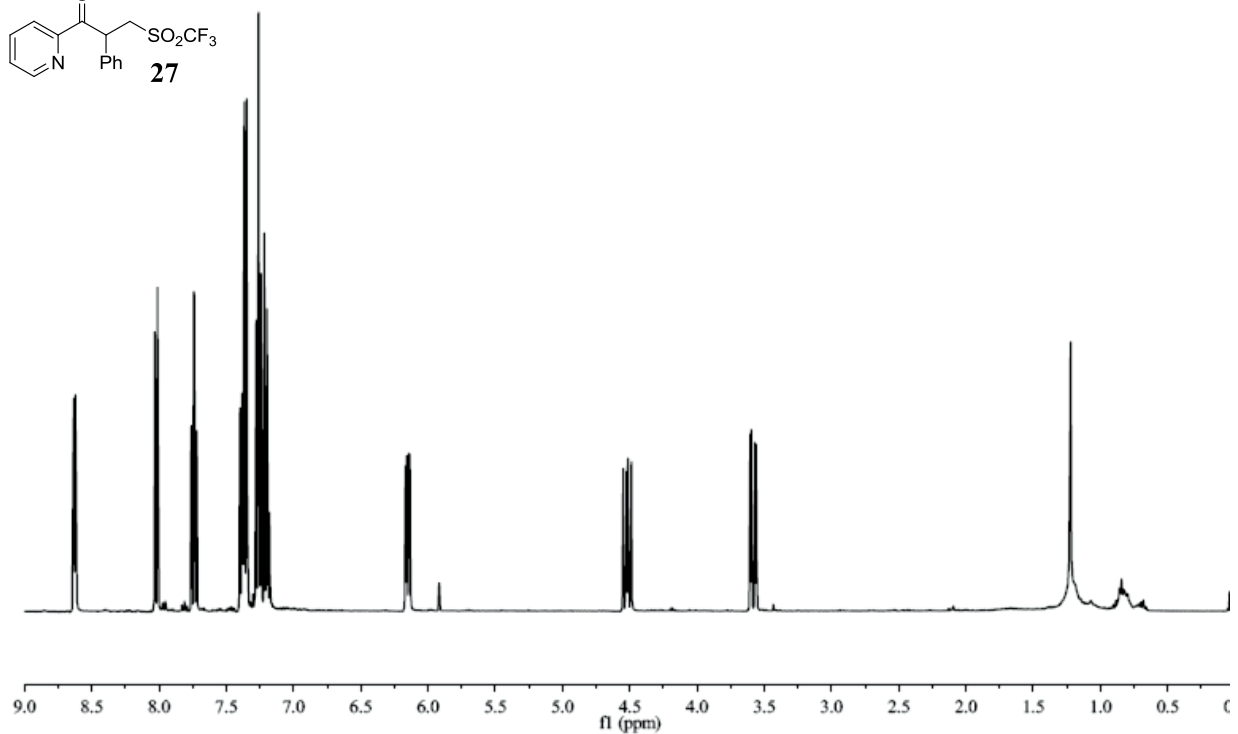
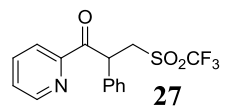
t-Butanol (0.7 mL) was added via syringe to a mixture of triazolium **30** (13.2 mg, 0.0289 mmol), **25** (41 mg, 0.174 mmol), catechol (15.5 mg, 0.141 mmol), and 5-bromo-2-pyridinecarbaldehyde (26.3 mg, 0.141 mmol) under argon. *i*-Pr₂NEt (4.9 μL , 0.0289 mmol) was added last. The reaction was stirred for 2 h at 23 °C, at which time acetic acid (5.5 μL) was added to quench the reaction (60% nmr yield, 74 %ee). A similar reaction was performed using achiral triazolium salt **26**, and was purified by column chromatography using a solvent system of 2:1 hexanes to CH_2Cl_2 to yield **50b** as a colorless oil. R_f (1:1 CH_2Cl_2 to hexanes) = 0.44; HPLC Analysis - Chiracel IC column, 199:1 hexanes to isopropanol, 2.0 mL/ min. Major enantiomer 8.30 minutes, minor enantiomer 11.09 minutes; ^1H -NMR (400 MHz; CDCl_3): δ 8.72 (dd, $J = 2.0, 0.9$ Hz, 1H), 7.97-7.91 (m, 2H), 7.38-7.35 (m, 2H), 7.33-7.28 (m, 2H), 7.28-7.23 (m, 1H), 6.06 (dd, $J = 9.9, 3.6$ Hz, 1H), 4.54 (ddd, $J = 14.6, 9.9, 0.9$ Hz, 1H), 3.60 (ddd, $J = 14.6, 3.6, 0.5$ Hz, 1H); ^{13}C NMR (100 MHz; CDCl_3): δ 195.1, 150.4, 149.3, 139.8, 134.8, 129.3, 128.6, 128.4, 126.1, 124.5, 52.0, 44.1; ^{19}F NMR (376 MHz; CDCl_3): δ -78.3; IR (NaCl, CDCl_3) 3062, 2935, 1703, 1566, 1456, 1368, 1208, 1120, 1088, 1009, 973, 931 cm^{-1} .

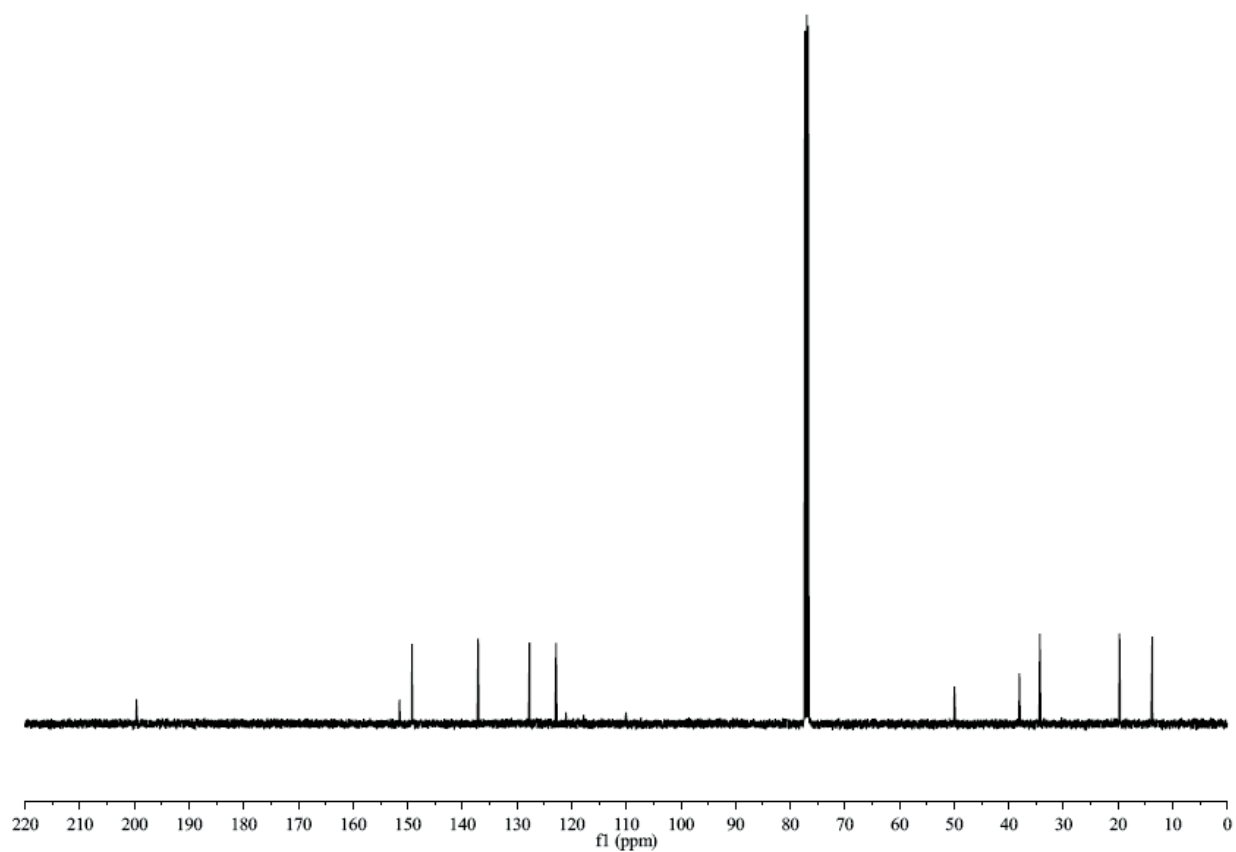
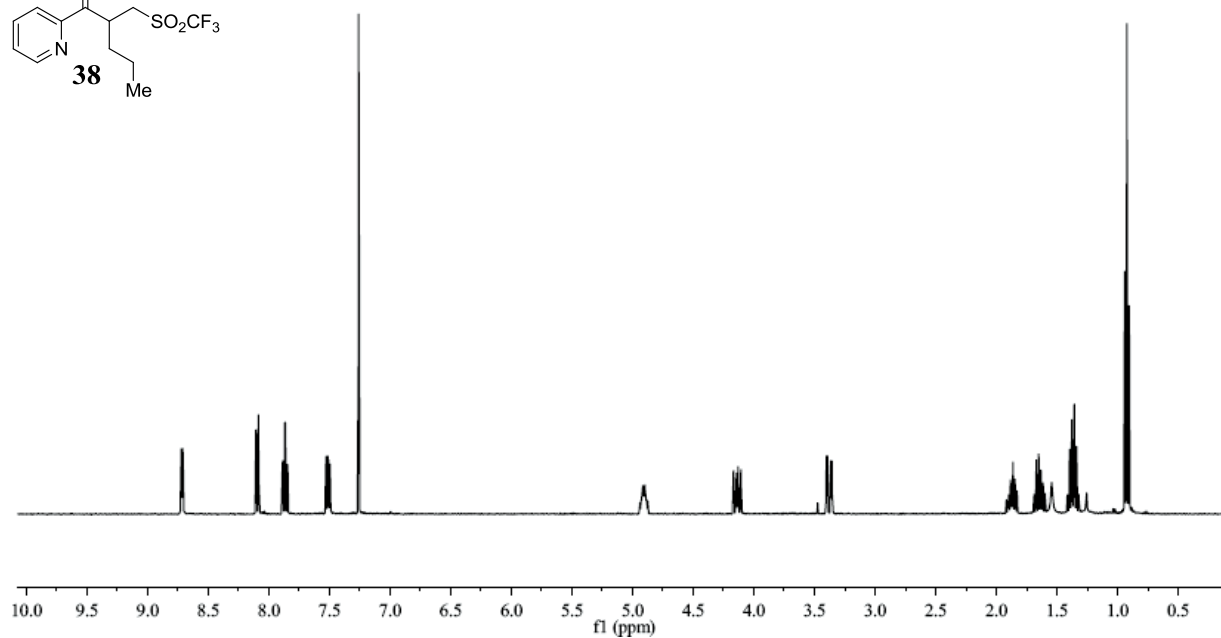
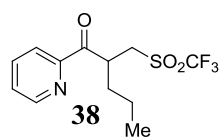
References

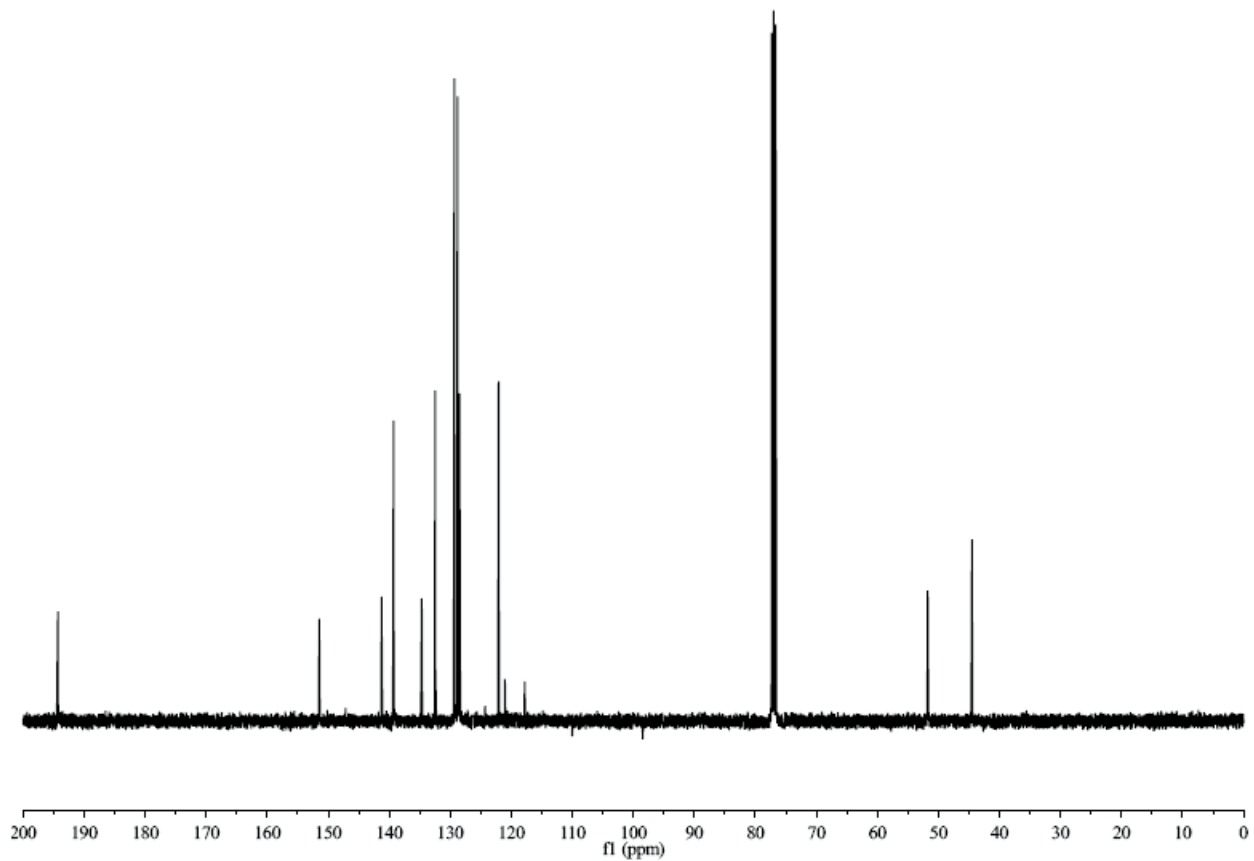
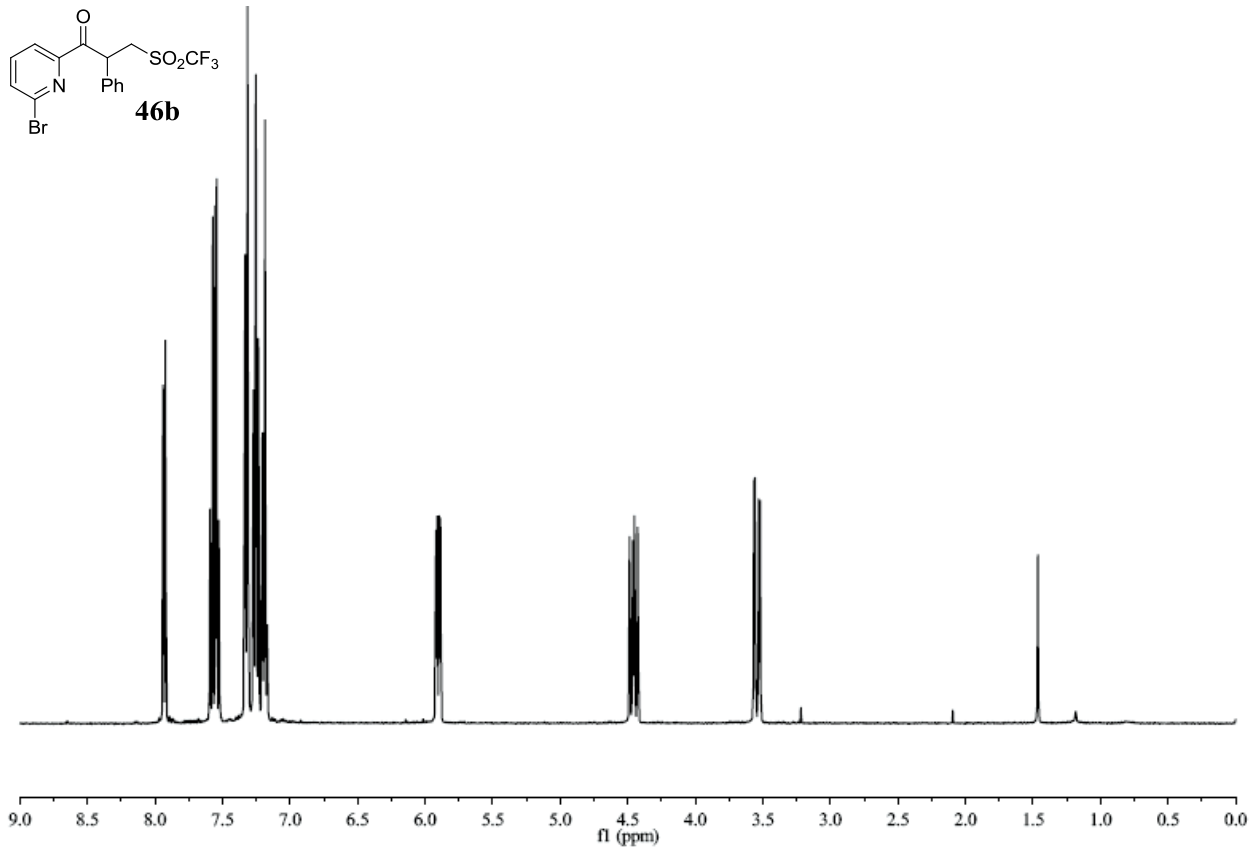
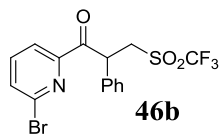
- 1.) Mahadevan, A.; Fuchs, P. L. *Tetrahedron Lett.* **1994**, *35*, 6025-6028.
- 2.) Arai, T.; Suzuki, K. *Synlett* **2009**, *19*, 3167-3170.

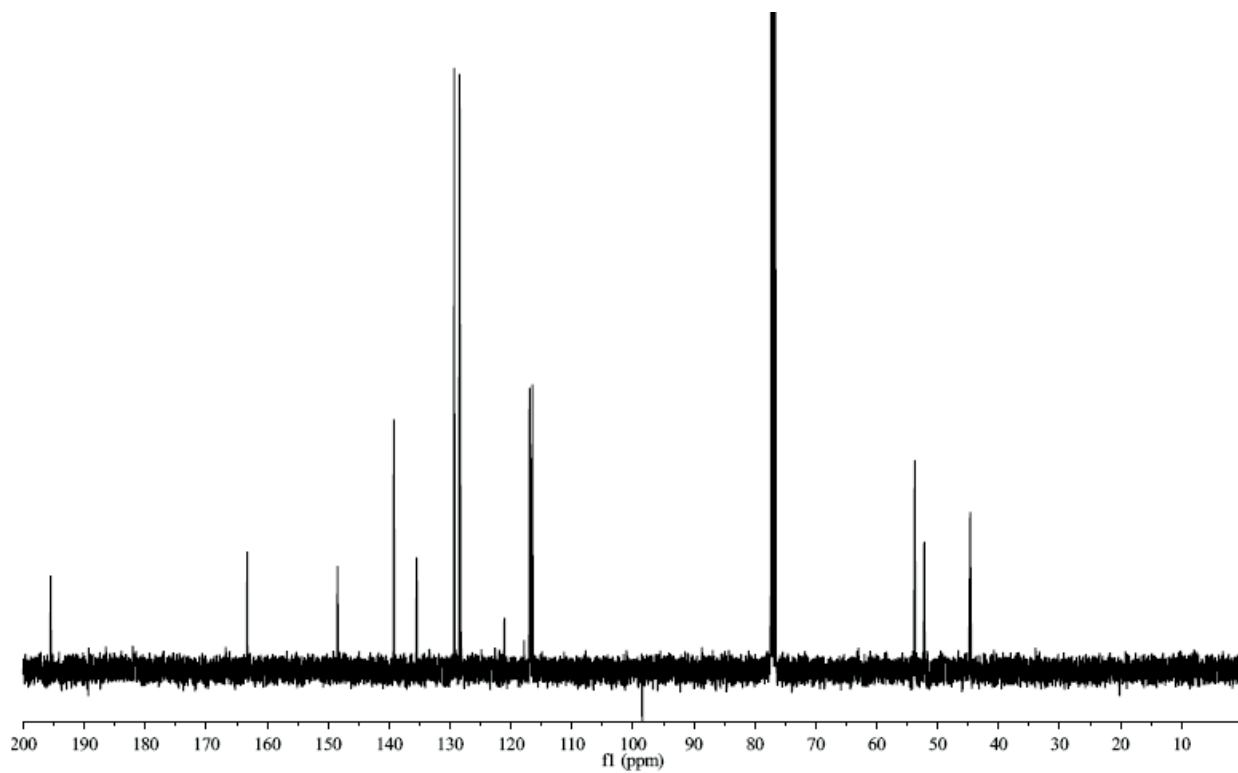
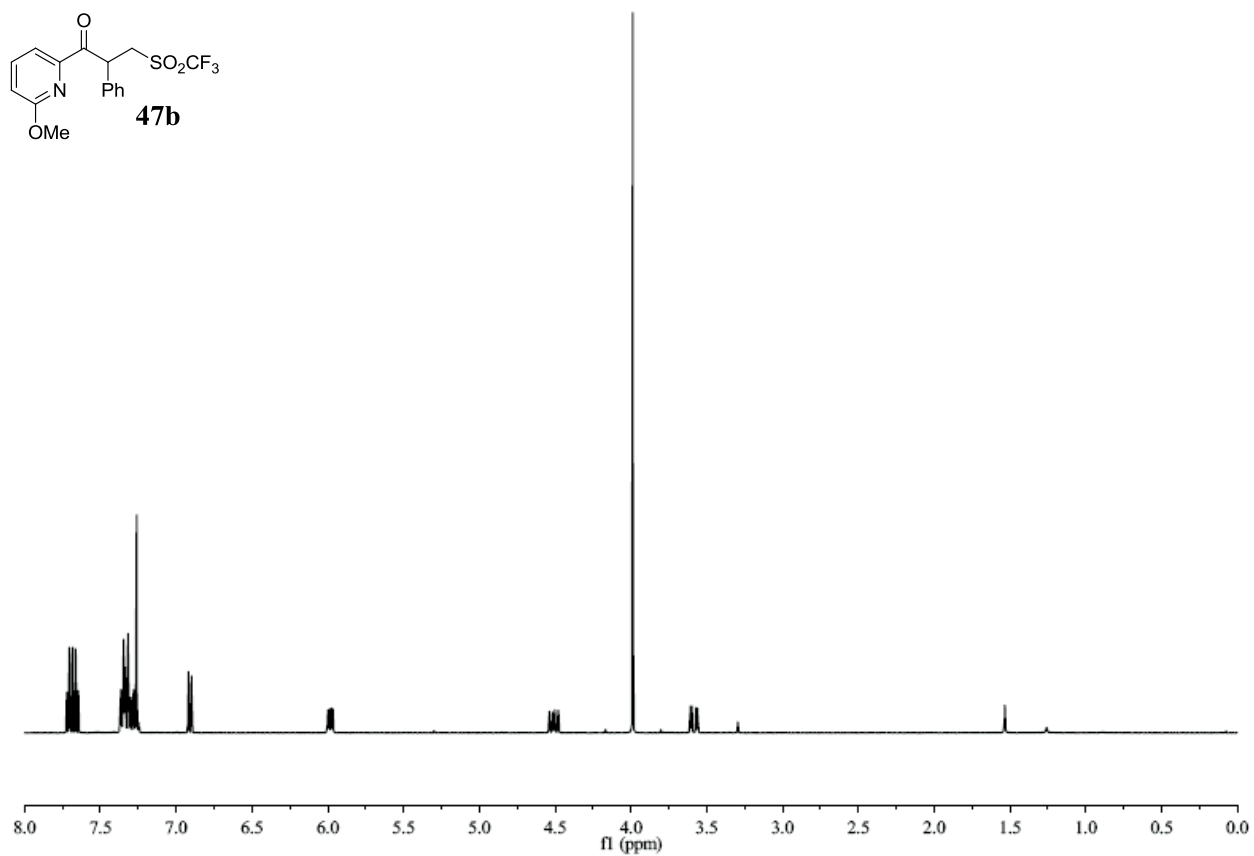
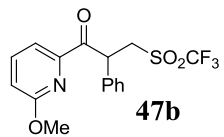


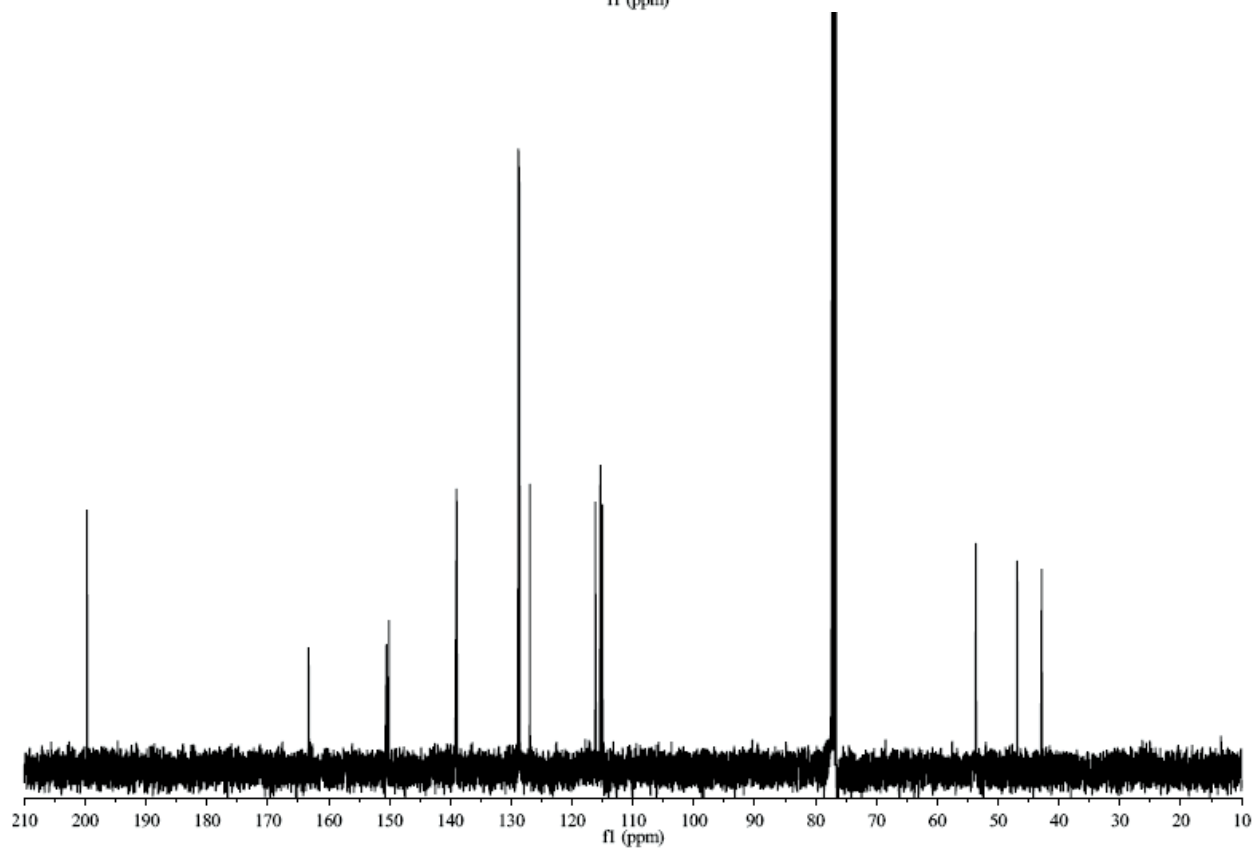
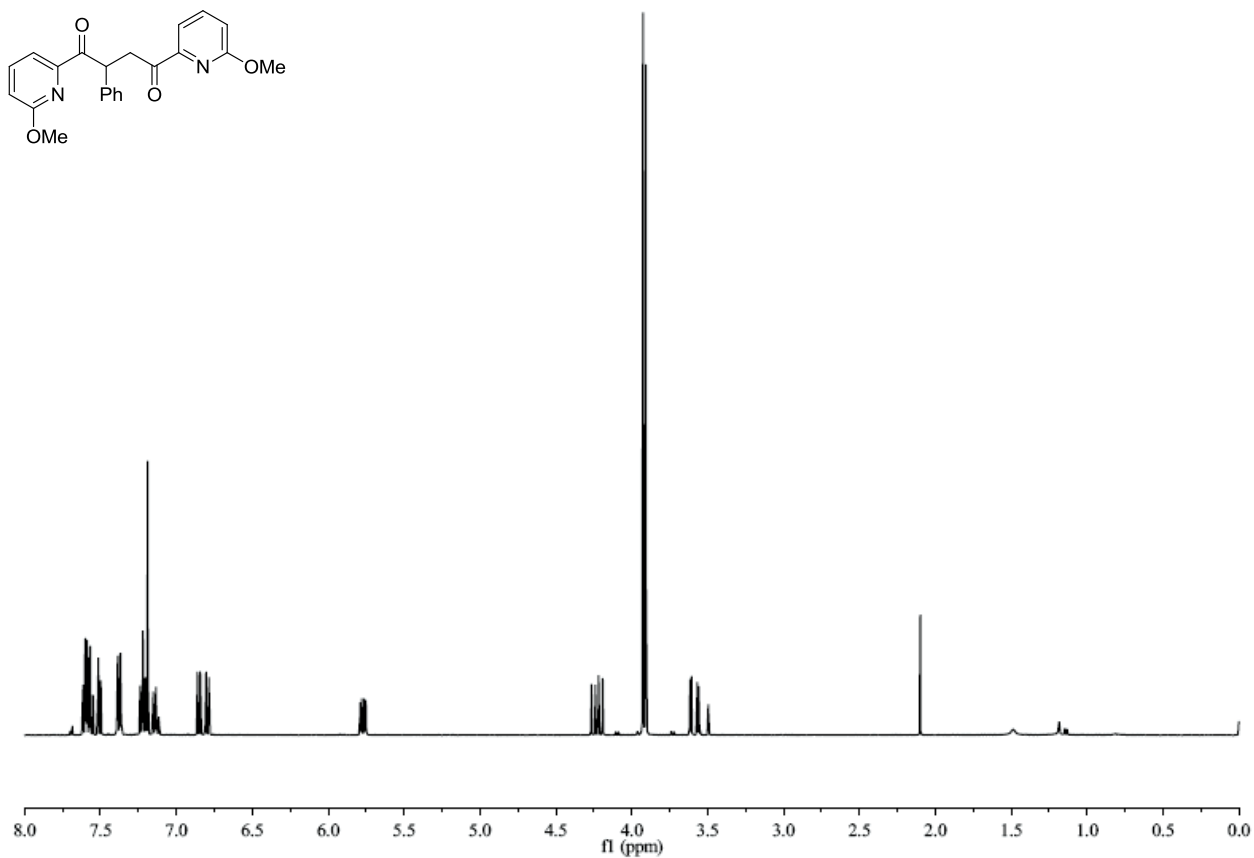
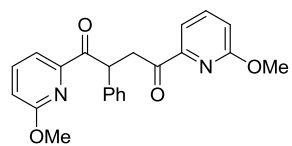


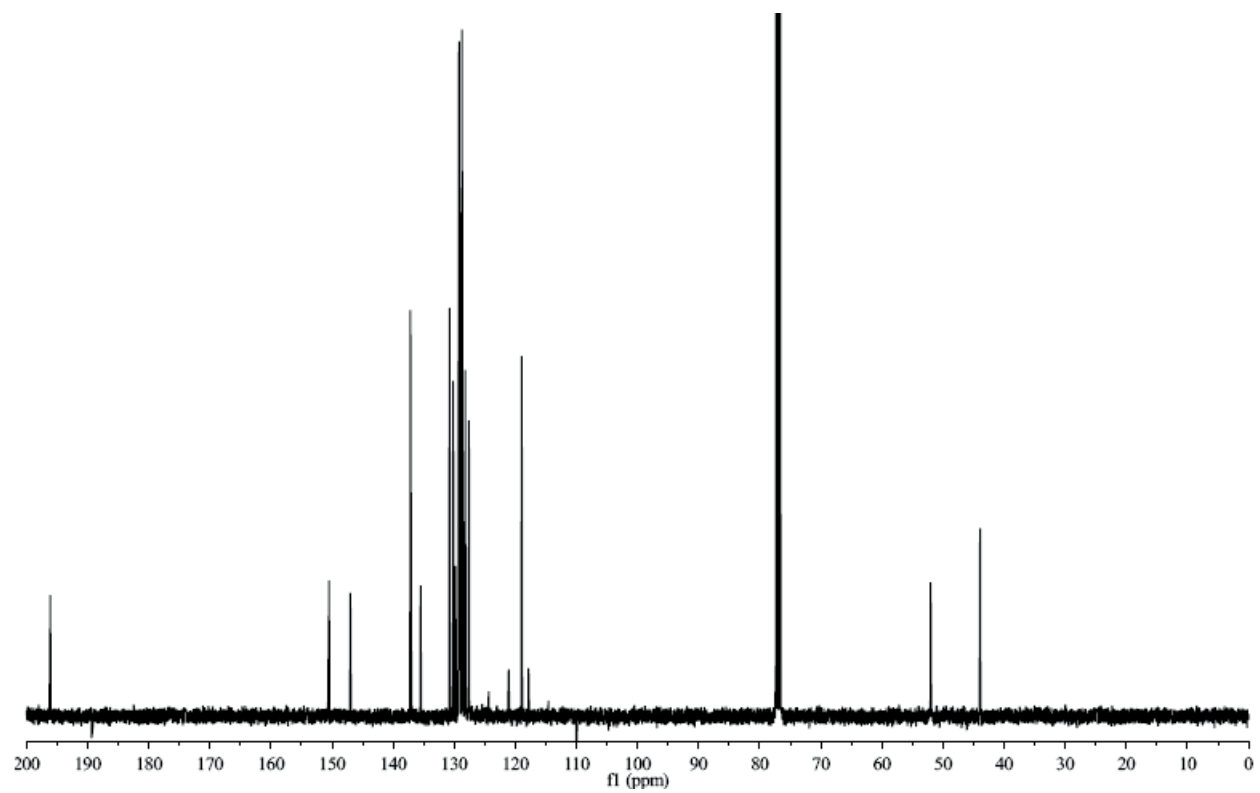
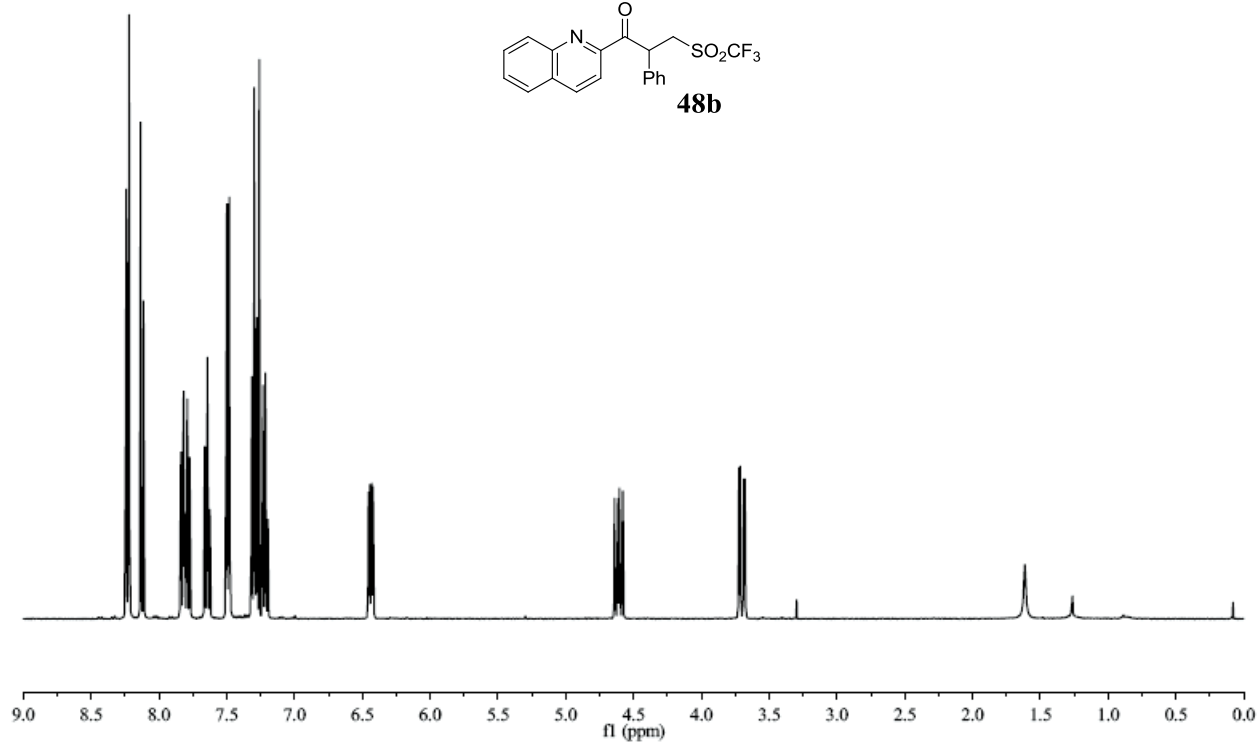
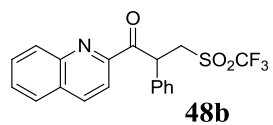


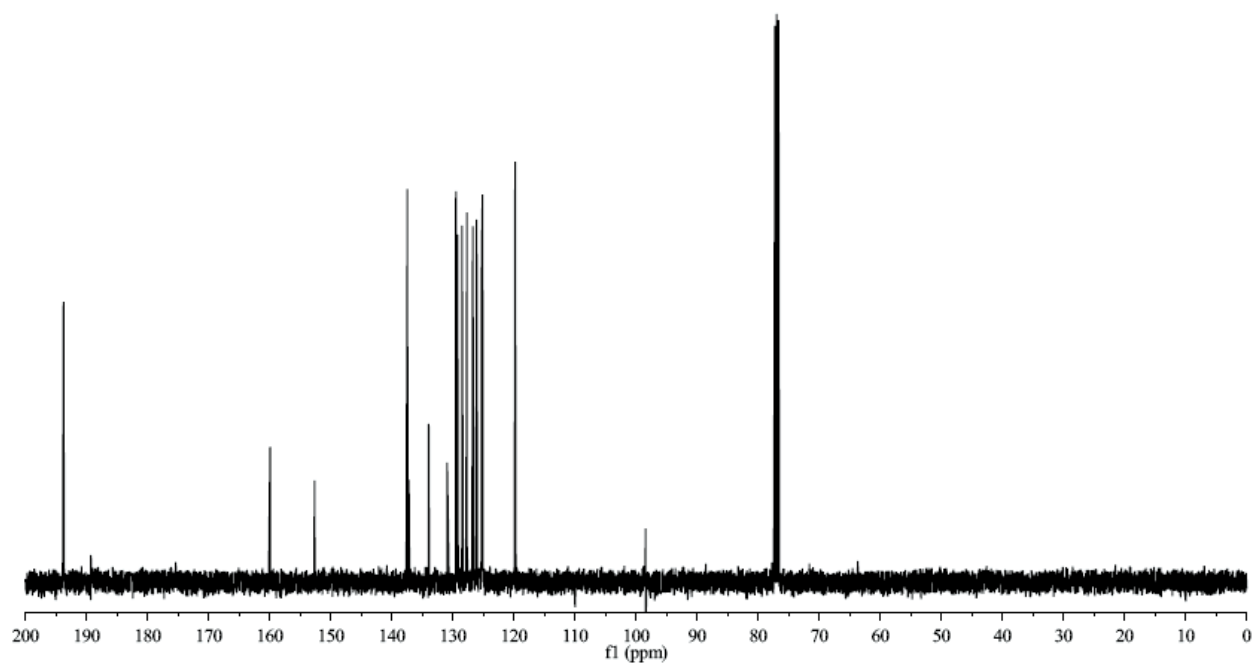
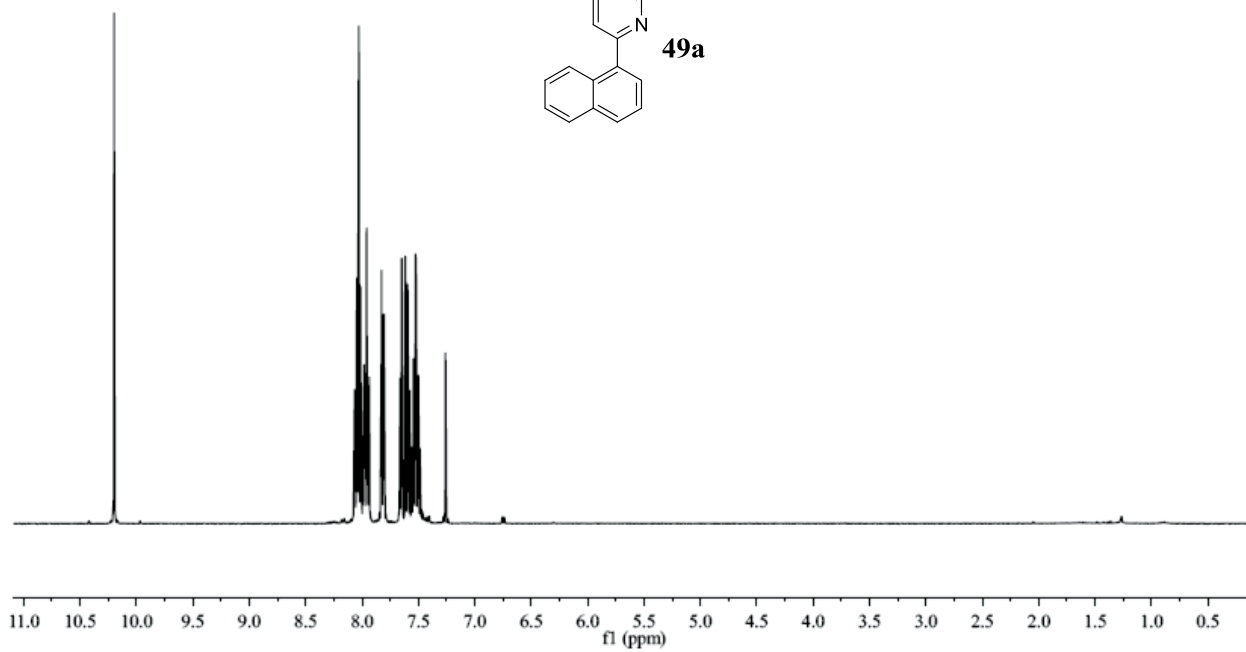
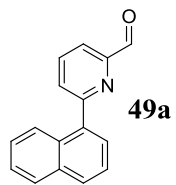


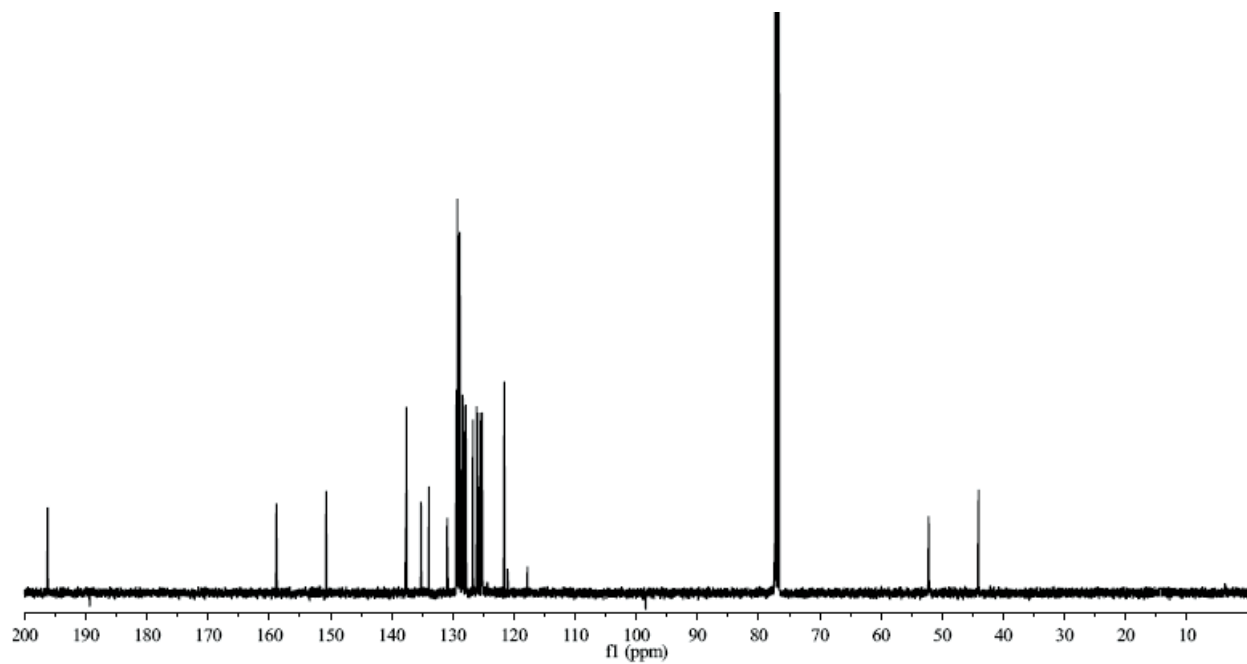
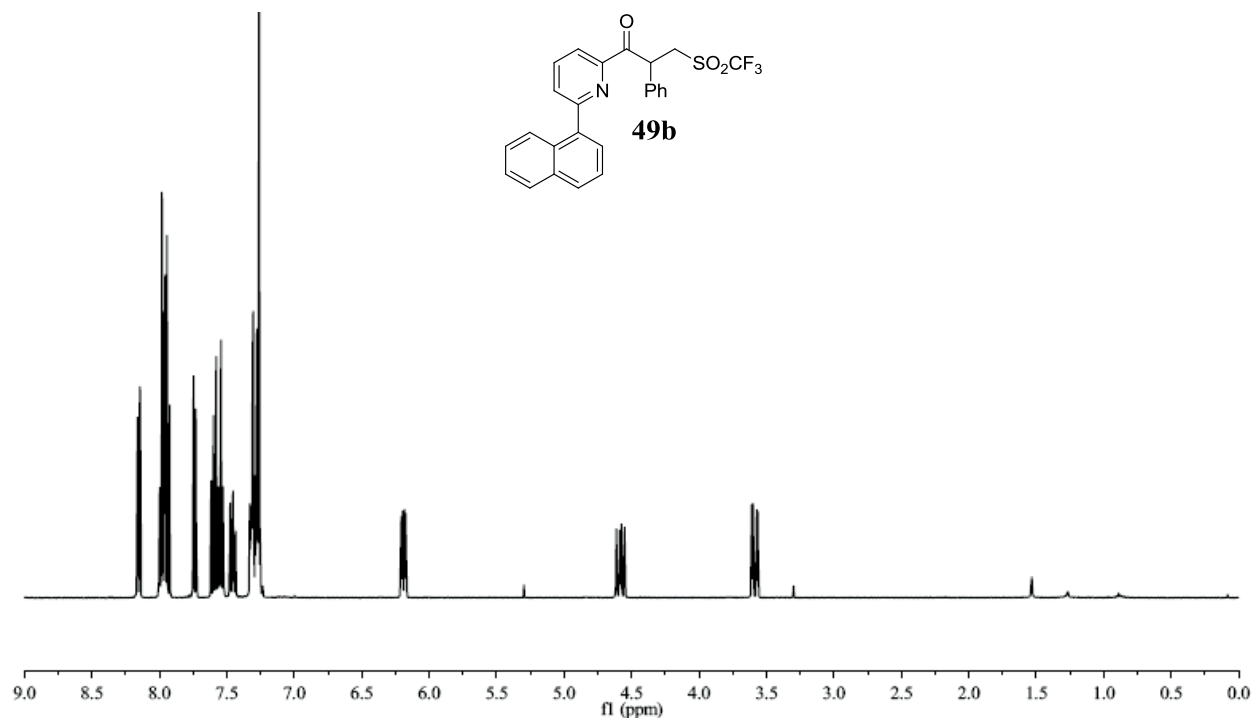
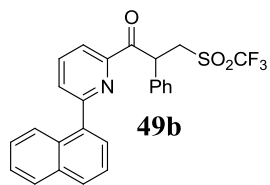


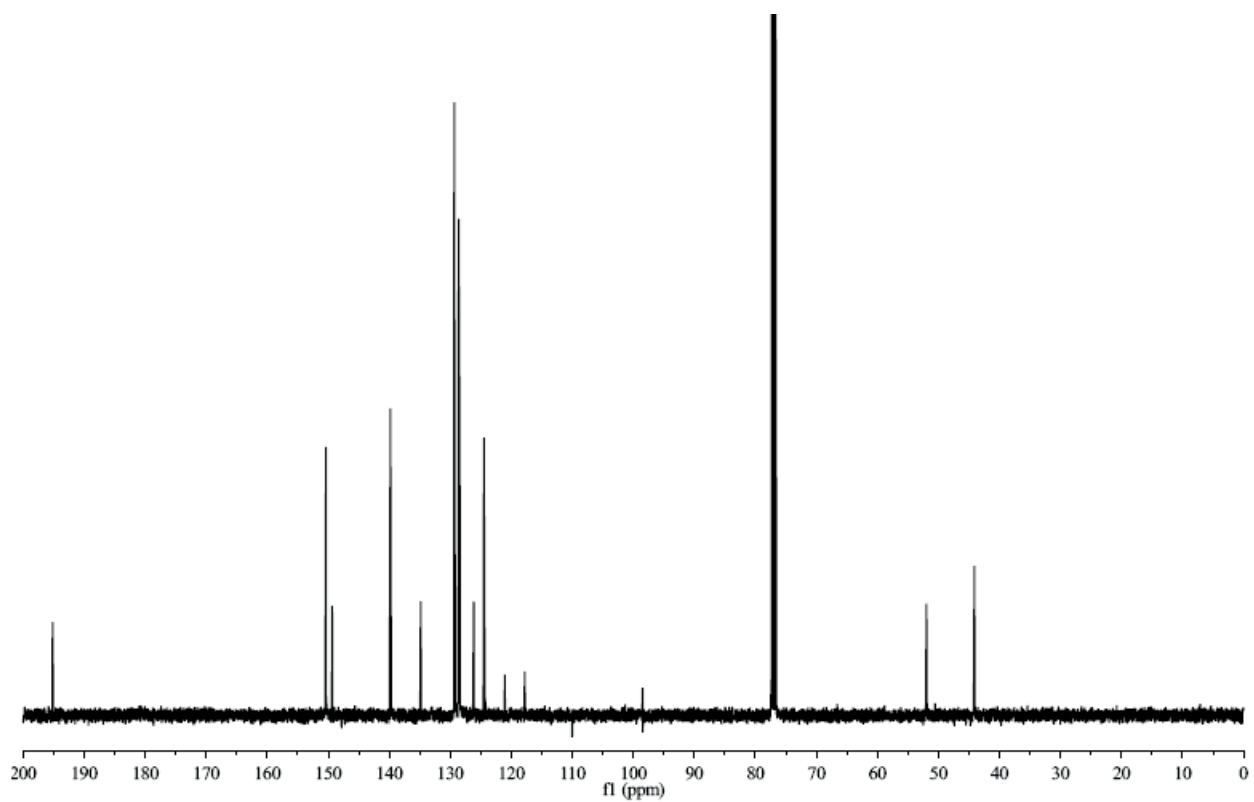
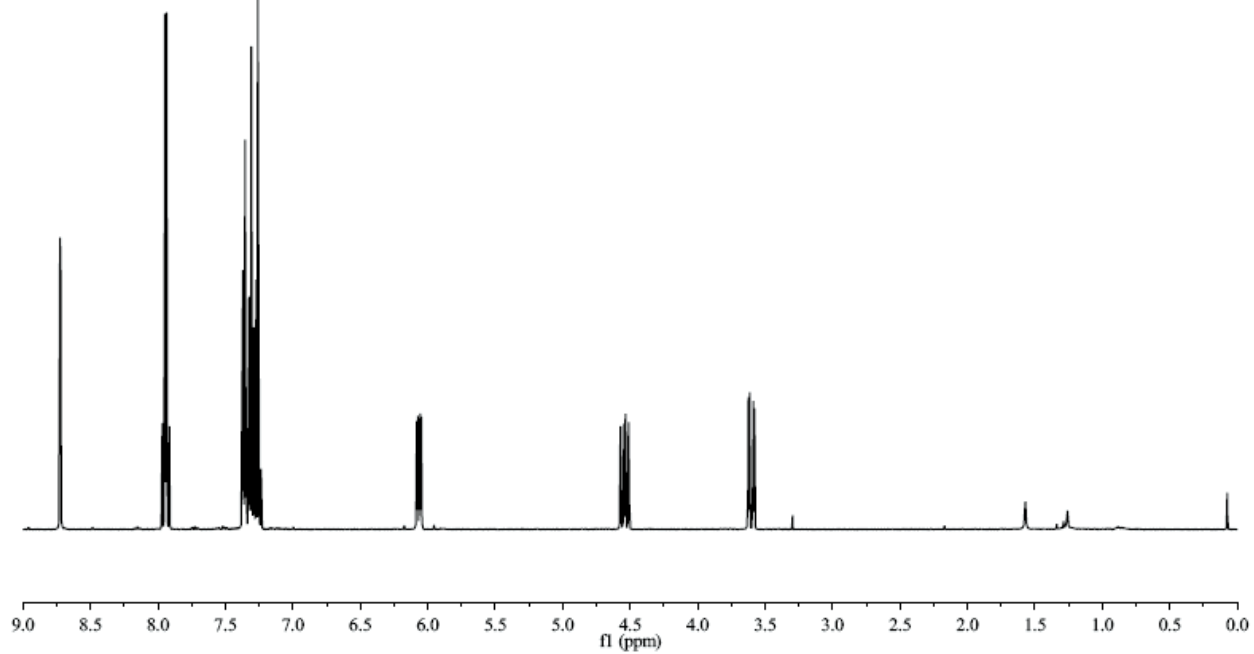
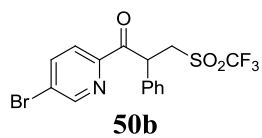












Appendix 2: Chapter 2 Experimental

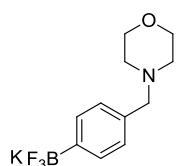
The Development of an Asymmetric Intermolecular Stetter Reaction

General Methods. All reactions were carried out under an atmosphere of argon in flame or oven-dried glassware with magnetic stirring. Commercial reagents were purchased from Sigma-Aldrich or Alfa Aesar and used without further purification, unless otherwise indicated.

Tetrahydrofuran, diethylether, and dichloromethane were degassed with argon and passed through two columns of neutral alumina. Toluene was degassed with argon and passed through one column of neutral alumina and one column of Q5 reactant. Methanol and acetone were purchased from Fisher Scientific and dried with activated 3Å molecular sieves. Column chromatography was performed on EM Science silica gel 60 (230-400 mesh). Thin layer chromatography was performed on SiliCycle® 250µm 60A plates. Visualization was accomplished with UV light or either KMnO₄ or *p*-anisaldehyde stain, followed by heating.

¹H, ¹³C, and ¹⁹F NMR spectra were recorded on a Varian 300 or 400 spectrometer at ambient temperature. All ¹H and ¹³C NMR spectra are referenced to TMS or the residual solvent signal. Data for ¹H NMR are reported as follows: chemical shift in parts per million (δ, ppm), multiplicity (s = singlet, bs = broad singlet, d = doublet, t = triplet, q = quartet, and m = multiplet), coupling constants (Hz), integration. ¹³C NMR data was recorded at 75 or 100 MHz, and are reported as follows: chemical shift (δ, ppm). ¹⁹F NMR data was recorded at 376 or 282 MHz, and are reported either as (δ, ppm), or as follows for spectra containing multiple signals: chemical shift (δ, ppm), multiplicity (s = singlet, d = doublet, t = triplet, q = quartet, m = multiplet), coupling constant (Hz), integration.

Melting points were measured with a MelTemp II melting point apparatus outfitted with an Omega type K thermocouple, and are uncorrected. Infrared spectra were obtained on a Nicolet Avatar 320 FT-IR spectrometer. High resolution mass spectra (HRMS) were recorded on an Agilent Technologies 6210 Time of Flight LC/MS. Low resolution mass spectra (LRMS) were recorded on an Agilent Technologies 6130 Quadrupole LC/MS.



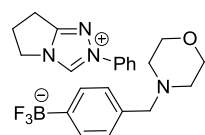
Potassium trifluoro(4-(morpholinomethyl)phenyl)borate (4): Prepared via a slightly modified literature procedure.¹ Potassium trifluoro(4-formylphenyl)borate (212 mg, 1.00 mmol), which was prepared from potassium trifluoro(4-formylphenyl)borate (**3**) via a known procedure,² was added to a roundbottom flask charged with KHF₂ (312 mg, 4.0 mmol) and a stirbar.

Methanol (8 mL) was added by syringe, followed by morpholine (173 µL, 2.00 mmol), and the slurry was stirred at 23 °C for 4 h. Pyridine-borane complex (8M, 123 µL, 0.98 mmol) was added dropwise over 5 minutes, and the reaction was stirred for another 18 h. The solvent was then removed, and the resulting white solid was triturated with ethyl ether (2 × 20 mL). Extraction with 10% methanol/acetone (3 × 20 mL) was followed by concentration to nearly the point of saturation. Ethyl ether was added to force precipitation, which was collected by filtration to afford 213 mg (75% yield) of **4** as a white solid. ¹H NMR (400 MHz, acetone-*d*₆) δ 7.42 (d, *J* =

7.7 Hz, 2H), 7.06 (d, $J = 7.5$ Hz, 2H), 3.58 (t, $J = 4.7$ Hz, 4H), 3.38 (s, 2H), 2.35 (t, $J = 4.5$ Hz, 4H); ^{13}C NMR (100 MHz; acetone- d_6): δ 135.2, 132.4, 128.1, 67.5, 64.5, 54.5; ^{19}F NMR (376 MHz; acetone- d_6): δ -142.5; IR (NaCl, acetone- d_6) 2938, 2856, 2808, 1703, 1455, 1397, 1222, 1200, 1113, 959 cm^{-1} ; LRMS (ES-) calcd for $\text{C}_{11}\text{H}_{14}\text{BF}_3\text{KNO}^-$ 244.11, found 244.1.

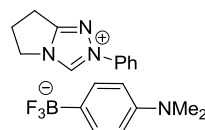
General procedure for counterion exchange to form base-activated NHC pre-catalysts

Triazolium pre-catalyst **7** (1.0 equiv.) and an aryltrifluoroborate (1.0 equiv.) were carefully weighed, then added to a screw-cap vial equipped with a stir bar. Under argon, dry acetone was added, and the vial capped. This mixture was stirred at 23 °C and then filtered through a 0.45 μm nylon syringe filter. The vial and syringe filter were rinsed with an equal amount of dry acetone. Evaporation of solvent afforded analytically pure product.



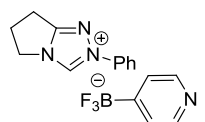
2-Phenyl-6,7-dihydro-5H-pyrrolo[2,1-c][1,2,4]triazol-2-ium trifluoro(4-(morpholinomethyl)phenyl)borate (8): According to the general procedure, **7** (15.6 mg, 0.0704 mmol) and **4** (20.0 mg, 0.0706 mmol) were stirred in 0.5 mL of acetone for 43 h. Upon work-up, 26 mg (86% yield) of **8** was isolated as a

yellow oil. ^1H NMR (400 MHz, acetone- d_6) δ 10.46 (s, 1H), 7.94-7.92 (m, 2H), 7.70-7.61 (m, 3H), 7.40 (d, $J = 7.4$ Hz, 2H), 7.04 (d, $J = 7.5$ Hz, 2H), 4.61-4.57 (m, 2H), 3.59 (t, $J = 4.7$ Hz, 4H), 3.38 (s, 2H), 3.33-3.28 (m, 2H), 2.95-2.87 (quintet, $J = 7.5$ Hz, 2H), 2.36 (t, $J = 4.5$ Hz, 4H); ^{13}C NMR (100 MHz; acetone- d_6): δ 135.5, 132.4, 131.4, 131.1, 128.1, 121.9, 67.4, 64.4, 54.5, 48.4, 27.6, 22.4; ^{19}F NMR (376 MHz; acetone- d_6): δ -141.9; IR (NaCl, acetone- d_6) 3133, 3032, 2958, 2855, 2810, 1700, 1594, 1455, 1392, 1216, 1189, 1116, 973 cm^{-1} .



2-Phenyl-6,7-dihydro-5H-pyrrolo[2,1-c][1,2,4]triazol-2-ium (4-(dimethylamino)phenyl) trifluoroborate (11b): According to the general procedure, **7** (15.5 mg, 0.0699 mmol) and **11a** (15 mg, 0.0665 mmol) were stirred in 1.0 mL of acetone for 8 h. Upon work-up, 18 mg (72% yield) of **11b**

was isolated as a colorless oil. ^1H NMR (300 MHz, acetone- d_6) δ 10.25 (s, 1H), 7.92-7.88 (m, 2H), 7.70-7.62 (m, 3H), 7.29 (d, $J = 8.4$ Hz, 2H), 6.54 (d, $J = 8.2$ Hz, 2H), 4.52 (t, $J = 7.4$ Hz, 2H), 3.27 (t, $J = 7.7$ Hz, 2H), 2.91 (quintet, $J = 7.6$ Hz, 2H), 2.78 (s, 6H); IR (NaCl, acetone- d_6) 3080, 2971, 2886, 2803, 1700, 1602, 1518, 1443, 1392, 1343, 1294, 1217, 1190, 1156, 972 cm^{-1} .

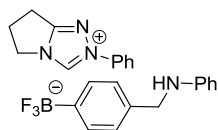


2-Phenyl-6,7-dihydro-5H-pyrrolo[2,1-c][1,2,4]triazol-2-ium

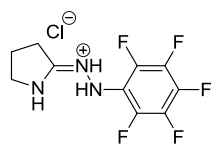
trifluoro(pyridin-4-yl)borate (12b): According to the general procedure, **7** (15.8 mg, 0.0713 mmol) and **12a** (13.2 mg, 0.0714 mmol) were stirred in 1.0

mL of acetone for 8 h. Upon work-up, 23 mg (96% yield) of **12b** was isolated as a colorless oil. Rf (95:5 CH_2Cl_2 to methanol) = 0.05; ^1H NMR (400 MHz, acetone- d_6) δ 10.43 (s, 1H), 8.26 (d, $J = 5.4$ Hz, 2H), 7.93-7.91 (m, 2H), 7.69-7.61 (m, 3H), 7.35 (d, $J = 4.5$ Hz, 2H), 4.60 (t, $J = 7.4$ Hz, 2H), 3.30 (t, $J = 7.7$ Hz, 2H), 2.91 (quintet, $J = 7.5$ Hz, 2H); ^{13}C NMR (100 MHz; acetone- d_6): δ 164.5, 147.9, 138.9, 136.9, 131.4, 131.0, 128.1, 121.9, 48.4, 27.6, 22.3; ^{19}F

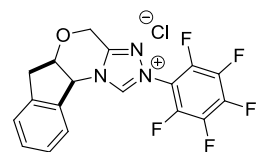
NMR (376 MHz; acetone-*d*₆): δ -144.3; IR (NaCl, acetone-*d*₆) 3134, 3060, 2975, 1594, 1439, 1391, 1296, 1198, 1090, 988 cm⁻¹.



2-Phenyl-6,7-dihydro-5H-pyrrolo[2,1-c][1,2,4]triazol-2-ium trifluoro(4-((phenylamino)methyl)phenyl)borate (13b): According to the general procedure, **7** (16.0 mg, 0.0722 mmol) and **13a** (20.6 mg, 0.0712 mmol) were stirred in 1.0 mL of acetone for 8 h. Upon work-up, 23 mg (74% yield) of **13b** was isolated as a colorless oil. ¹H NMR (400 MHz, acetone-*d*₆) δ 10.12 (s, 1H), 7.888-7.86 (m, 2H), 7.65-7.59 (m, 3H), 7.38 (d, *J* = 7.8 Hz, 2H), 7.10-7.02 (m, 4H), 6.66-6.63 (m, 2H), 6.53 (tt, *J* = 7.3, 1.1 Hz, 1H), 5.16 (bs, 1H), 4.42 (t, *J* = 7.4 Hz, 2H), 4.18 (s, 2H), 3.14 (t, *J* = 7.7 Hz, 2H), 2.74 (quintet, *J* = 7.5 Hz, 2H); ¹³C NMR (100 MHz; acetone-*d*₆): δ 164.2, 150.1, 138.8, 137.2, 136.9, 132.5, 131.3, 131.0, 129.6, 126.5, 121.8, 116.9, 113.4, 48.6, 48.2, 27.4, 22.2; ¹⁹F NMR (376 MHz; acetone-*d*₆): δ -141.9; IR (NaCl, acetone-*d*₆) 3408, 3022, 2926, 2850, 1699, 1602, 1508, 1434, 1391, 1326, 1251, 1213, 1183, 952 cm⁻¹.



(Z)-2-(Perfluorophenyl)-1-(pyrrolidin-2-ylidene)hydrazin-1-ium chloride (16): ¹H NMR (400 MHz, DMSO-*d*₆) δ 12.31 (s, 1H), 10.45 (s, 1H), 9.08 (s, 1H), 3.63 (t, *J* = 7.1 Hz, 2H), 2.91 (t, *J* = 8.0 Hz, 2H), 2.18 (quintet, *J* = 7.4 Hz, 2H); ¹⁹F NMR (376 MHz; DMSO-*d*₆): δ -155.7 (d, *J* = 24.8 Hz, 2F), -163.9 (td, *J* = 24.4, 3.6 Hz, 2F), -166.2 (t, *J* = 24.4 Hz, 1F); IR (NaCl, methanol) 3412, 3167, 2990, 2908, 2760, 1701, 1522, 1311, 1112, 1027, 972 cm⁻¹; LRMS (ES⁺) calcd for C₁₀H₉F₅N₃⁺ 266.07, found 266.1.

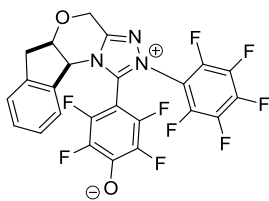


(5aR,10bS)-2-(Perfluorophenyl)-4,5a,6,10b-tetrahydroindeno[2,1-b][1,2,4]triazolo[4,3-d][1,4]oxazin-2-ium chloride (25): ¹H NMR (400 MHz, methanol-*d*₄) δ 7.59 (d, *J* = 7.6 Hz, 1H), 7.44-7.34 (m, 3H), 6.17 (d, *J* = 4.2 Hz, 1H), 5.28 (d, *J* = 16.4 Hz, 1H), 5.13 (d, *J* = 16.4 Hz, 1H), 5.05 (t, *J* = 4.3 Hz, 1H), 3.50 (dd, *J* = 17.1, 5.1 Hz, 1H), 3.30 (d, *J* = 16.8 Hz, 1H); ¹³C NMR (100 MHz; methanol-*d*₄): δ 152.7, 142.0, 136.2, 130.9, 128.7, 126.8, 125.0, 78.7, 63.8, 61.1, 38.2; ¹⁹F NMR (376 MHz; methanol-*d*₄): δ -147.2 – -147.3 (m, 2F), -150.07 (tt, *J* = 22.2, 4.0 Hz, 1F), -161.9 – -162.1 (m, 2F); IR (NaCl, methanol-*d*₄) 3046, 2914, 1595, 1527, 1481, 1465, 1386, 1075, 1001 cm⁻¹; LRMS (ES⁺) calcd for C₁₈H₁₁F₅N₃O⁺ 380.08, found 380.1.



(5aR,10bS)-2-(Perfluorophenyl)-1,2,4,5a,6,10b-hexahydroindeno[2,1-b][1,2,4]triazolo[4,3-d][1,4]oxazin-1-ol (29): Rf (1:1 hexanes to ethyl acetate) = 0.20; ¹H NMR (300 MHz, CDCl₃) δ 8.26 (d, *J* = 12.5 Hz, 1H), 7.30 (bs, 4H), 7.00 (bs, 0.5H), 6.31 (bs, 0.5H), 4.74-4.71 (m, 1H), 4.63 (t, *J* = 4.7 Hz, 1H), 4.38-4.21 (m, 2H), 3.26 (dd, *J* = 16.9, 5.1 Hz, 1H), 3.12 (d, *J* = 16.9 Hz, 1H); ¹³C NMR (75 MHz; CDCl₃): δ 163.8, 158.5, 139.3, 128.7, 128.4, 127.4, 125.3, 123.3, 64.3, 57.2, 37.9, 29.3; ¹⁹F NMR (282 MHz; CDCl₃): δ -142.8 (s, 0.5F), -143.2 (s, 0.5F), -145.8 (d, *J* = 19.8

Hz, 1F), -152.6 (t, $J = 21.4$ Hz, 0.5F), -153.4 (t, $J = 21.4$ Hz, 0.5F), -160.8 (t, $J = 19.5$ Hz, 1F), -161.5 (s, 1F); LRMS (ES+) calcd for $C_{18}H_{12}F_5N_3O_2$ 397.09, found 398.1.



2,3,5,6-Tetrafluoro-4-((5aR,10bS)-2-(perfluorophenyl)-4,5a,6,10b-tetrahydroindeno[2,1-b][1,2,4]triazolo[4,3-d][1,4]oxazin-2-ium-1-yl)phenolate (30): R_f (95:5 CH₂Cl₂ to methanol) = 0.08; ¹H NMR (300 MHz, CDCl₃) δ 7.35 (d, $J = 4.1$ Hz, 2H), 7.21-7.13 (m, 1H), 6.71 (d, $J = 7.8$ Hz, 1H), 6.01 (t, $J = 3.5$ Hz, 1H), 5.17-5.05 (m, 3H), 3.43 (dd, $J = 17.0, 4.5$ Hz, 1H), 3.34 (d, $J = 17.0$ Hz, 1H), 1.86-1.62 (bs, 2H – from H₂O); ¹³C NMR (100 MHz; CDCl₃): δ 150.7, 139.7, 134.4, 130.3, 128.6, 126.0, 123.8, 98.7, 77.8, 62.9, 62.8, 60.1, 36.9; ¹⁹F NMR (376 MHz; CDCl₃): δ -142.3 – -142.4 (m, 1F), -144.1 (tt, $J = 21.6, 4.4$ Hz, 1F), -144.2 – -144.3 (m, 1F), -144.6 – -144.7 (m, 1F), -147.3 – -147.4 (m, 1F), -156.5 (td, $J = 21.8, 6.8$ Hz, 1F), -156.8 (td, $J = 21.8, 6.8$ Hz, 1F), -163.2 (t, $J = 23.0$ Hz, 1F), -163.5 (t, $J = 23.0$ Hz, 1F); IR (NaCl, CDCl₃) 2926, 1650, 1579, 1508, 1481, 1432, 1299, 1093, 972 cm⁻¹; HRMS (ESI) calcd for $C_{24}H_{10}F_9N_3O_2$ 543.0629, found 544.0712.

References

- 1.) Molander, G. Cooper, D. *J. Org. Chem.* **2008**, 73, 3885–3891.
- 2.) Cousin, D.; Mann, J.; Nieuwenhuyzen, M. van den Berg, H. *Org. Biomol. Chem.*, **2006**, 4, 54–62.

X-Ray Crystal Structure: Chapter 2, Compound **8**

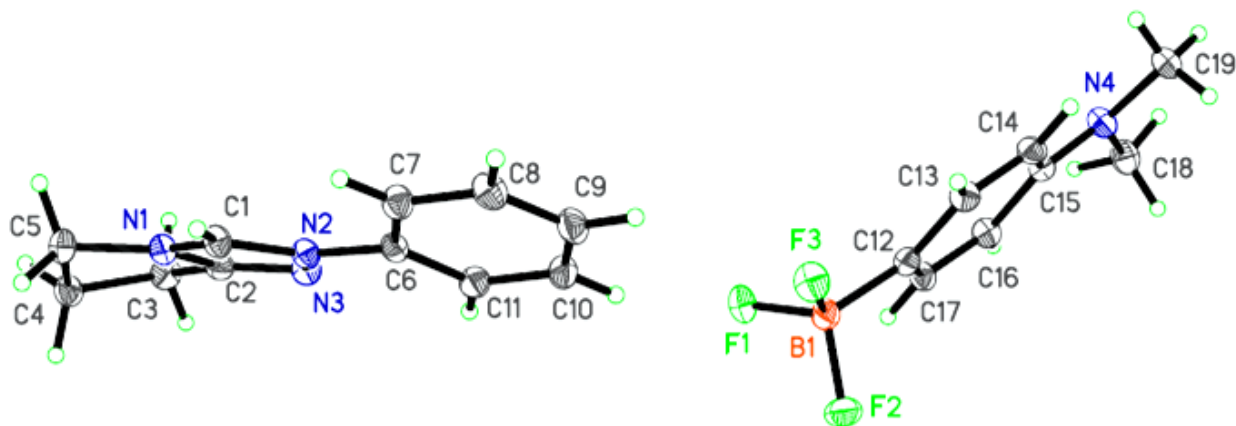


Table A.2.1 Crystal data and structure refinement for **8**

Identification code	rovis123	
Empirical formula	C ₁₉ H ₂₂ BF ₃ N ₄	
Formula weight	374.22	
Temperature	120 K	
Wavelength	0.71073 Å	
Crystal system	Orthorhombic	
Space group	<i>Pca</i> 2 ₁	
Unit cell dimensions	<i>a</i> = 14.2408(6) Å	∠ = 90°.
	<i>b</i> = 6.4514(3) Å	∠ = 90°.
	<i>c</i> = 19.1609(8) Å	∠ = 90°.
Volume	1760.37(13) Å ³	
<i>Z</i>	4	
Density (calculated)	1.412 Mg/m ³	
Absorption coefficient	0.107 mm ⁻¹	
<i>F</i> (000)	784	
Crystal size	0.22 x 0.22 x 0.14 mm ³	
Theta range for data collection	2.13 to 30.59°.	
Index ranges	-19 ≤ <i>h</i> ≤ 20, -9 ≤ <i>k</i> ≤ 9, -27 ≤ <i>l</i> ≤ 27	
Reflections collected	36075	
Independent reflections	5356 [R(int) = 0.0506]	
Completeness to theta = 30.59°	99.8 %	
Absorption correction	Semi-empirical from equivalents	
Max. and min. transmission	0.9851 and 0.9767	
Refinement method	Full-matrix least-squares on <i>F</i> ²	
Data / restraints / parameters	5356 / 1 / 246	

Goodness-of-fit on F^2	1.095
Final R indices [$I > 2\sigma(I)$]	R1 = 0.0387, wR2 = 0.0957
R indices (all data)	R1 = 0.0526, wR2 = 0.1123
Absolute structure parameter	0.0(5)
Largest diff. peak and hole	0.282 and -0.327 e.Å ⁻³

Table A.2.2. Atomic coordinates ($\times 10^4$) and equivalent isotropic displacement parameters ($\text{Å}^2 \times 10^3$) for compound **8**. U(eq) is defined as one third of the trace of the orthogonalized U^{ij} tensor.

	x	y	z	U(eq)
B(1)	2465(1)	2645(3)	1756(1)	19(1)
C(1)	1132(1)	8294(3)	5822(1)	18(1)
C(2)	424(1)	5412(3)	6081(1)	18(1)
C(3)	-113(1)	4234(3)	6620(1)	21(1)
C(4)	132(1)	5469(3)	7290(1)	22(1)
C(5)	361(1)	7701(3)	7052(1)	21(1)
C(6)	1552(1)	7328(3)	4602(1)	17(1)
C(7)	1736(1)	9338(3)	4394(1)	21(1)
C(8)	2067(1)	9674(3)	3719(1)	24(1)
C(9)	2207(1)	8021(3)	3269(1)	23(1)
C(10)	2038(1)	6016(3)	3491(1)	22(1)
C(11)	1707(1)	5657(3)	4165(1)	20(1)
C(12)	1958(1)	1989(3)	1041(1)	17(1)
C(13)	1827(1)	3355(3)	482(1)	20(1)
C(14)	1368(1)	2793(3)	-131(1)	19(1)
C(15)	998(1)	795(3)	-218(1)	18(1)
C(16)	1135(1)	-623(3)	336(1)	19(1)
C(17)	1595(1)	-9(3)	940(1)	19(1)
C(18)	349(1)	-1924(3)	-975(1)	25(1)
C(19)	476(1)	1667(3)	-1401(1)	25(1)
F(1)	1895(1)	2198(2)	2343(1)	25(1)
F(2)	3322(1)	1525(2)	1857(1)	29(1)
F(3)	2684(1)	4786(2)	1776(1)	26(1)
N(1)	665(1)	7317(2)	6326(1)	18(1)
N(2)	1162(1)	6974(2)	5286(1)	17(1)
N(3)	715(1)	5125(2)	5439(1)	19(1)
N(4)	500(1)	244(2)	-815(1)	22(1)

Table A.2.3. Bond lengths [\AA] and angles [$^\circ$] for compound **8**.

B(1)-F(3)	1.416(2)
B(1)-F(1)	1.417(2)
B(1)-F(2)	1.431(2)
B(1)-C(12)	1.606(2)
C(1)-N(1)	1.331(2)
C(1)-N(2)	1.335(2)
C(2)-N(3)	1.312(2)
C(2)-N(1)	1.360(2)
C(2)-C(3)	1.492(2)
C(3)-C(4)	1.552(2)
C(4)-C(5)	1.545(3)
C(5)-N(1)	1.4790(19)
C(6)-C(7)	1.382(2)
C(6)-C(11)	1.383(2)
C(6)-N(2)	1.4406(19)
C(7)-C(8)	1.393(2)
C(8)-C(9)	1.386(3)
C(9)-C(10)	1.383(3)
C(10)-C(11)	1.394(2)
C(12)-C(13)	1.399(2)
C(12)-C(17)	1.402(2)
C(13)-C(14)	1.393(2)
C(14)-C(15)	1.403(2)
C(15)-N(4)	1.392(2)
C(15)-C(16)	1.414(2)
C(16)-C(17)	1.389(2)
C(18)-N(4)	1.448(2)
C(19)-N(4)	1.450(2)
N(2)-N(3)	1.3837(19)
F(3)-B(1)-F(1)	107.65(14)
F(3)-B(1)-F(2)	107.50(14)
F(1)-B(1)-F(2)	106.15(14)
F(3)-B(1)-C(12)	112.25(14)
F(1)-B(1)-C(12)	111.53(13)
F(2)-B(1)-C(12)	111.46(13)
N(1)-C(1)-N(2)	105.77(14)
N(3)-C(2)-N(1)	111.77(14)

N(3)-C(2)-C(3)	137.63(16)
N(1)-C(2)-C(3)	110.59(14)
C(2)-C(3)-C(4)	101.31(13)
C(5)-C(4)-C(3)	106.37(13)
N(1)-C(5)-C(4)	100.58(13)
C(7)-C(6)-C(11)	121.73(15)
C(7)-C(6)-N(2)	118.97(14)
C(11)-C(6)-N(2)	119.27(15)
C(6)-C(7)-C(8)	118.59(16)
C(9)-C(8)-C(7)	120.43(17)
C(10)-C(9)-C(8)	120.21(16)
C(9)-C(10)-C(11)	119.95(16)
C(6)-C(11)-C(10)	119.07(17)
C(13)-C(12)-C(17)	115.17(14)
C(13)-C(12)-B(1)	123.17(15)
C(17)-C(12)-B(1)	121.65(14)
C(14)-C(13)-C(12)	122.95(16)
C(13)-C(14)-C(15)	121.04(15)
N(4)-C(15)-C(14)	121.55(14)
N(4)-C(15)-C(16)	121.43(15)
C(14)-C(15)-C(16)	117.01(14)
C(17)-C(16)-C(15)	120.39(16)
C(16)-C(17)-C(12)	123.42(15)
C(1)-N(1)-C(2)	107.75(13)
C(1)-N(1)-C(5)	138.55(15)
C(2)-N(1)-C(5)	113.69(14)
C(1)-N(2)-N(3)	111.84(12)
C(1)-N(2)-C(6)	127.66(14)
N(3)-N(2)-C(6)	120.44(13)
C(2)-N(3)-N(2)	102.88(13)
C(15)-N(4)-C(18)	119.73(14)
C(15)-N(4)-C(19)	119.11(14)
C(18)-N(4)-C(19)	116.39(14)

Symmetry transformations used to generate equivalent atoms:

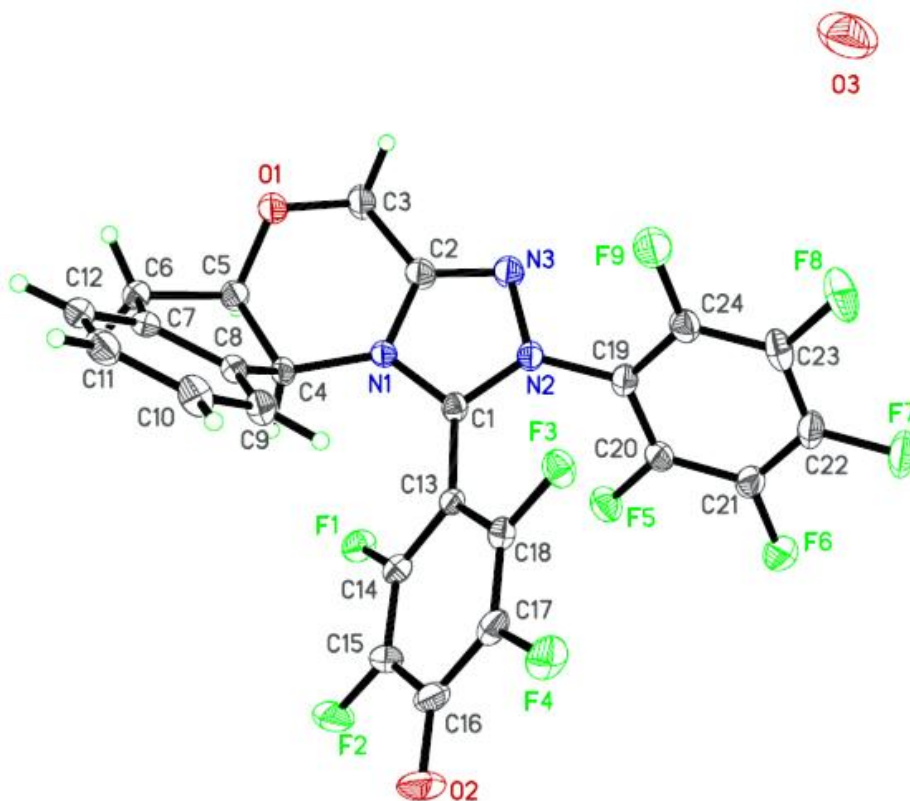
Table A.2.4. Anisotropic displacement parameters ($\text{\AA}^2 \times 10^3$) for compound **8**. The anisotropic displacement factor exponent takes the form: $-2h^2a^2U^{11} + \dots + 2hka^*b^*U^{12}$

	U11	U22	U33	U23	U13	U12
B(1)	21(1)	18(1)	18(1)	-2(1)	0(1)	1(1)
C(1)	20(1)	18(1)	17(1)	-1(1)	-1(1)	-4(1)
C(2)	18(1)	16(1)	19(1)	0(1)	-2(1)	-1(1)
C(3)	22(1)	20(1)	22(1)	2(1)	2(1)	-2(1)
C(4)	22(1)	26(1)	17(1)	2(1)	2(1)	0(1)
C(5)	24(1)	23(1)	17(1)	-2(1)	4(1)	-2(1)
C(6)	17(1)	20(1)	15(1)	0(1)	-2(1)	-1(1)
C(7)	25(1)	18(1)	19(1)	-1(1)	0(1)	-1(1)
C(8)	28(1)	21(1)	21(1)	5(1)	-1(1)	-4(1)
C(9)	22(1)	31(1)	17(1)	2(1)	1(1)	-2(1)
C(10)	23(1)	26(1)	19(1)	-5(1)	-1(1)	1(1)
C(11)	22(1)	17(1)	21(1)	-1(1)	0(1)	0(1)
C(12)	16(1)	18(1)	18(1)	-1(1)	2(1)	0(1)
C(13)	23(1)	15(1)	21(1)	0(1)	1(1)	-1(1)
C(14)	21(1)	17(1)	20(1)	5(1)	1(1)	2(1)
C(15)	17(1)	19(1)	17(1)	0(1)	1(1)	3(1)
C(16)	21(1)	16(1)	20(1)	1(1)	0(1)	-3(1)
C(17)	22(1)	19(1)	17(1)	3(1)	1(1)	-1(1)
C(18)	29(1)	27(1)	21(1)	-1(1)	-1(1)	-5(1)
C(19)	27(1)	30(1)	18(1)	2(1)	-4(1)	2(1)
F(1)	30(1)	29(1)	16(1)	1(1)	2(1)	-4(1)
F(2)	24(1)	32(1)	32(1)	-10(1)	-8(1)	9(1)
F(3)	32(1)	19(1)	26(1)	-3(1)	-1(1)	-5(1)
N(1)	19(1)	19(1)	16(1)	-1(1)	-1(1)	-1(1)
N(2)	19(1)	16(1)	16(1)	0(1)	-1(1)	-2(1)
N(3)	22(1)	15(1)	20(1)	1(1)	0(1)	-3(1)
N(4)	26(1)	21(1)	18(1)	1(1)	-3(1)	-1(1)

Table A.2.5. Hydrogen coordinates ($\times 10^4$) and isotropic displacement parameters ($\text{\AA}^2 \times 10^3$) for compound **8**.

	x	y	z	U(eq)
H(1)	1386	9622	5840	22
H(3A)	99	2808	6651	25
H(3B)	-782	4257	6525	25
H(4A)	-396	5470	7610	26
H(4B)	669	4856	7524	26
H(5A)	-188	8589	7071	25
H(5B)	860	8308	7330	25
H(7)	1641	10443	4697	25
H(8)	2196	11016	3570	28
H(9)	2415	8261	2816	28
H(10)	2145	4908	3191	27
H(11)	1592	4313	4319	24
H(13)	2057	4700	522	23
H(14)	1306	3758	-489	23
H(16)	915	-1975	295	23
H(17)	1667	-973	1297	23
H(18A)	939	-2563	-1088	38
H(18B)	-70	-2041	-1365	38
H(18C)	79	-2604	-577	38
H(19A)	255	2995	-1246	37
H(19B)	62	1137	-1753	37
H(19C)	1097	1811	-1591	37

X-Ray Crystal Structure: Chapter 2, Compound **30**



*Note: O3 represents a molecule of H₂O

Table A.2.6. Crystal data and structure refinement for compound **30**

Identification code	rovis129_0m	
Empirical formula	C ₂₄ H ₁₀ F ₉ N ₃ O ₃	
Formula weight	559.35	
Temperature	120 K	
Wavelength	0.71073 Å	
Crystal system	Orthorhombic	
Space group	<i>P</i> 2 ₁ 2 ₁ 2 ₁	
Unit cell dimensions	<i>a</i> = 6.0808(3) Å	∠ = 90°.
	<i>b</i> = 17.0420(7) Å	∠ = 90°.
	<i>c</i> = 20.4648(9) Å	∠ = 90°.
Volume	2120.75(17) Å ³	
Z	4	
Density (calculated)	1.752 Mg/m ³	
Absorption coefficient	0.170 mm ⁻¹	
F(000)	1120	

Crystal size	0.32 x 0.24 x 0.23 mm ³
Theta range for data collection	1.55 to 30.73°.
Index ranges	-8<=h<=8, -24<=k<=24, -29<=l<=29
Reflections collected	46309
Independent reflections	6580 [R(int) = 0.0451]
Completeness to theta = 30.73°	99.8 %
Absorption correction	Semi-empirical from equivalents
Max. and min. transmission	0.9621 and 0.9482
Refinement method	Full-matrix least-squares on F ²
Data / restraints / parameters	6580 / 0 / 352
Goodness-of-fit on F ²	1.105
Final R indices [I>2sigma(I)]	R1 = 0.0410, wR2 = 0.1044
R indices (all data)	R1 = 0.0623, wR2 = 0.1305
Absolute structure parameter	0.3(5)
Largest diff. peak and hole	0.382 and -0.480 e.Å ⁻³

Table A.2.7. Atomic coordinates (x 10⁴) and equivalent isotropic displacement parameters (Å²x 10³) for compound **30**. U(eq) is defined as one third of the trace of the orthogonalized U^{ij} tensor.

	x	y	z	U(eq)
C(1)	3075(3)	2211(1)	2429(1)	16(1)
C(2)	2919(4)	3098(1)	3210(1)	24(1)
C(3)	2600(5)	3402(1)	3887(1)	32(1)
C(4)	2197(4)	1713(1)	3587(1)	18(1)
C(5)	1595(4)	2133(1)	4235(1)	22(1)
C(6)	2156(4)	1523(1)	4756(1)	23(1)
C(7)	4040(3)	1076(1)	4459(1)	21(1)
C(8)	4111(3)	1186(1)	3779(1)	18(1)
C(9)	5681(4)	812(1)	3400(1)	22(1)
C(10)	7256(4)	349(1)	3711(1)	26(1)
C(11)	7206(4)	246(1)	4385(1)	27(1)
C(12)	5577(4)	599(1)	4759(1)	25(1)
C(13)	2999(3)	1496(1)	2052(1)	16(1)
C(14)	1237(3)	966(1)	2116(1)	19(1)
C(15)	1209(4)	253(1)	1809(1)	24(1)
C(16)	2916(4)	-4(1)	1382(1)	26(1)
C(17)	4638(4)	557(1)	1306(1)	23(1)

C(18)	4683(3)	1261(1)	1622(1)	18(1)
C(19)	4012(3)	3169(1)	1556(1)	19(1)
C(20)	2553(4)	3020(1)	1051(1)	20(1)
C(21)	3073(4)	3221(1)	415(1)	24(1)
C(22)	5054(4)	3590(1)	286(1)	26(1)
C(23)	6488(4)	3759(1)	784(1)	26(1)
C(24)	5987(4)	3546(1)	1415(1)	23(1)
F(1)	-517(2)	1179(1)	2476(1)	25(1)
F(2)	-546(2)	-219(1)	1897(1)	35(1)
F(3)	6430(2)	1741(1)	1543(1)	24(1)
F(4)	6317(2)	371(1)	899(1)	32(1)
F(5)	622(2)	2677(1)	1174(1)	27(1)
F(6)	1658(3)	3071(1)	-65(1)	39(1)
F(7)	5571(3)	3787(1)	-326(1)	40(1)
F(8)	8385(2)	4125(1)	655(1)	40(1)
F(9)	7429(2)	3692(1)	1890(1)	35(1)
N(1)	2685(3)	2307(1)	3075(1)	18(1)
N(2)	3521(3)	2938(1)	2206(1)	19(1)
N(3)	3460(3)	3498(1)	2692(1)	26(1)
O(1)	3016(3)	2790(1)	4342(1)	28(1)
O(2)	2877(3)	-663(1)	1099(1)	37(1)
O(3)	2155(5)	7857(2)	1724(2)	91(1)

Table A.2.8. Bond lengths [\AA] and angles [$^\circ$] for compound **30**

C(1)-N(2)	1.348(2)
C(1)-N(1)	1.353(2)
C(1)-C(13)	1.442(2)
C(2)-N(3)	1.303(3)
C(2)-N(1)	1.382(2)
C(2)-C(3)	1.494(3)
C(3)-O(1)	1.421(2)
C(4)-N(1)	1.487(2)
C(4)-C(8)	1.522(3)
C(4)-C(5)	1.551(3)
C(5)-O(1)	1.431(3)
C(5)-C(6)	1.527(3)
C(6)-C(7)	1.504(3)
C(7)-C(12)	1.381(3)

C(7)-C(8)	1.405(3)
C(8)-C(9)	1.385(3)
C(9)-C(10)	1.395(3)
C(10)-C(11)	1.390(3)
C(11)-C(12)	1.389(3)
C(13)-C(14)	1.407(3)
C(13)-C(18)	1.410(3)
C(14)-F(1)	1.346(2)
C(14)-C(15)	1.368(3)
C(15)-F(2)	1.349(3)
C(15)-C(16)	1.425(3)
C(16)-O(2)	1.264(2)
C(16)-C(17)	1.427(3)
C(17)-F(4)	1.354(2)
C(17)-C(18)	1.363(3)
C(18)-F(3)	1.351(2)
C(19)-C(20)	1.385(3)
C(19)-C(24)	1.392(3)
C(19)-N(2)	1.420(2)
C(20)-F(5)	1.336(2)
C(20)-C(21)	1.382(3)
C(21)-F(6)	1.330(3)
C(21)-C(22)	1.384(3)
C(22)-F(7)	1.335(2)
C(22)-C(23)	1.372(3)
C(23)-F(8)	1.337(3)
C(23)-C(24)	1.376(3)
C(24)-F(9)	1.332(2)
N(2)-N(3)	1.379(2)
N(2)-C(1)-N(1)	104.74(16)
N(2)-C(1)-C(13)	126.97(17)
N(1)-C(1)-C(13)	128.28(16)
N(3)-C(2)-N(1)	111.99(17)
N(3)-C(2)-C(3)	127.30(17)
N(1)-C(2)-C(3)	120.70(17)
O(1)-C(3)-C(2)	109.25(16)
N(1)-C(4)-C(8)	115.58(17)
N(1)-C(4)-C(5)	109.61(14)
C(8)-C(4)-C(5)	103.43(16)
O(1)-C(5)-C(6)	106.92(16)

O(1)-C(5)-C(4)	110.45(16)
C(6)-C(5)-C(4)	103.23(15)
C(7)-C(6)-C(5)	103.57(16)
C(12)-C(7)-C(8)	119.83(19)
C(12)-C(7)-C(6)	129.39(18)
C(8)-C(7)-C(6)	110.78(17)
C(9)-C(8)-C(7)	120.96(19)
C(9)-C(8)-C(4)	130.81(18)
C(7)-C(8)-C(4)	108.16(17)
C(8)-C(9)-C(10)	118.6(2)
C(11)-C(10)-C(9)	120.6(2)
C(12)-C(11)-C(10)	120.5(2)
C(7)-C(12)-C(11)	119.53(19)
C(14)-C(13)-C(18)	115.32(16)
C(14)-C(13)-C(1)	121.15(17)
C(18)-C(13)-C(1)	123.48(17)
F(1)-C(14)-C(15)	118.72(19)
F(1)-C(14)-C(13)	118.73(16)
C(15)-C(14)-C(13)	122.51(19)
F(2)-C(15)-C(14)	118.6(2)
F(2)-C(15)-C(16)	118.30(18)
C(14)-C(15)-C(16)	123.1(2)
O(2)-C(16)-C(15)	122.7(2)
O(2)-C(16)-C(17)	124.0(2)
C(15)-C(16)-C(17)	113.28(18)
F(4)-C(17)-C(18)	118.8(2)
F(4)-C(17)-C(16)	117.68(18)
C(18)-C(17)-C(16)	123.53(19)
F(3)-C(18)-C(17)	119.51(18)
F(3)-C(18)-C(13)	118.25(17)
C(17)-C(18)-C(13)	122.20(19)
C(20)-C(19)-C(24)	118.87(18)
C(20)-C(19)-N(2)	120.91(19)
C(24)-C(19)-N(2)	120.21(19)
F(5)-C(20)-C(21)	119.05(19)
F(5)-C(20)-C(19)	120.24(18)
C(21)-C(20)-C(19)	120.7(2)
F(6)-C(21)-C(20)	120.0(2)
F(6)-C(21)-C(22)	120.58(18)
C(20)-C(21)-C(22)	119.4(2)

F(7)-C(22)-C(23)	119.7(2)
F(7)-C(22)-C(21)	119.9(2)
C(23)-C(22)-C(21)	120.42(18)
F(8)-C(23)-C(22)	119.99(19)
F(8)-C(23)-C(24)	119.9(2)
C(22)-C(23)-C(24)	120.1(2)
F(9)-C(24)-C(23)	119.28(19)
F(9)-C(24)-C(19)	120.24(18)
C(23)-C(24)-C(19)	120.5(2)
C(1)-N(1)-C(2)	107.15(15)
C(1)-N(1)-C(4)	129.88(15)
C(2)-N(1)-C(4)	122.91(15)
C(1)-N(2)-N(3)	112.78(15)
C(1)-N(2)-C(19)	127.95(17)
N(3)-N(2)-C(19)	119.27(15)
C(2)-N(3)-N(2)	103.33(15)
C(3)-O(1)-C(5)	111.49(17)

Symmetry transformations used to generate equivalent atoms:

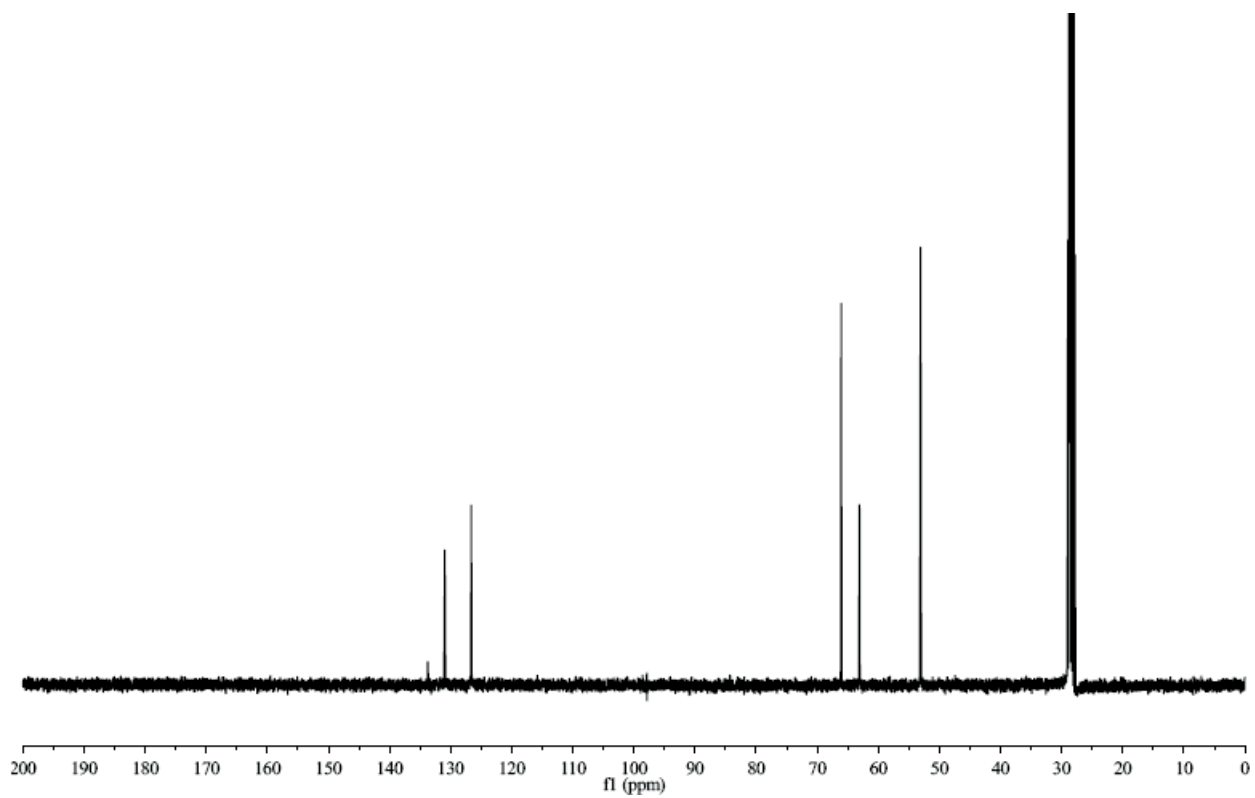
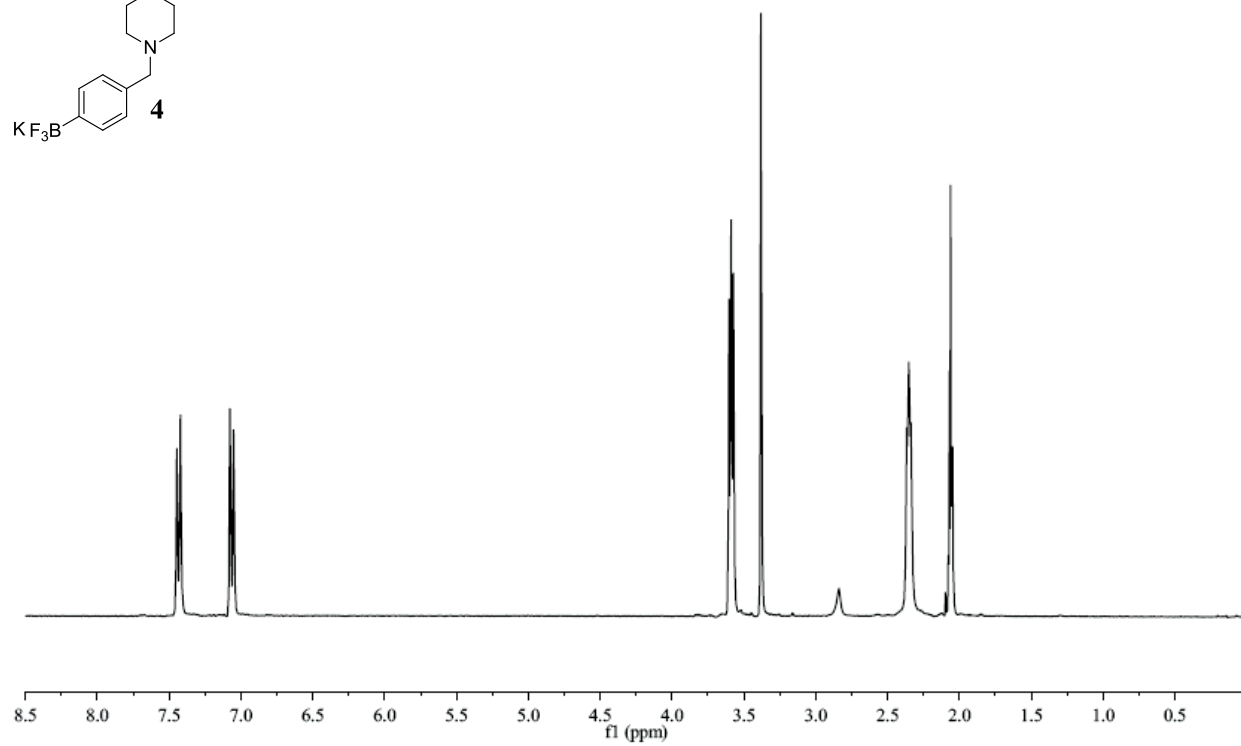
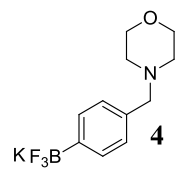
Table A.2.9. Anisotropic displacement parameters ($\text{\AA}^2 \times 10^3$) for compound **30**. The anisotropic displacement factor exponent takes the form: $-2 \sum [h^2 a^* 2U^{11} + \dots + 2 h k a^* b^* U^{12}]$

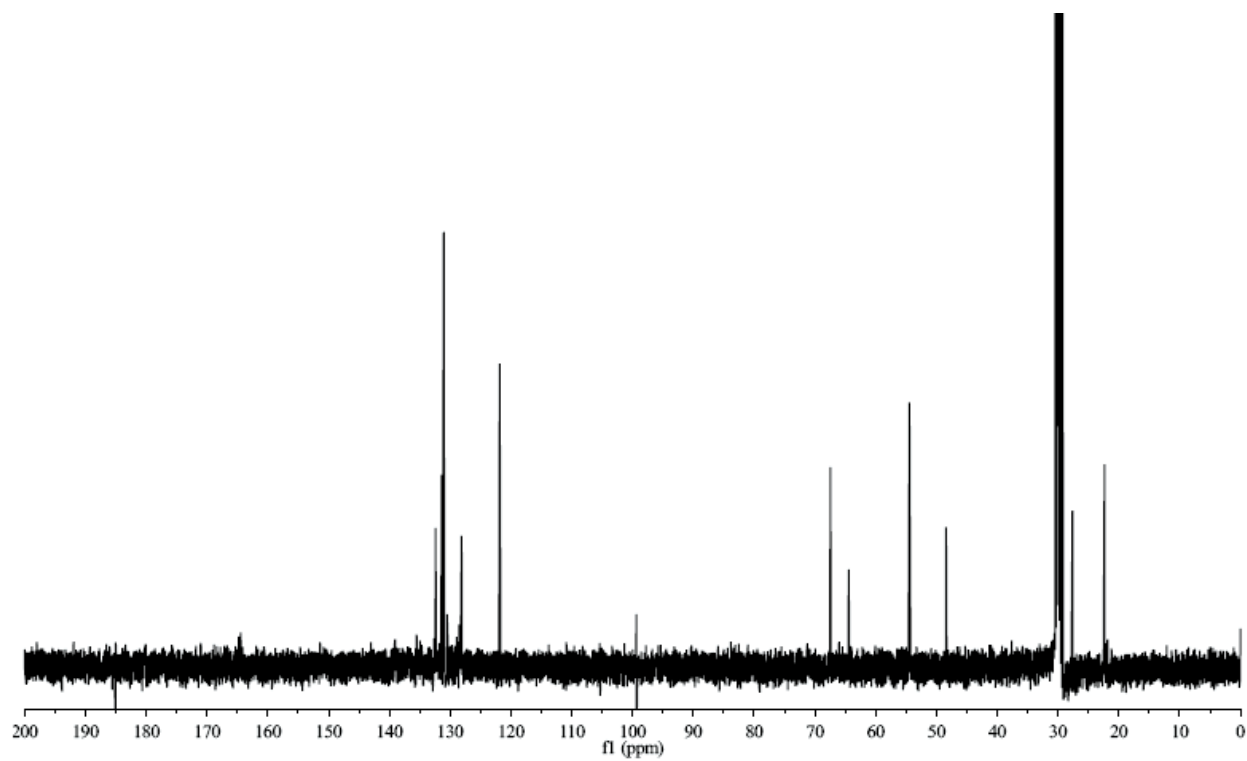
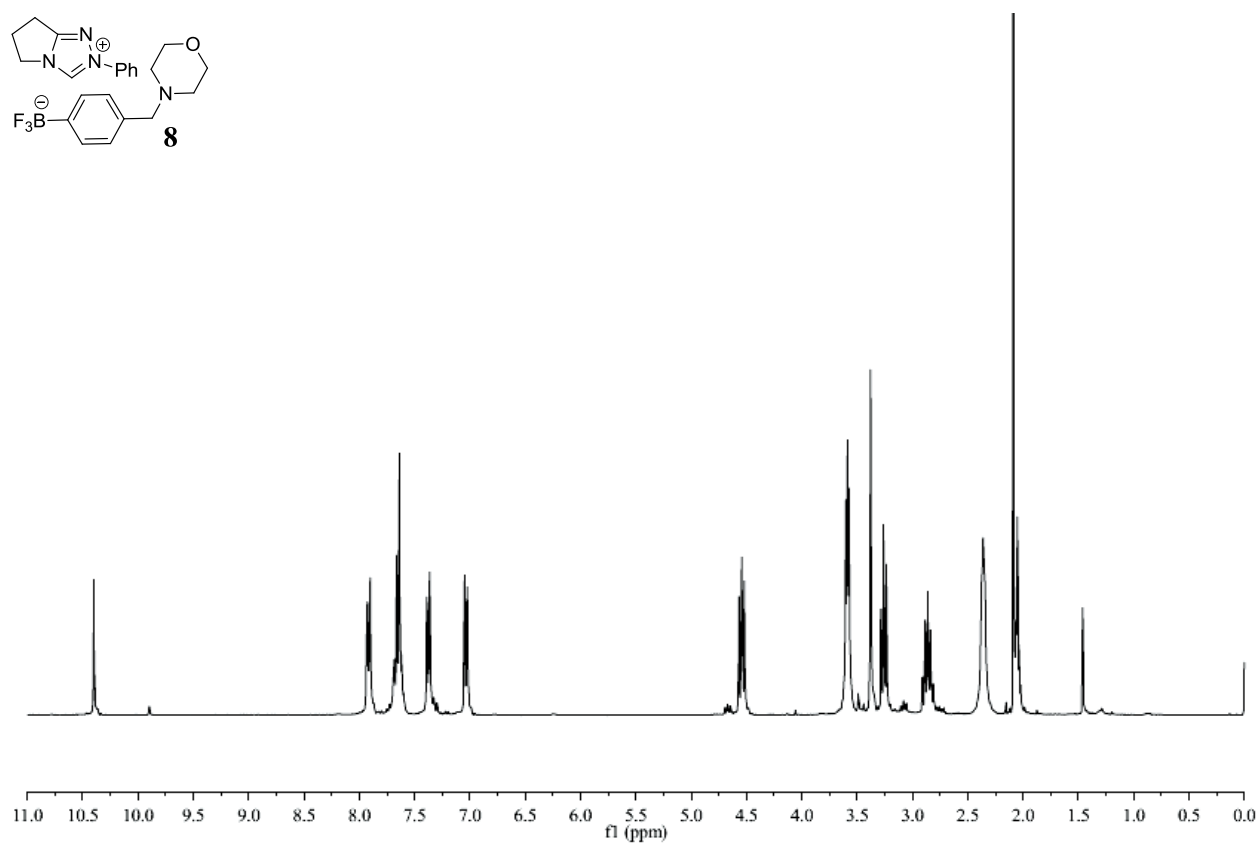
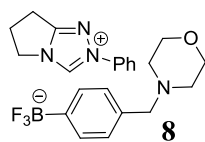
	U ¹¹	U ²²	U ³³	U ²³	U ¹³	U ¹²
C(1)	18(1)	16(1)	16(1)	1(1)	4(1)	2(1)
C(2)	37(1)	15(1)	21(1)	-2(1)	4(1)	0(1)
C(3)	61(2)	15(1)	19(1)	-2(1)	10(1)	-2(1)
C(4)	25(1)	15(1)	14(1)	1(1)	4(1)	-2(1)
C(5)	32(1)	18(1)	17(1)	-2(1)	6(1)	0(1)
C(6)	33(1)	20(1)	16(1)	-1(1)	3(1)	-4(1)
C(7)	28(1)	16(1)	18(1)	-1(1)	-2(1)	-6(1)
C(8)	22(1)	16(1)	17(1)	1(1)	1(1)	-3(1)
C(9)	24(1)	20(1)	22(1)	4(1)	2(1)	-1(1)
C(10)	25(1)	22(1)	32(1)	5(1)	4(1)	1(1)
C(11)	29(1)	19(1)	32(1)	5(1)	-7(1)	-3(1)
C(12)	35(1)	18(1)	22(1)	2(1)	-7(1)	-5(1)
C(13)	22(1)	15(1)	13(1)	0(1)	0(1)	1(1)
C(14)	21(1)	22(1)	15(1)	-2(1)	1(1)	1(1)
C(15)	29(1)	22(1)	21(1)	-3(1)	-3(1)	-7(1)

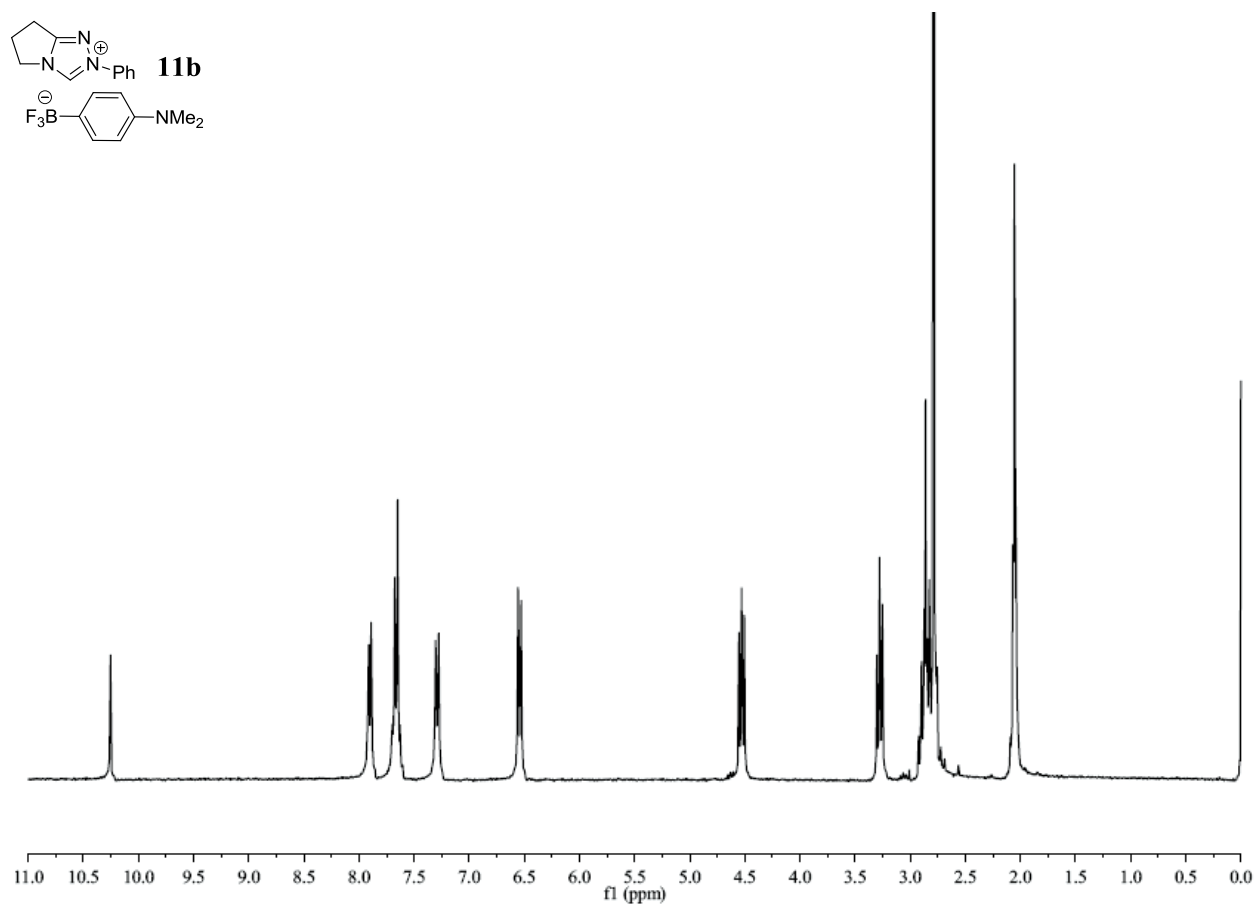
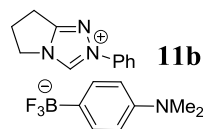
C(16)	36(1)	23(1)	18(1)	-5(1)	-5(1)	2(1)
C(17)	29(1)	24(1)	15(1)	-1(1)	1(1)	8(1)
C(18)	20(1)	20(1)	16(1)	3(1)	1(1)	2(1)
C(19)	23(1)	17(1)	17(1)	2(1)	4(1)	3(1)
C(20)	24(1)	15(1)	22(1)	1(1)	0(1)	0(1)
C(21)	37(1)	19(1)	18(1)	2(1)	-2(1)	2(1)
C(22)	39(1)	19(1)	19(1)	3(1)	9(1)	4(1)
C(23)	24(1)	23(1)	30(1)	8(1)	10(1)	1(1)
C(24)	25(1)	20(1)	23(1)	4(1)	-2(1)	-1(1)
F(1)	21(1)	33(1)	22(1)	-5(1)	5(1)	-5(1)
F(2)	38(1)	31(1)	36(1)	-8(1)	1(1)	-17(1)
F(3)	23(1)	22(1)	26(1)	2(1)	7(1)	0(1)
F(4)	38(1)	31(1)	27(1)	-5(1)	11(1)	12(1)
F(5)	24(1)	28(1)	30(1)	6(1)	-2(1)	-6(1)
F(6)	59(1)	33(1)	23(1)	4(1)	-12(1)	-10(1)
F(7)	63(1)	34(1)	22(1)	7(1)	15(1)	1(1)
F(8)	29(1)	43(1)	47(1)	17(1)	11(1)	-6(1)
F(9)	31(1)	42(1)	33(1)	9(1)	-9(1)	-10(1)
N(1)	27(1)	13(1)	15(1)	-2(1)	3(1)	-1(1)
N(2)	27(1)	16(1)	16(1)	1(1)	2(1)	0(1)
N(3)	41(1)	15(1)	20(1)	-2(1)	5(1)	0(1)
O(1)	48(1)	18(1)	19(1)	-2(1)	4(1)	-5(1)
O(2)	51(1)	26(1)	34(1)	-16(1)	-1(1)	0(1)
O(3)	91(2)	77(2)	105(2)	18(2)	-46(2)	-34(2)

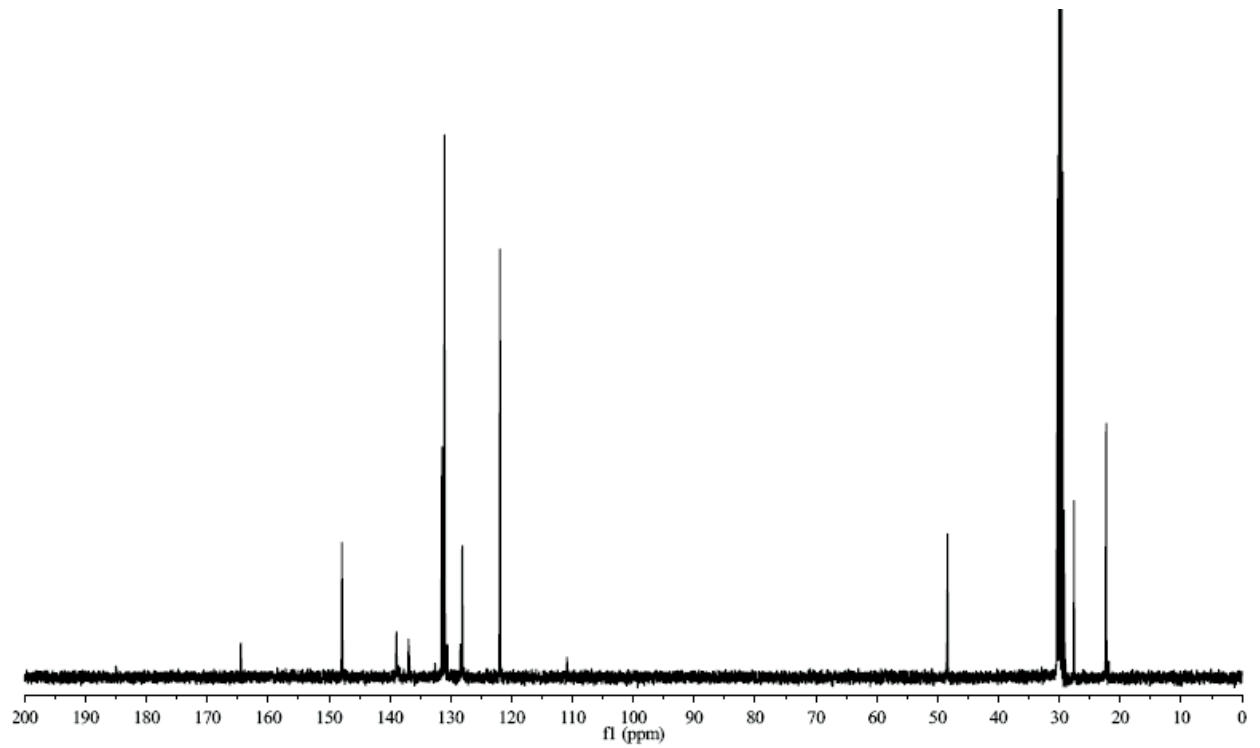
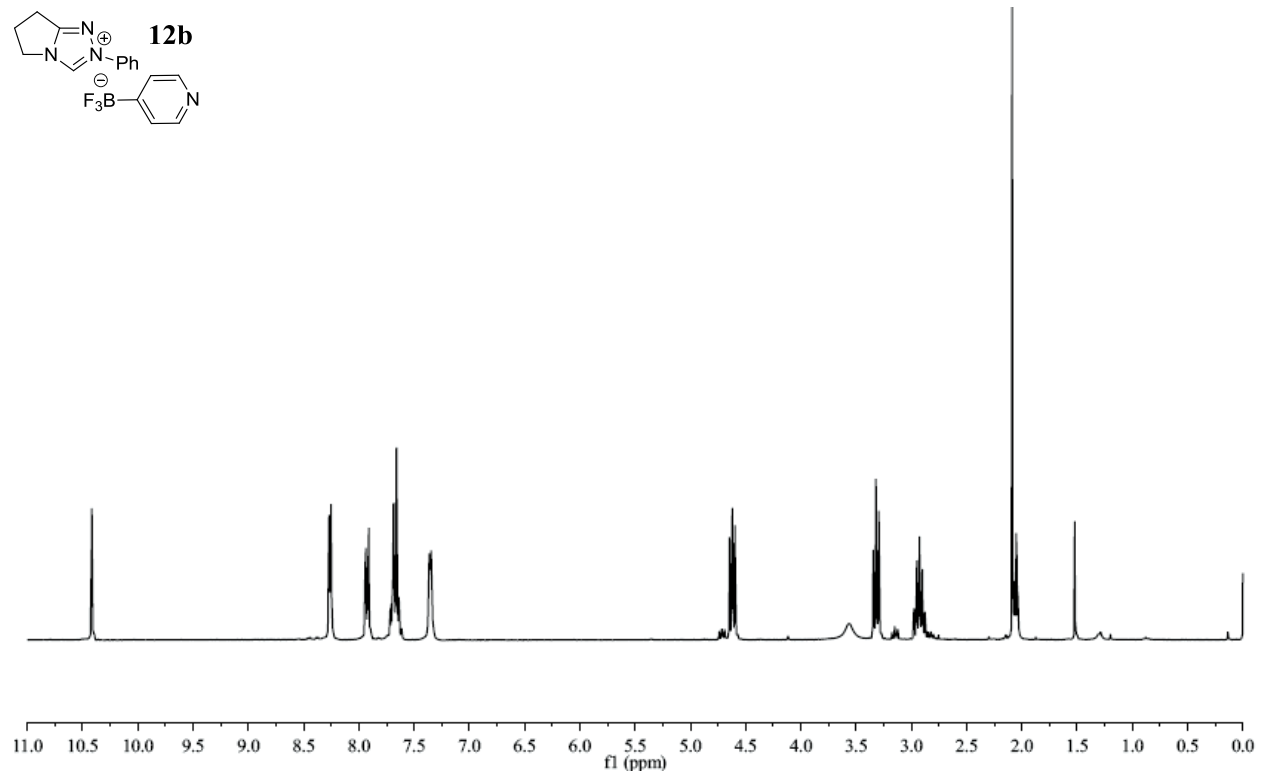
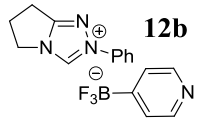
Table A.2.10. Hydrogen coordinates ($\times 10^4$) and isotropic displacement parameters ($\text{\AA}^2 \times 10^3$) for compound **30**.

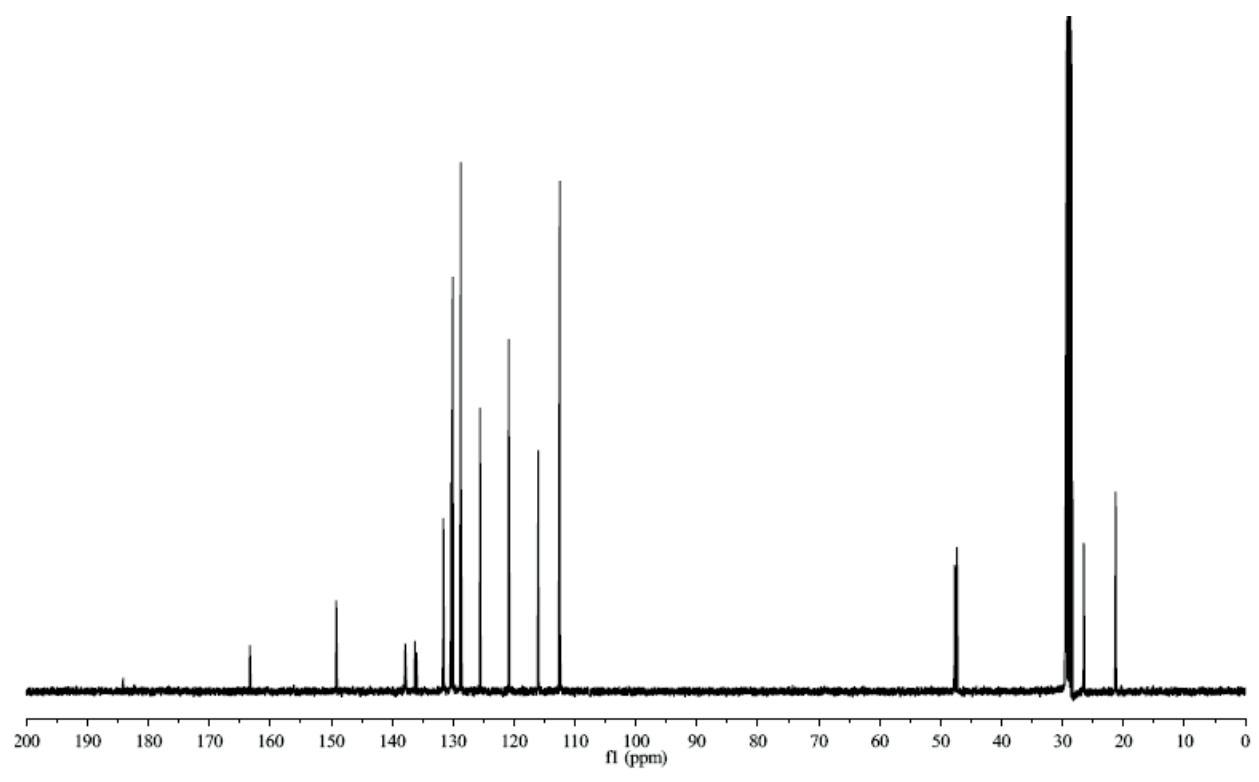
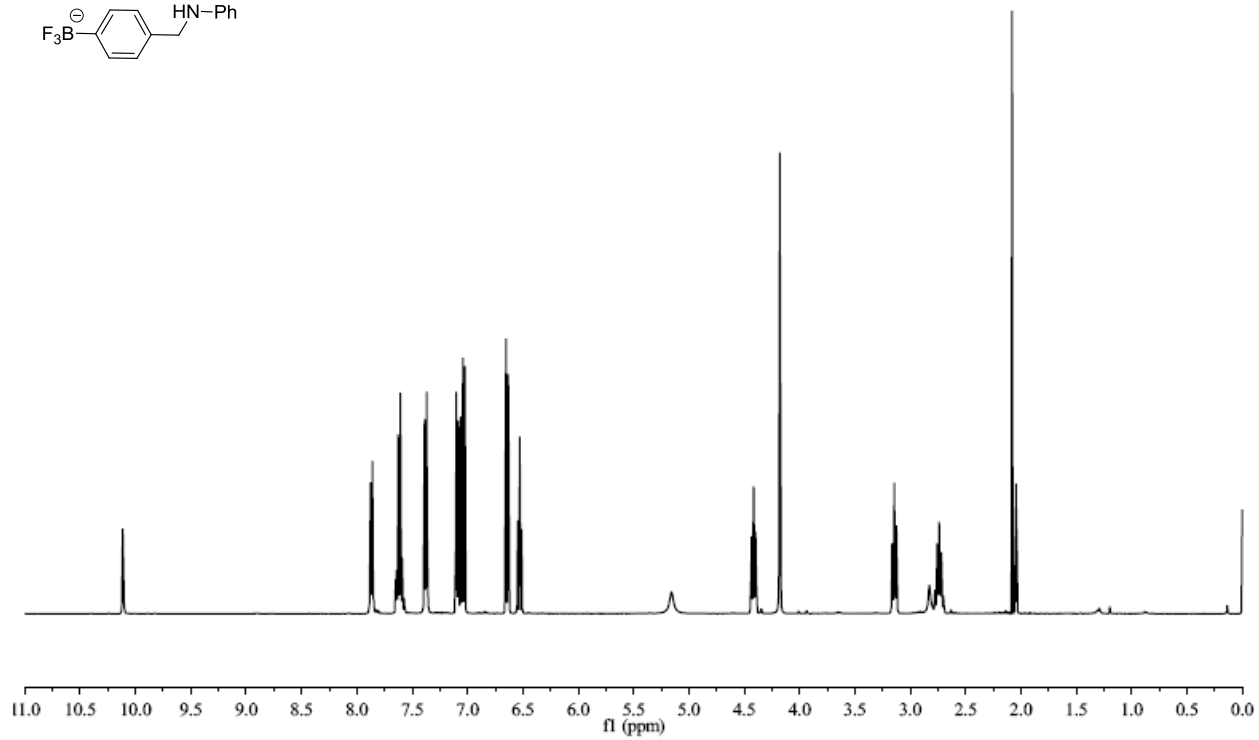
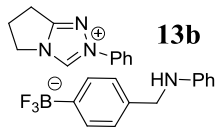
	x	y	z	U(eq)
H(3A)	3597	3837	3967	38
H(3B)	1106	3592	3939	38
H(4)	956	1388	3446	22
H(5)	40	2284	4249	27
H(6A)	2592	1773	5161	28
H(6B)	914	1181	4839	28
H(9)	5685	869	2948	26
H(10)	8349	107	3466	32
H(11)	8271	-62	4587	32
H(12)	5523	516	5208	30

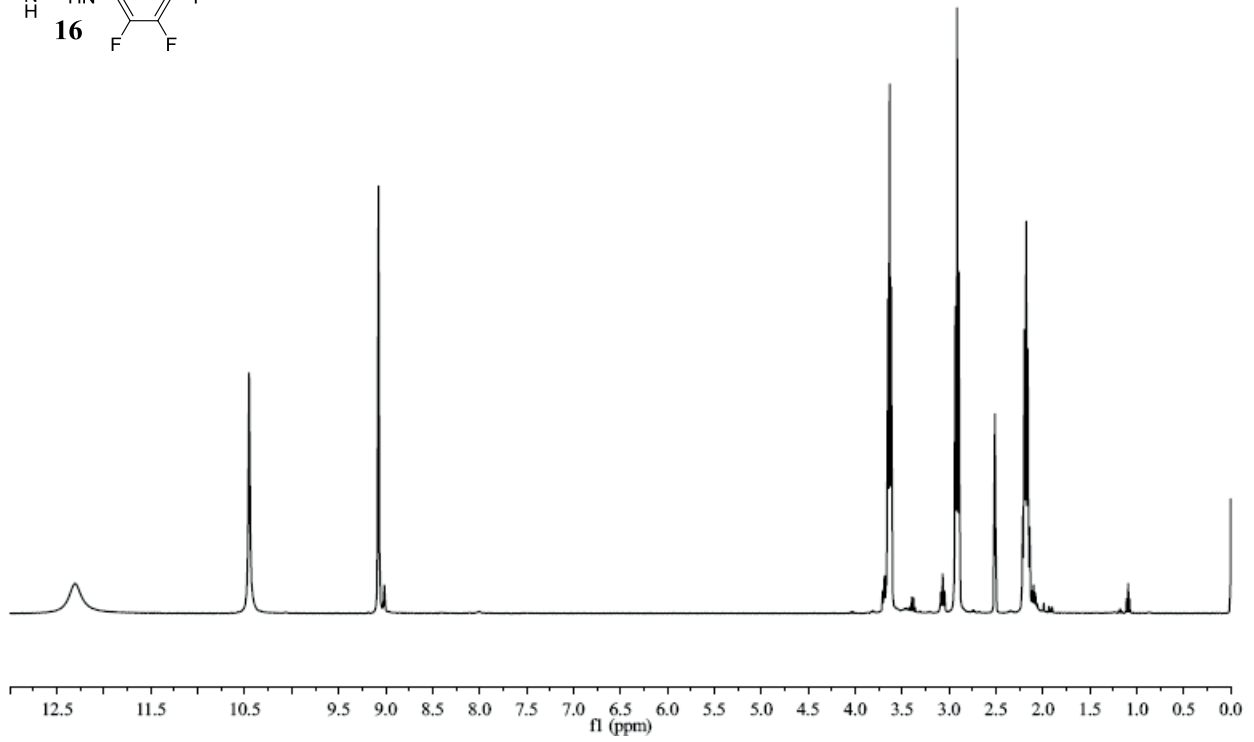
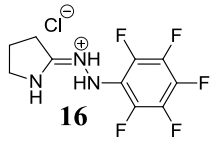




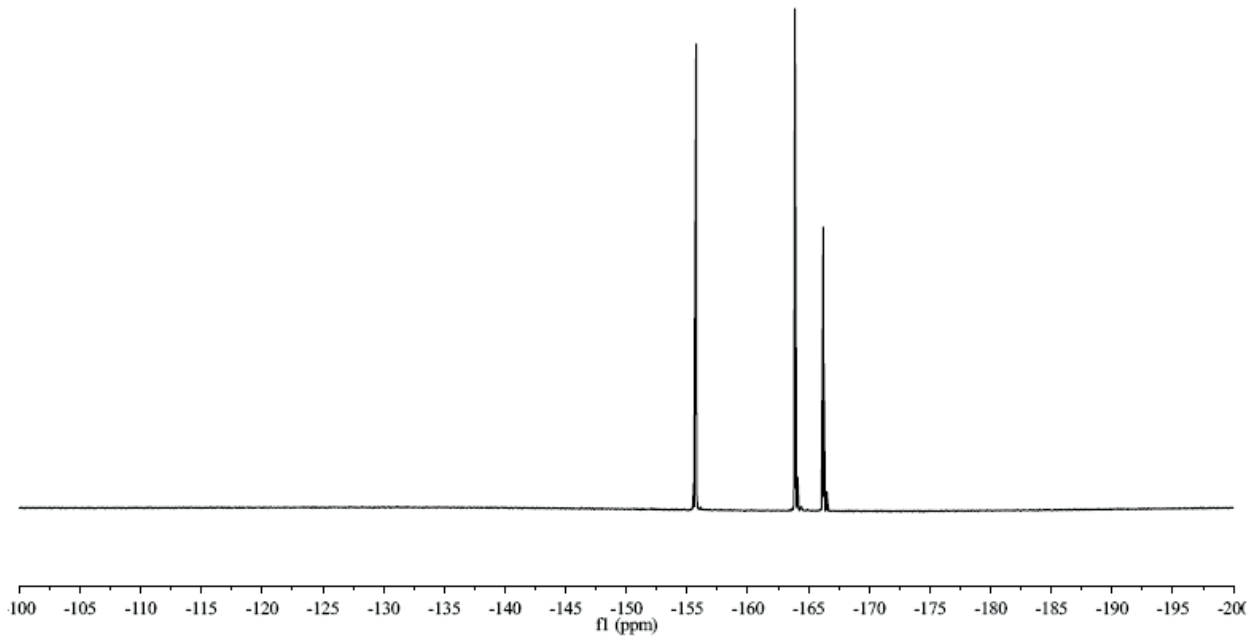


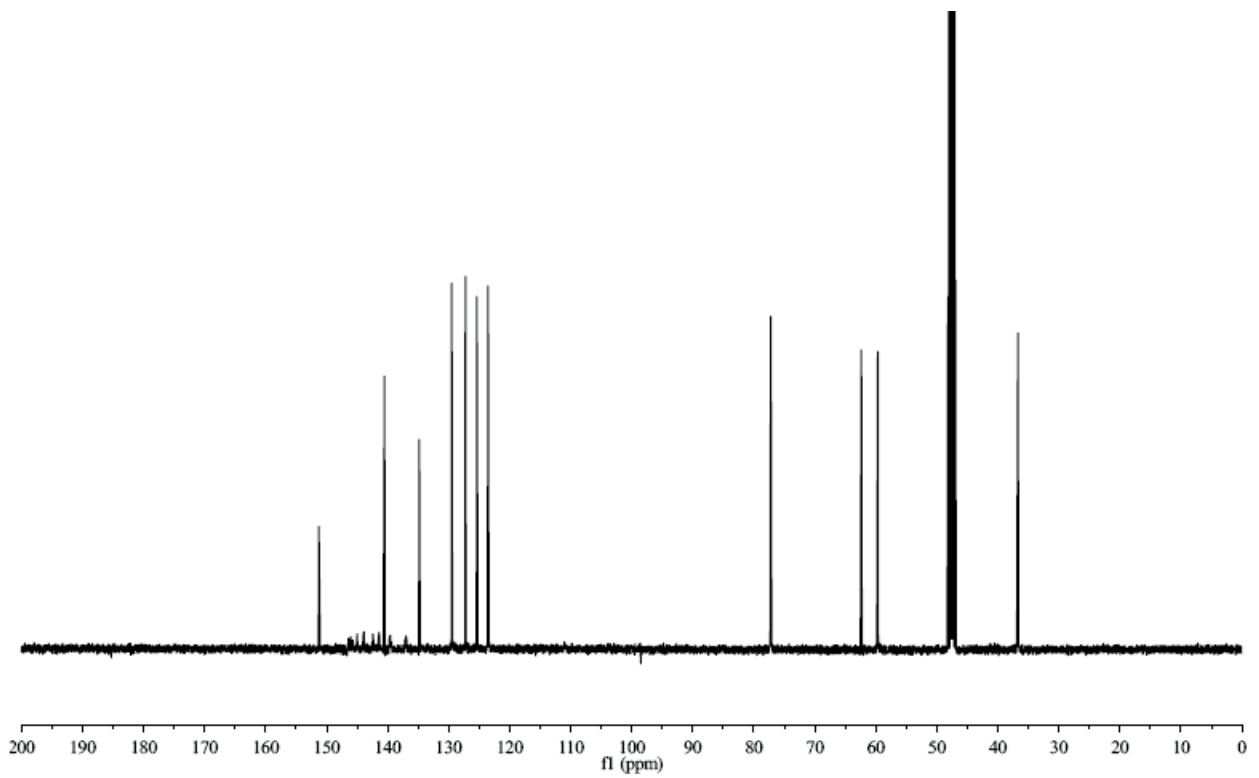
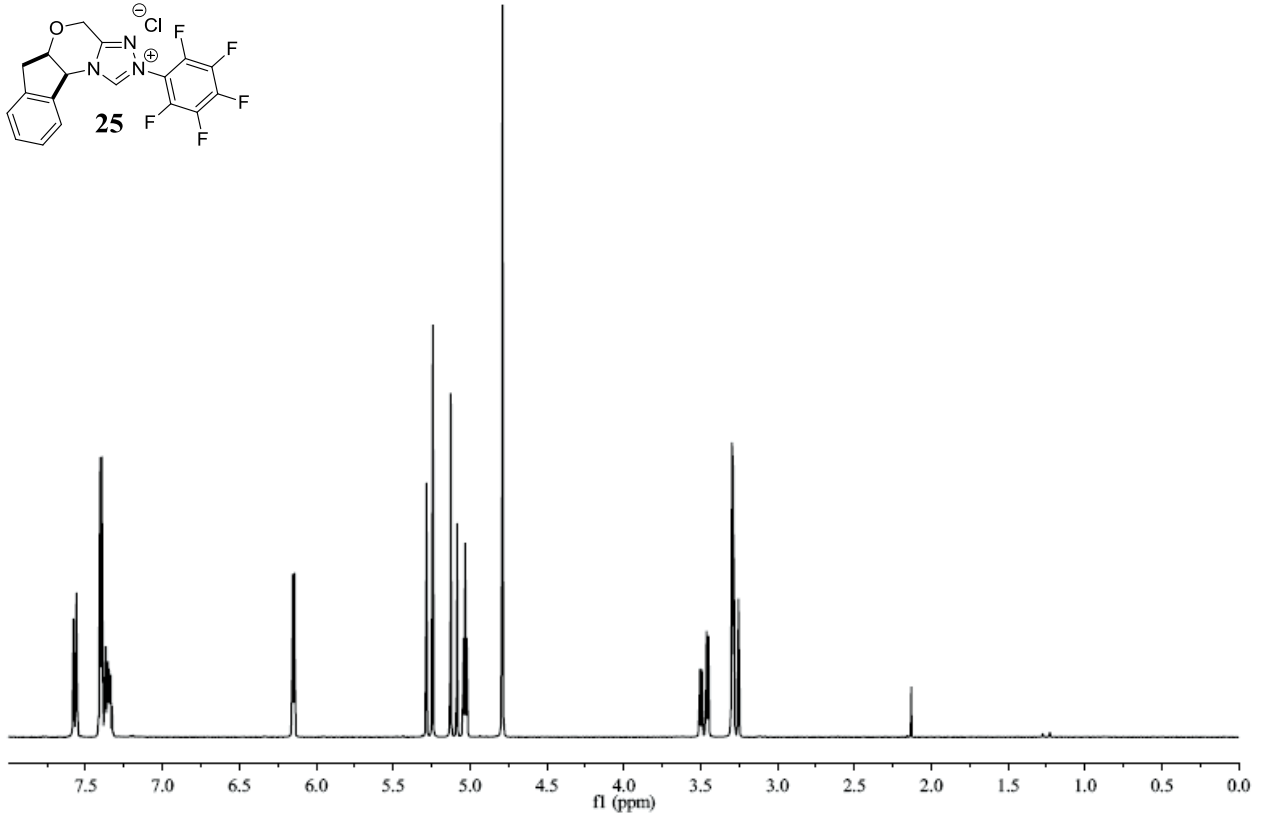
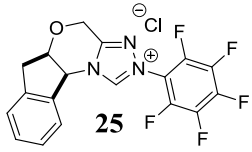


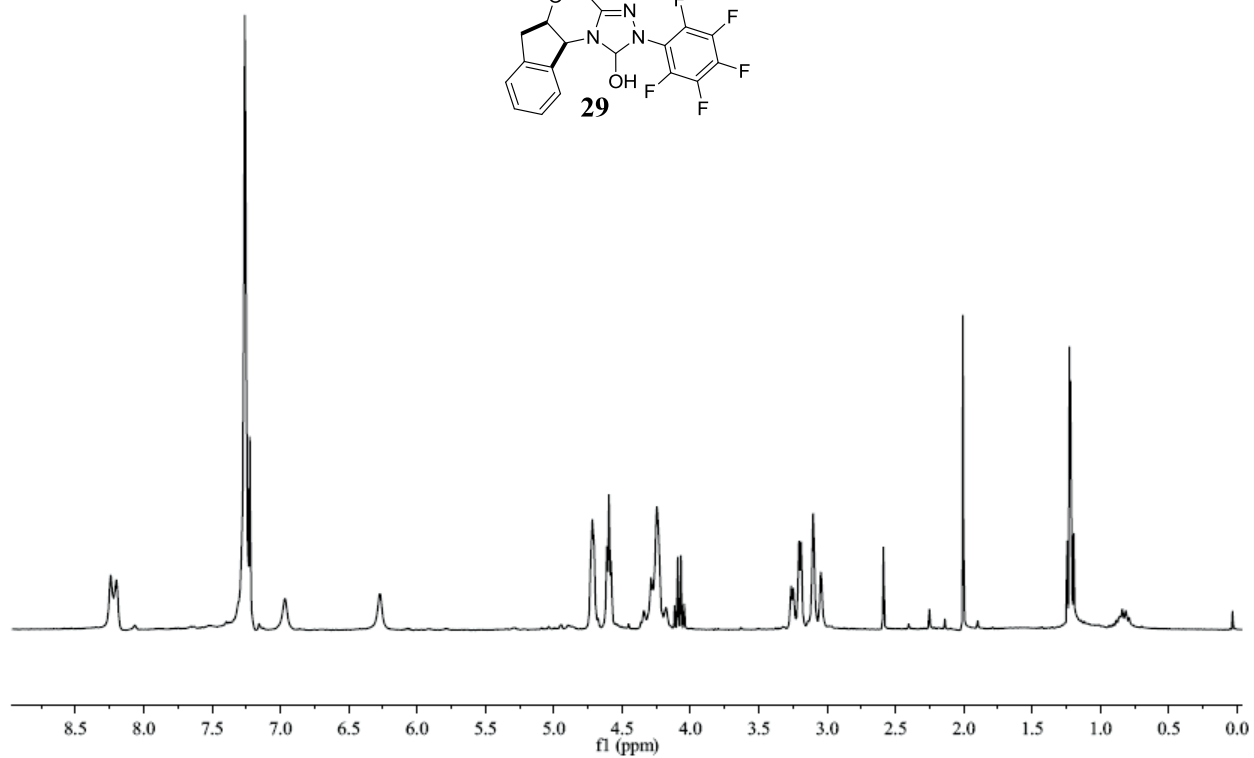
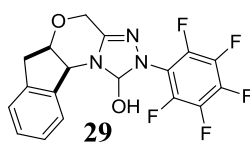
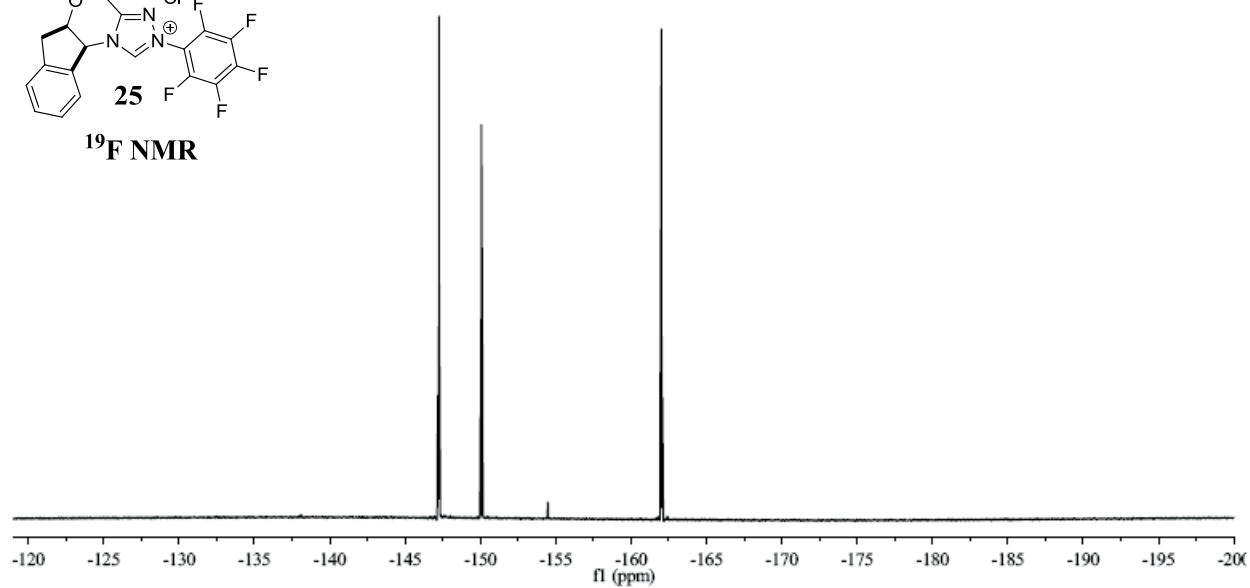
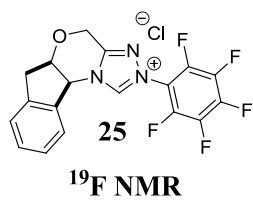


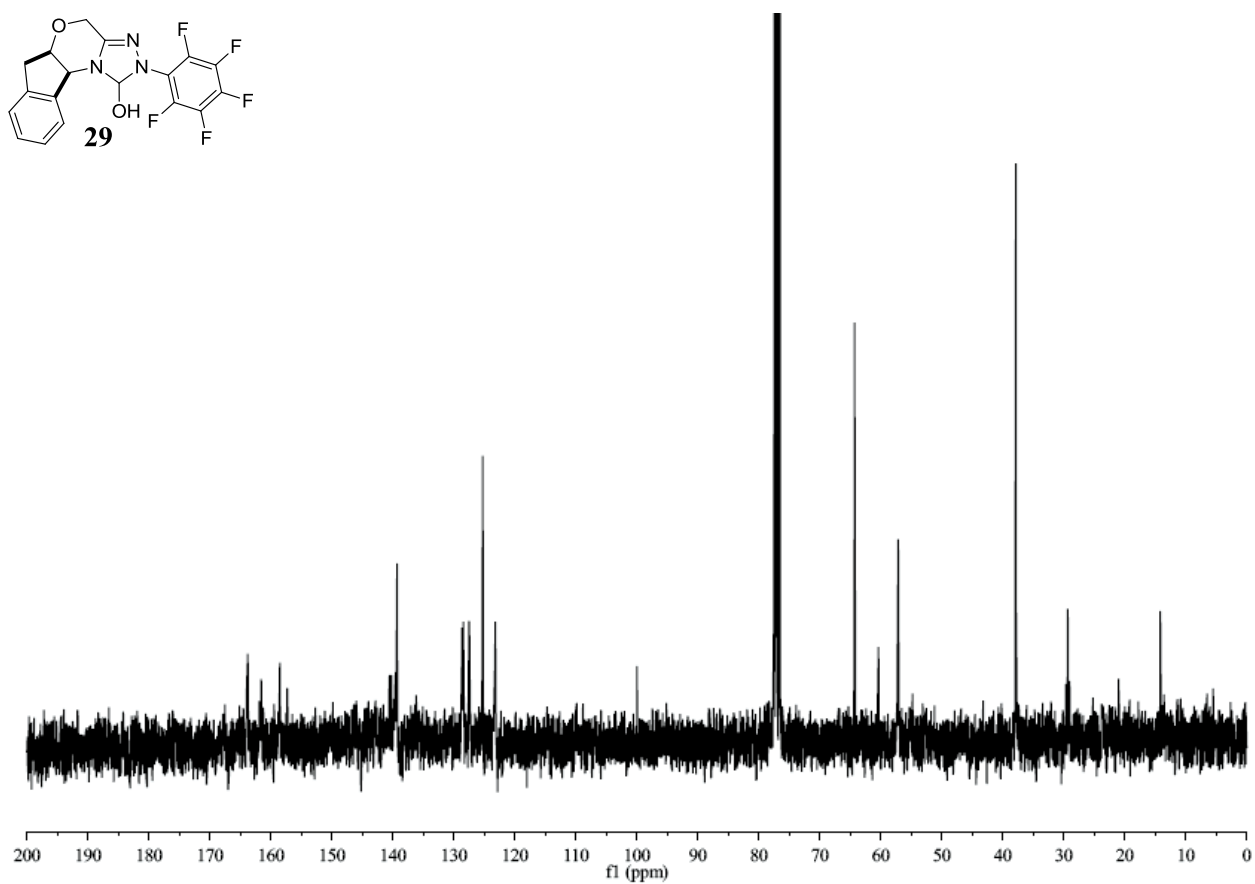
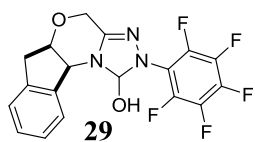


¹⁹F NMR









¹⁹F NMR

